Designing a Test Asset and Validating the Accuracy of GPS/GNSS Speed Measurement

A thesis submitted in fulfilment of the requirements for the degree of Master of Science

ANDRIY DYUKOV

Bachelor (Hons) in Electrical Engineering, Kharkov Polytechnic Institute

School of Science

College of Science, Engineering and Health

RMIT University

December 2017

DECLARATION

I certify that except where due acknowledgement has been made, the work is that of the author alone; the work has not been submitted previously, in whole or in part, to qualify for any other academic award; the content of the thesis is the result of work which has been carried out since the official commencement date of the approved research program; any editorial work, paid or unpaid, carried out by a third party is acknowledged; and, ethics procedures and guidelines have been followed.

I acknowledge the support I have received for my research through the provision of an Australian Government Research Training Program Scholarship.

Andriy Dyukov

20 November 2017

ACKNOLEDGEMENTS

I would like to thank my supervisors: Dr Suelynn Choy and Dr David Silcock. This thesis would not have been completed without their guidance, encouragement and support. Both my supervisors patiently guided me through the process of scientific research, had numerous meetings with me when we discussed the results and future steps of my research journey.

I would like to also thank my wife Elena for her full support that kept me moving forward. When the testing stage of this research started, she kindly provided her vehicle Mazda 3 to make modifications to it to be able to conduct practical testing. Moreover, she went with me on a few occasions when practical tests were conducted. In particular, Elena participated in a long trial test drive from Melbourne to Echuca and we both enjoyed not only a ride itself, but also went to one of Echuca's Murray River 100 years old paddle steamers named as Pride of Murray.

I would like to finally express my gratitude to my Mom for her loving support. During my research time and dedication to this project I paid less attention to my Mom. This is because I sometimes spent hours during weekends on this project while these hours could be devoted to my Mom instead. For that I dedicate this work to my Mother and wife.

ABSTRACT

Global Navigation Satellite System (GNSS) receivers are now widely used for navigation and speed measurements. The increasing demand for vehicles monitoring in regulatory and non-regulatory environments has led to a growing number of GNSS applications in the automobile industry. In addition, GNSS receivers are commonly used by civilian users for navigation and speed measurements.

Manufacturers of GNSS receivers supply speed accuracy parameters in the receiver specification data sheets. However, little information is provided regarding specific conditions when the specified speed accuracy of GNSS receivers might be met. Also, there is limited research available about practical speed accuracy parameters of receivers in a variety of challenging GNSS environments. Finally, to the author's knowledge, there is no research conducted to understand if adding more satellites from different constellations to GPS, for example, GLONASS provides an improvement in GNSS speed accuracy reporting.

This thesis presents the design of a test asset system capable of testing GNSS receivers for speed accuracy and the Uncertainty of Measurements (UOM) analysis for this system. The test asset system utilises a variety of engineering solutions and is capable of maintaining high accuracy benchmarks in speed measurements. The test asset system has an UOM equal 0.4 km/h for the entire range of speeds used for GNSS speed testing. The system was designed, assembled and tested to ensure the system maintains its integrity and capability to test GNSS receivers for speed measurement. Subsequently, several field experiments were performed to collect GNSS speed data records in a variety of driving environments using different receivers. The receivers ranged from geodetic grade to low cost receivers. Test routes were selected specifically to reflect real world and challenging GNSS environments, such as freeways with overpasses and roads with tree canopies.

Detailed analyses of outliers and statistical results are presented to demonstrate that GNSS receivers may not measure speed correctly under challenging environments. The results also show that different GNSS receivers perform differently in measuring speed. Methods to filter potentially unreliable speed records were also investigated.

Key words: GPS, accuracy, speed, testing, challenging environment, outlier.

Contents

APPENDICES

LIST OF FIGURES

LIST OF TABLES

ACRONYMS

Acronym	Meaning
DGPS	Differential GPS
DOP	Dilution of Precision
EDM	Electronic Distance Measurement
EEPROM	Electrically Erasable Programmable Read-Only Memory
GDA94	Geocentric Datum of Australia 1994
GLONASS	Globalnaya Navigazionnaya Sputnikovaya Sistema, or Global Navigation Satellite System (Russia)
GNSS	Global Navigation Satellite System
GPS	Global Positioning System
HDOP	Horizontal Dilution of Precision
LOS	Line of Sight
NANU	Notice Advisory for Navstar Users
NMEA	National Marine Electronics Association
NMI	National Measurement Institute
PCB	Printed Circuit Board
PDOP	Position Dilution of Precision
PIC	Peripheral Interface Controller
PLL	Phase Lock Loop
PSI	Pounds per Square Inch
RMS	Root Mean Square
PPR	Pulses Per Revolution
PRN	Pseudo Random Noise
QZSS	Quazi-Zenith Satellite System (Japan)
RF	Radio Frequency
SBAS	Satellite-Based Augmentation System
SD	Secure Digital

SDOP	Speed Dilution of Precision
SNR	Signal to Noise Ratio
UART	Universal Asynchronous Receiver / Transmitter
UOM	Uncertainty of Measurements
UFDC	Universal Frequency to Digital Converter
UHF	Ultra-High Frequency
UTC	Coordinated Universal Time
VDOP	Vertical Dilution of Precision

SUMMARY OF PUBLICATIONS

The following is a list of works published by the author during his research.
All these works are cited in the text and therefore also appear in the References section.

Journal papers
Dyukov, A 2016, 'Development of an Electronic Speed Measurement System for Evaluating the Accuracy of GNSS Receivers and Statistical Analysis of Their Performance in Speed Measurements', *Universal Journal of Electrical and Electronic Engineering*, Vol.4(2), pp.33-50.

Dyukov, A 2016, 'Mask Angle Effects on GNSS Speed Validity in Multipath and Tree Foliage Environments', *Asian Journal of Applied Sciences*, Vol.04, Issue 02, pp.309-321.

Dyukov, A 2016, 'Test Vehicle Speed Error as a Function of Tyre Pressure', *Journal of Traffic and Transportation Engineering*, Vol.4, No2, pp.102-107.

Dyukov, A, Choy, S & Silcock, D 2015, 'Accuracy of Speed Measurements using GNSS in Challenging Environments', *Asian Journal of Applied Sciences*, Vol.03, Issue 06, pp.794-811.

The following is a list of works published by the author before this research was undertaken and cited in this thesis.

Dyukov, A 1988, *A Device to Control the Necessary Diameter of a Reel*, Patent of the USSR No 1388374.

Dyukov, A 1990, *A Device to Control the Cartridge Glue Machine Tool*. Patent of the USSR No1535812.

1 INTRODUCTION

1.1 Background

Speed measurement systems are currently used across a range of industry sectors such as road transport, aviation, agriculture, maritime, rail and consumer. In the last 15 years, the use of Global Navigation Satellite Systems (GNSS), in particular the United States Global Positioning System (GPS) for speed determination has become well known, as it offers advantages over other methods, particularly in its accuracy of measurements. However, GPS based speed measurement solutions are vulnerable in areas where GPS satellites visibility drops or degrades, e.g. in urban canyons, along roads with tree canopies, overpasses and gantries. There are only a few practical research projects to date investigating the performance of GPS receivers for speed measurements under various environments. Also, there is limited research that quantifies the amount of speed outliers generated by the receivers in such environments. This thesis covers the design of a test asset to test GPS/GNSS receivers for speed accuracy. Subsequently, it presents the performance analysis of low cost consumer grade, medium range and geodetic quality GNSS receivers in challenging environments. Finally, this research also analyses methods for detection of GPS speed outliers.

This chapter reviews some background information pertaining to this thesis. A discussion covering prior theoretical and practical research is included, and a summary of the research contribution highlights the original research conducted as part of this Master study. The chapter concludes with a preview of the remaining chapters.

1.2 Research motivation

The use of GNSS technology is rapidly increasing and speed records provided by GNSS are currently used in the court of law (Truebridge 2014; Wainwright 2007). It is important to understand how GNSS speed records might be used for evidentiary purposes and specific circumstances when GNSS cannot be relied upon (Huang 2013).

A few research activities focus attention on the theoretical performance of GPS receivers to measure speed (Zhang 2007; How, Pohlman & Park 2002; Zhuang 1994; Zhang et al 2006). Such research has advanced our theoretical knowledge on how speed is determined by GPS receivers and the error sources. On the other hand, theoretical research results do not necessarily reflect the practical performance of GPS receivers in a real world environment.

A number of experiments have been conducted by researchers to estimate the speed accuracy of GNSS receivers when they are stationary (Chalko 2009; Ding & Wang 2011; Durrant & Hill 2005).

However, such experiments were usually conducted in open sky conditions and the GNSS receivers reported speed was very close to zero because the receivers were not operating under challenging environments. In such experiments, these GNSS receivers performed well and practically within their specifications provided.

Also, a few research activities were performed in kinematic mode where GPS receivers were installed on test vehicles and driven along a specific route while their speed was compared to specific speed references (Chalko 2009; Witte & Wilson 2004; Ogle et al 2002; Al-Gaadi 2005; Chowdhury, Chakravarty & Balamuralidhar 2014; Ding & Wang 2011; Serrano et al 2004; Szarmes et al 1997; Keskin, Sekerli, & Kahraman 2014; Supej & Cuk 2014; Zhao, Goodchild & McKormack 2011). While some of these research tests were conducted in a variety of GPS environments, there have been limitations:

a) No information was provided in any research as to whether a test vehicle was calibrated and whether its accuracy can be traceable to national standards.
   Traceability to national standards means that a test vehicle shall be calibrated in such a way when its speed measurements or distance and time measurement results can be related to stated references, usually national or international standards, through an unbroken chain of comparisons all having stated uncertainties. For example, if calibration of a test vehicle is conducted on a chassis dynamometer, the dynamometer's installation shall have its frequency counter calibrated and its drums calibrated.
   In addition, all the above calibrations shall be conducted by reference instruments with an unbroken chain of comparisons to national or international standards of frequency and length; and their uncertainties properly calculated and understood (Asia Pacific Legal Metrology Forum 2004).
   It is worth noting that the accuracy of the test vehicle designed in this research is traceable to National standards through the proven calibration procedure and a chain of recorded calibrations. This will be shown in Chapter 4 relating to the Uncertainty of Measurements (UOM).
b) There has been minimal investigation conducted focusing on specific environments when a receiver operates in the GNSS challenging environment, e.g. near high rise buildings, tree canopies or overpasses. Such environments may create the degradation of the GPS signal or multipath.
c) No work has been conducted to investigate simple quality indicators which can be used to indicate the reliability of the speed records.
   It should be noted that some of these simple quality indicators are widely available from GPS/GNSS receivers, e.g. the number of satellites tracked or Horizontal Dilution of Precision (HDOP).

d) No work has been conducted to assess the performance / accuracy of speed measurements using different GNSS receivers based on their cost and functionality under a variety of test conditions.

Practical research has been conducted by Brzostowski et al (2012) to understand how different GPS receivers perform in kinematic mode under challenging environments. The receivers tested were NovAtel OEMV-3, U-block IEA-6, X-Sens MTI-G and others. However, this research only focused on positional accuracy but not speed accuracy.

Limited research activities have also been conducted using GPS simulators (Sathyamorthy, Shafii, Amin, Jusoh & Ali 2015), and in real world environments with calibrated vehicles (Bai et al 2015). It should be noted that the emphasis of the research was on the fact that a test asset, i.e. a GPS simulator or a test vehicle, was calibrated and therefore its accuracy parameters or UOM are well known and stated in the research.
The first part of the research published the results of testing with GPS simulators but did not provide any real-world challenge to the receivers under test. Therefore, testing for speed with simulators had relatively minor value and could only highlight issues when the receivers had firmware issues in their speed measurement algorithms. Further, the second part of this research focused on a test with a calibrated test vehicle equipped with a Correvit speed measurement system on board (Corrys Datron Sensor Systems 2008). However, the focus of this real-world test described by Bai et al (2015) was with one specific GPS receiver and it was evident that testing was conducted on a highway with good GNSS visibility. The results showed the receiver performed very well throughout the journey. Also, Bai et al (2015) focused on one receiver operating in GPS mode rather than on a combined GNSS solution.

Speed tests have also been conducted by GNSS chipset and receiver manufacturers. However, it is usually a challenge to find the results of such tests because they are mainly available for manufacturers use only. It is common that GNSS chipset data sheets contain speed accuracy parameters. However, it remains unclear whether such parameters were tested with GNSS simulators or in static / kinematic modes, and the conditions of the test. For example, the U-blox (2011; 2014) datasheets state that the accuracy of speed determination is 0.1 m/s but with a note that such accuracy is achievable under good GNSS conditions for U-blox 6 and 50% of measurements for U-blox 7. However, it is not specified what good conditions might mean or the speed accuracy performance in poor conditions. The documents from SIRF Technology, Inc (2007; 2010) also states the technical specifications of velocity accuracy of 0.01 m/s without specifying when this parameter is guaranteed. As a result, it appears that datasheets for these well-known GNSS receivers do not contain any specific conditions when speed records may fall

outside the compliance limits. Therefore, a consumer may be tempted to assume that speed accuracies are always guaranteed.

Durrant & Hill (2005) represent a report developed by a manufacturer of GPS receiver. The report describes the performance of the receiver for speed measurements. However, this report described two test scenarios only. The first was in open sky static testing; and the second was a brief dynamic test in an open sky environment. In the latter test, the speed of a vehicle was measured precisely during a short timing interval when a vehicle passed a little section of the road where laser trap systems were installed. In addition, there was no analysis of the uncertainty of speed measurement. Finally, only one GPS receiver was tested.

Another example of manufacturer GPS testing was described in U-blox (2013a). Although this report was very comprehensive, it did not focus on speed accuracy but demonstrated willingness of the GPS chipset manufacturer to test a few critical parameters using a GPS simulator. Such testing did not consider the accuracy of speed measurements in real-world situations.

Speed Dilution of Precision (SDOP) is outputted by some GPS chipsets as a parameter to indicate possible quality of speed records (Chalko 2009). SDOP is a parameter determined based on the Kalman Filter covariance computed during each 1-second cycle of the SiRF3 chipset (Chalko 2009). It should be noted that SiRF is a trademark of SiRF Technology, Inc. which pioneered in the commercial use of GPS technology for consumer applications. Chalko (2009) suggested the following benefits of using SDOP for determining errors of GPS-Doppler speed measurements:

- the SDOP parameter reflects the influence of atmospheric phenomena and satellite constellation geometry at the time of each GPS-Doppler speed measurement (Chalko 2009).
- the GPS Doppler speed accuracy can be computed for each speed measurement individually. This is important when speeds are measured in varying atmospheric conditions.
- the method of evaluating speed measurement errors based on SDOP parameters is self-adjusting to the measurement conditions.
- the speed values displayed by the GPS receiver in real time can be corrected for speed error.
- the logged GPS-Doppler speeds corrected by SDOP can potentially serve as proof of speed, including in the court of law.

There are disadvantages of using SDOP. They could be summarised as follows:

- SDOP is not a parameter used in many GPS chipsets even after years of implementing it in SIRF type GPS chipsets. SDOP is not outputted as a parameter in most low cost or mid-

range receivers, but also not always in geodetic quality receivers. For example, advanced NovAtel receivers (NovAtel Inc 2014a) used in this project, plus the Leica receivers (Leica Geosystems 2004) used in the survey industry do not output SDOP.

- The determination of SDOP values is hidden behind proprietary algorithms, which are often not disclosed nor available to researchers. This may introduce doubts when such speed records are used for evidentiary purposes in legal proceedings.

The above disadvantages of SDOP indicate a need to have other simple quality indicators which might be used to filter the potential unreliable speed records generated by GPS chipsets / receivers.

As mentioned previously, little research activities have been conducted to investigate GNSS speed accuracy in challenging environments. GNSS signals are radio navigation waves and therefore can be impacted by multipath, tree foliage or other obstructions in the real-world environment.

Multipath occurs when the GNSS signal is reflected from surrounding objects, such as buildings, bridges, road gantries and other structures. It is considered that multipath represents one of the largest sources of error in GNSS measurements (Mekik & Can 2010) and specifically in speed related applications (Zhang 2007). For multipath mitigation, existing approaches can be classified into several groups (Inside GNSS 2016): tracking loop based, antenna based, mask angle based and extra information based. The first approach focuses on tracking loop improvements and the other receiver based techniques (Van Dierendonck, Fenton & Ford 1992). Antenna based methods include the use of special antennas (Tranquilla, Carr & Al-Rizzo 1994). The extra information based method might use several sub-methods trying to improve the performance in multipath environments. Such sub-methods might include determination of SNR and the subsequent determination of probable multipath based on SNR values (Comp & Axelrad 1998; John A Dutton e-Education Institute 2015) or elevation enhanced maps (Pinana-Diaz, Toledo-Moreo, Betaille & Gomez-Scarmeta 2011).

All the above methods are relevant to situations when GNSS receivers or antennas are designed rather than used by the end user and therefore may be applicable for research and development rather than practical applications. As a result, the only method available to the end user to mitigate multipath is to change the mask angle through the receiver configuration settings, if such settings are available. This method has been described in several sources (John A Dutton e-Education Institute 2015; Roberts 2015; Abd-Elazeem, Farah & Farrag 2010; Heng, Walter, Enge & Gao 2015). Mask angle, also very often referred to as cut-off angle, is a parameter in the receiver configuration when signals below a particular elevation angle would be effectively filtered out by the receiver and would not be used in positional or speed computations. Therefore, the use of the cut-off angle to mitigate multipath related problems might be a sound strategy. In theory, it is considered that such strategy would help to improve speed accuracy parameter of GNSS receivers (Zhang 2007) or positional accuracy (John A Dutton e-Education Institute 2015; Roberts 2015;

Abd-Elazeem, Farah & Farrag 2010). On the other hand, implementing higher mask angles would drop the availability of satellites used for navigation and speed measurements and therefore reduce the number of speed records available. Hence, a compromise is needed between high mask angle to mitigate multipath and low mask angle to have sufficient satellite availability. It is worth noting that the above-mentioned research did not stipulate dependency between cut-off angle and speed accuracy. It is only considered in theory that the higher the cut-off angle, the better the speed accuracy (Zhang 2007).

It is also worth mentioning that if reflected GNSS signals come from an object located by more than 160 meters from a receiver, it is highly unlikely that such signals could cause errors in GNSS performance (Hannah 2001). However, the majority of overpasses located along freeways or buildings are located close to the road. Therefore, overpasses shall be taken into consideration when analysing GNSS speed errors. As a result, it is important to understand if the strategy of elevating the mask angle would practically help to improve the speed accuracy in such environments.

In addition to that, it is also known that tree foliage and canopy might affect the performance of GPS receivers (Goldhirsh & Vogel 1998). However, the research on investigating the impact of trees on GPS receivers focused on positional accuracy only (Klimanek 2010; Lachapelle, Henriksen & Melgard 1994), and only on GPS rather than GNSS receivers. Therefore, it is unclear how GNSS receivers would perform in tree foliage environments and whether such conditions represent more or less challenge to the receivers compared to multipath related environments. It is also unclear if elevation cut-off angle variations would influence the performance of GNSS receivers in tree foliage related environments.

Trees can be a significant source of signal loss. Several parameters are involved in such a loss, among them: the specific type of a tree, whether trees are dry or wet, and in the case of deciduous trees, whether the leaves are present or not. It was expected that even isolated trees might represent a problem for GNSS signals; however, a dense group of trees or trees staying all along a section of the road might represent a major problem. The expectation was based on the fact that the attenuation of RF and GPS signals in particular depends on the distance the signal must penetrate through the forest or leaves, and the attenuation increases with frequency. According to McLarson (1997), the attenuation of RF signals is in general approximately 0.05 dB/m at 200 MHz, 0.1 dB/m at 500 MHz, 0.2 dB/m at 1 GHz, 0.3 dB/m at 2 GHz and 0.4 dB/m at 3 GHz. As GNSS L1 frequency equals to 1575.42 MHz, the GNSS signal sits in the middle of Ultra High Frequency (UHF) range and therefore is vulnerable to propagation along tree lined roads.

However, the challenge of tree foliage environments is not only related to obstructions and signal propagation. The second challenge relates to the test vehicle moving along the road when unobstructed line of sights (LOS) for every epoch is achieved for relatively short periods of time. In such instances, the satellite availability would vary significantly from one second to another. This

means the receivers are put under challenge of operating with constantly changing satellites because of LOS variability and signal variability from each satellite due to GNSS signal attenuation.

As a result, it is important to quantify whether multipath or tree foliage environments represents a major challenge for GNSS receivers to measure speed. It is also important to investigate methods of determination of potentially unreliable speed records in such environments.

1.3 Research objectives

The aim of this research is to assess the performance of various GNSS receivers for measuring speed. The research has the following objectives:

- Development of a speed measurement system for the test vehicle that can accurately measure the accuracy of speed measurements from GNSS receivers. This development includes the full design, assembly of a prototype, development of calibration methods and validation of proper operation of the test vehicle;
- Analysis of the UOM for the developed speed measurement system in the test vehicle.
- Assessment of speed accuracy provided by low cost consumer grade, medium range and high end geodetic quality GNSS receivers, particularly in GNSS challenging environments. The objective is also to quantify whether overpasses or areas with tree canopies represent most challenging environment for GNSS speed measurements;
- Assessment of using HDOP parameter to filter potentially unreliable GNSS speed records;
- Assessment of the effectiveness of using elevation mask angle to reduce the number of speed outliers in GNSS challenging environments;
- Analysis of the benefits of adding Globalnaya Navigazionnaya Sputnikovaya Sistema (GLONASS) satellites to a Global Positioning System (GPS) only constellation to improve the accuracy of speed measurements;
- Assessment of using Signal to Noise Ratio (SNR) to filter out unreliable speed records.

1.4 Research approach and contributions

In this thesis, a test vehicle with a speed measurement system was specifically designed and implemented to assess the accuracy of speed measurements provided by GNSS receivers.

Modern GNSS chipsets which represent an integral part of GNSS receivers usually have a minimum sampling and processing rate of at least 1 Hz or higher. The majority of GNSS chipset manufacturers claim that the measured speed accuracy is about 0.1-0.4 km/h or better. However, a challenge in proving the GNSS speed accuracy parameter was to have an electronic speed

measurement system on the test vehicle capable of generating speed records synchronised to Universal Coordinated Time (UTC). Such synchronisation would provide a timing match between speed records produced by a test vehicle and speed records generated by the GNSS receivers under test.

The second challenge was to design an electronic speed measurement system of the test vehicle with the UOM better than, or compatible to the speed errors of GNSS receivers. The calibrated speed of a test vehicle represents the reference speed for all comparisons. Therefore, it is important that the reference speed inaccuracies are well understood and estimated via proper UOM techniques. The speed measurement system must be calibrated for every run/test. Thus, the test vehicle must be driven with all GNSS receivers on observation days after each calibration. Also, after each test, the vehicle's calibration was checked again to ensure that the calibration parameters are still maintained.

The third challenge relates to reporting of an instantaneous speed value using raw Doppler measurement used by the GNSS receivers to compute speed. However, the speed measurement system of the test vehicle always reports an average value of speed for a specific timing interval, e.g., 1 sec. Indeed, GNSS receivers using Doppler to calculate speed are not able to provide one record per second when speed is reported as an average value for the entire second. Such GNSS receivers report speed which is immediate and corresponds to the end of each second, whereas the speed measurement system of the test vehicle averages the speed within the second of conducting a measurement.

To address the above challenges, a specific test vehicle's electronic speed measurement system was designed, assembled, pilot tested and implemented. Subsequently, the test vehicle was driven on specific routes selected such that the research objectives can be addressed. For example, to test GNSS receivers in challenging environments, the routes were selected either on freeways with multiple overpasses or countryside roads with multiple tree canopies or forest areas. Also, several GPS/GNSS receivers were tested simultaneously to compare their performance against each other and against the speed measurement system under the same GNSS environments. Data from these receivers were collected and subsequently analysed to address the research objectives.

The contributions of this research can be divided into two distinct categories. The first relates to the engineering design of the speed measurement system; and the second relates to actual experiments with the GNSS receivers, their data analysis and results. Therefore, the research contributions are as follows:

1.4.1 Engineering design

The contributions related to the engineering design of the speed measurement system:

- Design of a speed measurement system for the test vehicle. This system is used to effectively test GNSS receivers for speed accuracy.
- Analysis of the UOM of the speed measurement system.
- Development of a calibration methodology for the speed measurement system and electronic calibration diagrams to ensure that the desired UOM is maintained.

The designed and calibrated speed measurement system has its UOM well understood and comparable to what GNSS receivers may achieve in stationary mode. This will be described in chapters 4 and 6 of this thesis. Also, the developed calibration methodology provides traceability to national standards of distance and time.

1.4.2 Experiments, data analysis and formulating outcomes

The contributions related to actual experiments with GNSS receivers, their data analysis and results:

- Assessment of the accuracy of speed measurement provided by various GNSS receivers in the real-world environment. Real-world challenging conditions include close proximity to bridges, overpasses, road gantries and roads with tree canopies / forests. This information is valuable in understanding whether the receivers speed records can be trusted. The research also attempts to investigate the quality of the speed measurement provided by different receiver types, e.g. geodetic quality, medium and consumer grade GNSS receivers. These receivers use the same algorithm for speed determination, i.e. the Doppler method.
- Evaluation of the benefits of adding an additional GNSS constellation, such as GLONASS, to improve speed measurement accuracy, particularly in challenging environments.
- Investigation on whether HDOP or SNR could be used for identification and detection of unreliable speed records.
- Investigation on whether satellite mask angle can be used for filtering speed outliers generated by GNSS receivers in challenging environments.

1.5 Thesis outline

This thesis will present the details of the designed speed measurement system for testing GNSS receivers for speed accuracy, as well as the results from practical field experiments.

Chapter 2 contains a detailed discussion of the methods and algorithms utilised in GNSS for speed determination. This chapter also describes the practical implementation of such methods in modern GNSS chipsets and the sources of error.

Chapter 3 contains a detailed discussion of the speed measurement system developed and used as reference in the research. This chapter includes information on the existing non-GPS based speed measurement methods and their analysis, peculiarities of the designed system based on the microcontroller, features of the speed sensor, and aspects of the hardware / firmware components of the non-GPS based speed measurement system.

Chapter 4 focuses on the UOM of the speed measurement system. Relevant uncertainties of the calibration and speed measurement are analysed. The UOM provides a basis to benchmark, compare and quantify the accuracy of speed measurement provided by GNSS receivers.

Chapter 5 describes the GNSS receivers tested in this research. In addition, this chapter details the test methodology used in the experiments. It also highlights the approach for validating each experimental run through checking the performance of GNSS constellation. Finally, this chapter contains a description of a trial test conducted to demonstrate that the test vehicle, with its speed measurement system, operated as expected, and proving that the test methodology was sound.

Chapter 6 describes the outcomes from each experiment. The first part of the chapter concentrates on static speed tests for all GNSS receivers. It describes the results of the static speed tests conducted in ideal open sky environments and under various environments where a test vehicle was stationary. This aimed to determine the speed measurement noise for each GNSS receiver. Then, this chapter provides the results of the dynamic tests in open sky and challenging GNSS environments. Challenging environments were classified into two types: routes with overpasses / road gantries, and routes with forest / tree canopy. GNSS plus GLONASS speed measurements were compared to GPS only results. Test results are presented to analyse both speed outliers generated by GNSS receivers and their statistical performance.

Chapter 7 presents an investigation into whether it is possible to filter individual speed outliers or potentially unreliable speed records using GNSS parameters such as HDOP, the number of satellites, SNR or satellite elevation.

Chapter 8 contains discussions and conclusions reviewing the contributions of the research, and provides some recommendations for future work.

2 SPEED DETERMINATION WITH GPS/GNSS

2.1 Overview

GNSS receivers are widely used today for obtaining positional and speed information. Speed records produced by GNSS are used in a variety of applications, such as monitoring driver behaviour (SeaStar Solutions 2015), in court for challenging speed fines (Expert Law 2012), in the telematics industry to monitor if drivers of heavy vehicles are speeding (Fleetmatics 2015; United States Department of Transportation 2014), unmanned aerial vehicles (Christophersen et al 2006) and Intelligent Transport Systems (ITS). Sometimes, speed records from GNSS are used to monitor drivers who have committed numerous driving offences, such as through the Intelligent Speed Assist initiative launched by VicRoads (VicRoads 2016).

GNSS receivers measure speed using multiple methods. Three methods will be described: speed through position records, speed based on Doppler method, and speed based on Carrier-phase method. It should be noted that modern GNSS receivers may use a combination of the above methods.

In this thesis, reference to GNSS includes GPS or GPS plus GLONASS.

2.2 Speed based on position records

The least accurate method of speed determination is via the use of position records and knowing the time interval between them. This method has been used by GPS receivers in the past, but is no longer a popular method.

This method uses the following simple equation to calculate speed:

$$\text{Speed} = \text{Distance} / \text{Time} \tag{2.1}$$

Since GPS provides position at very precise moments, it is possible to compute average speeds for these intervals. All computations are made by the GPS receiver.

The accuracy of this speed measurement method is lower compared to the Doppler derived or carrier phase methods. The accuracy entirely depends on the positional accuracy, which varies from a few centimetres to 20-30 meters or so. As a result, if the speed is low, the positional inaccuracy would provide large speed errors. Also, the accuracy will vary with the time period considered, i.e. the higher the sampling rate, the better the accuracy on a condition of maintaining a constant speed within this interval. Thus, for each segment between two track points, the receiver calculates an average speed over this time period. However, no instantaneous speed information is provided as a result.

In Figure 2-1, the blue track is the straight line projection of the real red track. The length of the blue track is shorter than the red one. Therefore, the straight speed (blue) is different from the real one. In fact, the more the track has a zigzag shape, the bigger the difference between these two values.

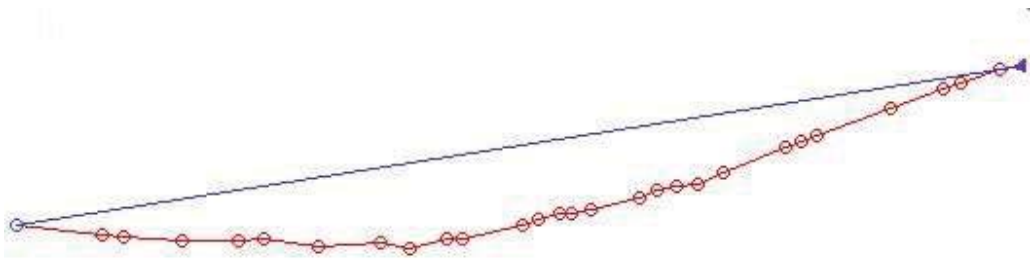

Figure 2-1: Speed through distance over time

In this method, measurements should be done faster to provide higher speed accuracy, otherwise zig-zag movements would result in an error. On the other hand, if the measurements are observed rapidly, say 100 times per second, then positional inaccuracies would come into play. Thus, speed measurements may become totally inaccurate.

These limitations prevent its use in modern GNSS receivers.

2.3 Speed based on Doppler method

People are experiencing Doppler effects in their lives all the time. For example, when people swim against waves rather than with the wave. Another example is when an emergency vehicle drives with a siren and the siren is heard differently depending on whether the vehicle is travelling towards or away from an observer. This is because of the relative speed between two objects, i.e. the person on the one hand and the waves / car on the other. This principle of measurement is shown in Figure 2-2.

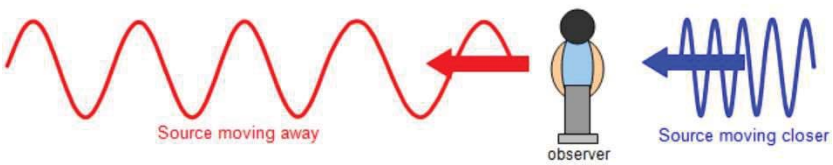

Figure 2-2: Doppler effect

When a source transmitting electromagnetic waves is moving relative to an observer, a frequency shift between the transmitted signal and the received signal will be observed. This effect is known as the Doppler effect and the frequency change is known as the Doppler shift or the Doppler frequency. The Doppler frequency shift speed calculation in GPS receivers is a direct measurement of speed. The L1 carrier frequency of the GPS satellite will appear to be shifted in

frequency by the relative motion between the satellite and the receiver. This is shown in Figure 2-3.

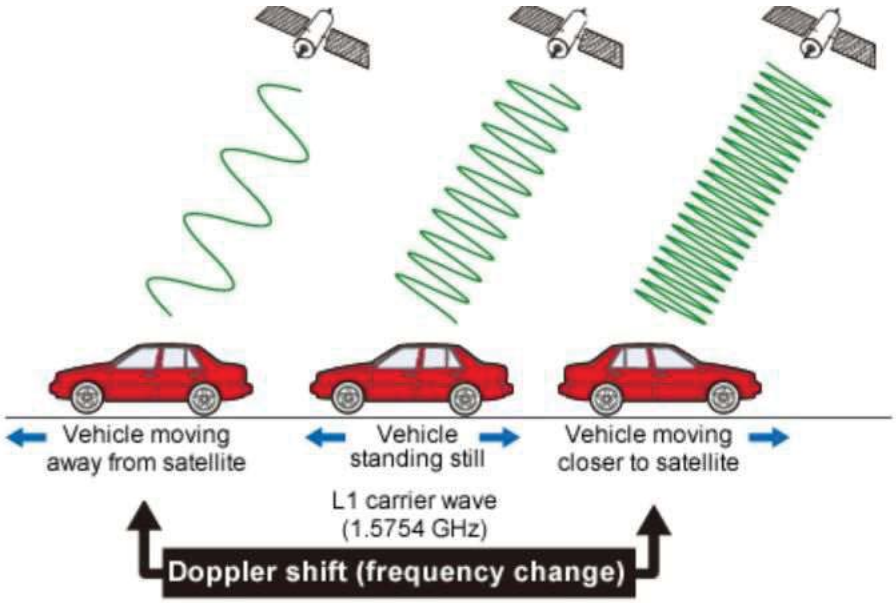

Figure 2-3: Doppler shift and GPS speed measurements (Ono Sokki Co, Ltd 2017)

Since each satellite emits a steady frequency, the different frequencies measured by the GPS receiver are caused by the motion of the receiver, provided that the speed and trajectory of the satellites are well known. Observing several satellites, the GPS receiver can determine its instant speed. This value is accurate according to GPS chipset and receiver manufacturers' documentation and the accuracy could be as good as 0.1 km/h or better (SIRF Technology Inc 2010; NovAtel Inc 2007; Libelium Comunicaciones Distribuidas 2014).

In the context of GNSS, the frequency experienced by the receiver can be represented as (Bahrami 2008),

$$\mathrm{Fr} = \left(1 + \frac{\mathrm{Vradial}}{\mathrm{Vprop}}\right) * \mathrm{F_t} \quad \text{if moving toward; and} \tag{2.2}$$

$$\mathrm{Fr} = \left(1 - \frac{\mathrm{Vradial}}{\mathrm{Vprop}}\right) * \mathrm{F_t} \quad \text{if moving from the receiver,} \tag{2.3}$$

where

- F_t and F_r are the transmitted and received frequencies, respectively;
- V_{prop} is the propagation speed of the waves which equals the speed of light in a vacuum in this context;
- V_{radial} is the relative radial velocity between the signal emitter (i.e. the satellite) and the receiver in the Line-of-Sight (LOS) direction.

Re-arranging the above formula, the Doppler shift can be presented as,

$$\Delta Fr = (Fr - Ft) = \pm (Vradial/C) * Ft = \pm (Vradial / \lambda_{ft}), \quad (2.4)$$

where

- λ_{ft} is the nominal/transmitted frequency wavelength; and
- C is the speed of light.

The above equation confirms that if there is a means to measure the Doppler shift ΔFr, then it is possible to get the radial velocity to a satellite. Subsequently, by forming a system of equations, one should be able to estimate the receiver velocity vector assuming that the satellite velocities can be modelled and well understood.

This Doppler computed speed is commonly used by GNSS receivers to provide instant speed measurements. The receiver provides the raw Doppler measurements that are the direct output of the Phase Lock Loop (PLL) filter (Borio, Sokolova & Lachapelle 2009), as shown in Figure 2-4.

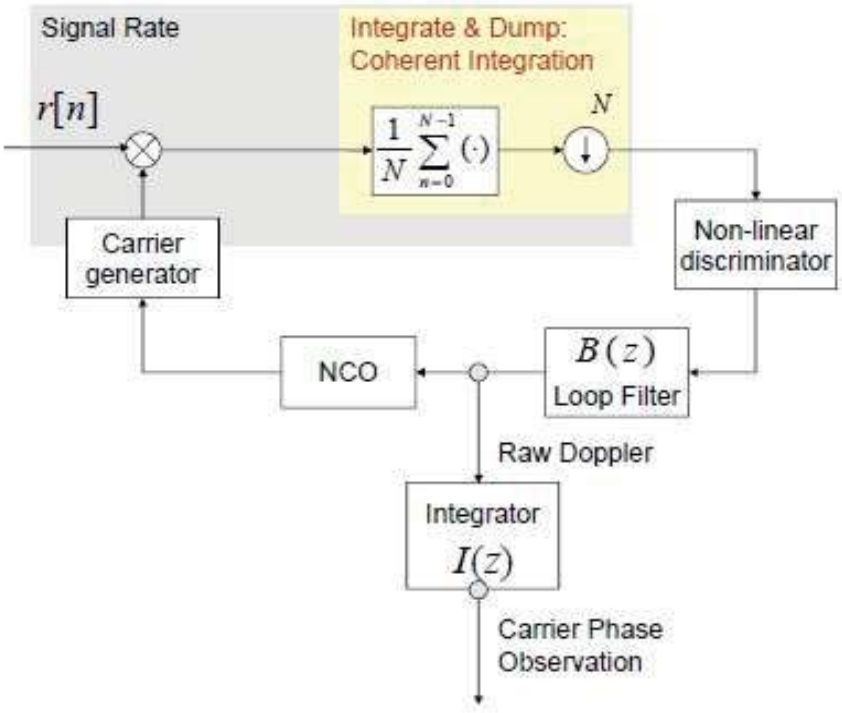

Figure 2-4: Phase lock loop (Borio, Sokolova & Lachapelle 2009)

In Figure 2-4, the Loop Filter output is the raw estimate of the carrier Doppler, and the Integrator's output represents carrier phase observations. The loop filter output is an instantaneous measure produced over a small-time interval, namely the coherent integration time.

The Doppler shift is therefore the frequency difference between the received signal and the source signal. This results from the relative motion between a GNSS receiver and any GNSS satellite. The GNSS receiver in this instance measures the Doppler frequency shift.

2.4 Speed based on the carrier phase method

A carrier phase measurement is the measurement of the phase of the arriving carrier wave signal from the GPS satellite. As the radio signal from a GPS satellite travels from the satellite to the receiver, it completes numerous whole and a fractional number of cycles of oscillation, i.e. the distance is represented by some fractional number of wavelengths, for example, 67 million and 1/2 wavelengths. In this case, the carrier phase measurement gives the fractional value of 1/2 wavelength, or 180 degrees of phase. This in itself has almost no value. However, the GPS chipset can determine the phase change, or the number of wavelengths of distance change, between the satellite and the receiver from one measurement epoch to the next. In this instance, there is a measurement of the change in distance between the satellite and the receiver over a known period of time. Given that the location and velocity of all the satellites are known, the GPS receiver can use this information to calculate the 3D velocity. It is possible to do the same thing with both pseudo-range or Doppler measurements, which the receiver also generates. However, carrier phase measurements have the potential to be more accurate. The following is required to conduct the carrier phase speed calculations:

- raw carrier phase measurement data; and
- GPS broadcast ephemeris to compute the position of all the GPS satellites.

In this process, the receiver clock drift rate may be significant and should also be considered in calculations.

Figure 2-5 represents a visual interpretation of this method considering what is shown in Figure 2-4 and how the PLL operates. The carrier phase measurement of a GPS receiver is actually the integrated Doppler shift measurements (Borio, Sokolova & Lachapelle 2009).

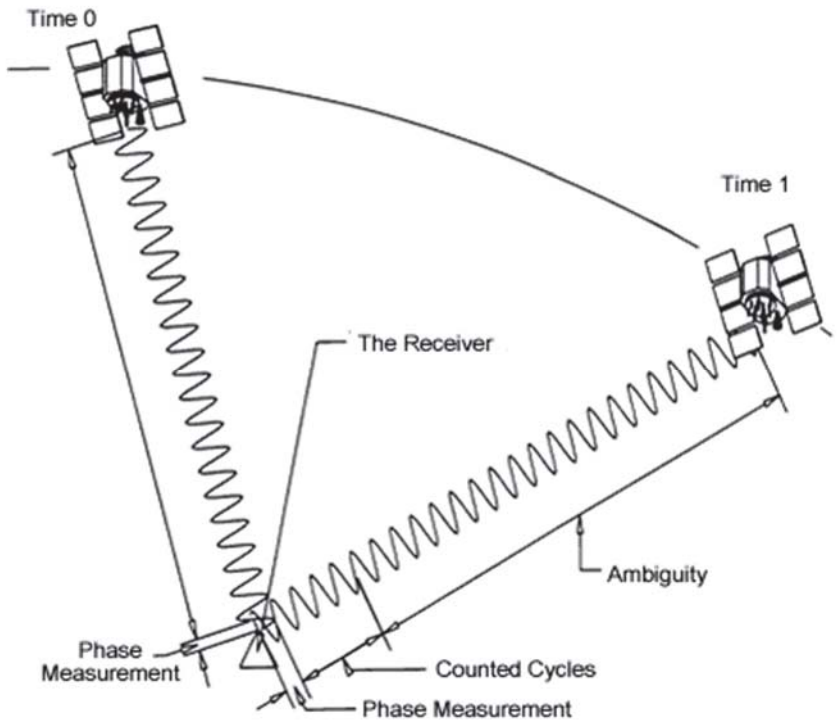

Figure 2-5: Carrier phase method (Perez-Ruiz & Upadhyaya 2012)

2.5 Practical implementation of speed measurements in modern GNSS chipsets

One of the most comprehensive explanations about how GPS chipsets may use several methods to measure speed depending on settings is presented in Table 2-1 (U-blox 2013b; U-blox 2013c).

Table 2-1: Dynamic platform models of U-blox 6 and U-blox 7 (U-blox 2013b; U-blox 2013c)

Dynamic Platform Model

Platform	*Description*
Portable	Default setting. Applications with low acceleration, e.g. portable devices. Suitable for most situations. MAX Altitude [m]: 12000, MAX Velocity [m/s]: 310, MAX Vertical Velocity [m/s]: 50, Sanity check type: Altitude and Velocity, Max Position Deviation: Medium
Stationary	Used in timing applications (antenna must be stationary) or other stationary applications. Velocity restricted to 0 m/s. Zero dynamics assumed. MAX Altitude [m]: 9000, MAX Velocity [m/s]: 10, MAX Vertical Velocity [m/s]: 6, Sanity check type: Altitude and Velocity, Max Position Deviation: Small
Pedestrian	Applications with low acceleration and speed, e.g. how a pedestrian would move. Low acceleration assumed. MAX Altitude [m]: 9000, MAX Velocity [m/s]: 30, MAX Vertical Velocity [m/s]: 20, Sanity check type: Altitude and Velocity, Max Position Deviation: Small
Automotive	Default setting for ADR. Used for applications with equivalent dynamics to those of a passenger car. Low vertical acceleration assumed. MAX Altitude [m]: 6000 (5000 for firmware versions 6.00 and below), MAX Velocity [m/s]: 84 (62 for firmware versions 4.00 to 5.00), MAX Vertical Velocity [m/s]: 15, Sanity check type: Altitude and Velocity, Max Position Deviation: Medium
At sea	Recommended for applications at sea, with zero vertical velocity. Zero vertical velocity assumed. Sea level assumed. MAX Altitude [m]: 500, MAX Velocity [m/s]: 25, MAX Vertical Velocity [m/s]: 5, Sanity check type: Altitude and Velocity, Max Position Deviation: Medium
Airborne <1g	Used for applications with a higher dynamic range and vertical acceleration than a passenger car. No 2D position fixes supported. MAX Altitude [m]: 50000, MAX Velocity [m/s]: 100, MAX Vertical Velocity [m/s]: 100, Sanity check type: Altitude, Max Position Deviation: Large
Airborne <2g	Recommended for typical airborne environment. No 2D position fixes supported. MAX Altitude [m]: 50000, MAX Velocity [m/s]: 250, MAX Vertical Velocity [m/s]: 100, Sanity check type: Altitude, Max Position Deviation: Large
Airborne <4g	Only recommended for extremely dynamic environments. No 2D position fixes supported. MAX Altitude [m]: 50000, MAX Velocity [m/s]: 500, MAX Vertical Velocity [m/s]: 100, Sanity check type: Altitude, Max Position Deviation: Large

Table 2-1 demonstrates that the U-blox GPS chipsets is very flexible in selecting a number of modes of operation to measure speed. However, not all chipsets and GPS receivers allow this. The method of using position records to calculate speed is not used in the U-blox chipset. This is simply because positional inaccuracy parameters would cause errors in speed determination, particularly at low speeds. The Doppler and Carrier Phase methods are flexibly used in the U-blox GPS chipset to provide high accuracy speed determination (Sbisa 2013).

The speed calculation method depends on the chosen dynamic platform (refer to Table 2-1). Some dynamic platforms enable speed calculation based on Doppler only, while others permit the use carrier phase measurements as well (Sbisa 2013). When Doppler measurements are used to calculate speed, then the solution relates to the exact moment when the solution is derived. When carrier phase measurements are used, then the speed solution relates to the mid-time between

the current and the last epoch. This is because the Doppler measurement is a measure of instantaneous speed, whereas a temporal difference of carrier phase is the measure of mean velocity between observation epochs (Hou 2014; Ding & Wang 2011). Thus, at a 1 Hz navigation rate, the speed solution in the carrier phase method relates to the time 0.5 seconds prior to the position solution.

For example, when the speed dramatically changes within one epoch, the delay within one epoch in the speed measurement would be significant (integration effect). For that reason, in case of higher acceleration, U-blox chipsets switch back to the speed measurement based on the Doppler method (Sbisa 2013).

Table 2-2 shows the U-blox 6 GPS chipset default modes of operation depending on the chosen dynamic platform (Sbisa 2013). It should be noted that the chipset automatically changes its default settings using the above approach depending on acceleration.

Table 2-2: Dynamic platforms and speed determination for U-blox 6 GPS chipset (Sbisa 2013)

Platform	**Speed determination via Doppler**	**Speed determination via carrier Phase**
Portable	No	YES
Stationary	No	YES
Pedestrian	No	YES
Automotive	No	YES
At sea	No	YES
Airborne <1g	YES	No
Airborne <2G	YES	No
Airborne <4g	YES	No

Thus, GPS chipsets such as U-blox 6 can provide significant flexibility in the selection of the required method to measure speed. Moreover, depending on the acceleration of the chipset the default mode of operation may change from Doppler based to carrier phase or vice versa.

2.6 The sources of GPS speed errors

Zhang (2007) states that the various methods of speed measurements have the following sources of errors:

- atmospheric interference;
- multipath;
- GPS satellite frequency and velocity errors (United States of America Department of Defence 2008);
- GPS receiver errors related to frequency and phase shift determination.

Atmospheric interference is related to the moisture and ions in the earth's atmosphere which can change the speed at which the satellite radio waves travel. Additionally, the radio waves are bent (refracted) when they enter the earth's atmosphere, which changes the length of the path the radio signal takes to get to the receiver.

Atmospheric errors are usually greater for satellites in the low horizon. Therefore, some GPS receivers allow the user to mask satellites below a set angle (refer to Figure 2-6). For many receivers, the mask angle is implemented with 5° above the horizon as default. For more advanced receivers used in this research, the angle varied between 5° and 15° in different experiments. The effects of mask angle on speed measurement accuracy will be studied in chapter 7.

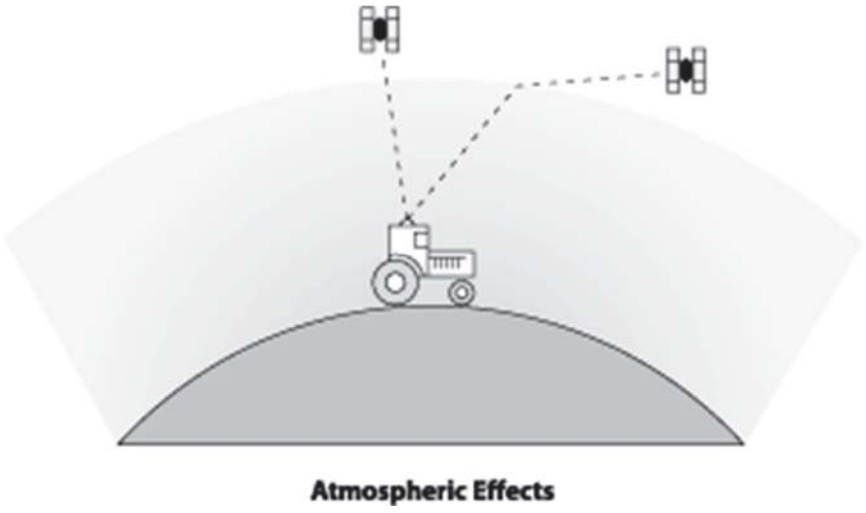

Figure 2-6: Atmospheric errors

Multipath means that the same radio signal is received several times through different paths. For instance, a radio wave could leave a satellite and travel directly to the receiver, but also bounces off a building and arrives at the receiver later. The most common causes of multipath are buildings, overpasses and road gantries. With advanced antenna-filtering techniques, some GPS receivers might be less prone to multipath errors.

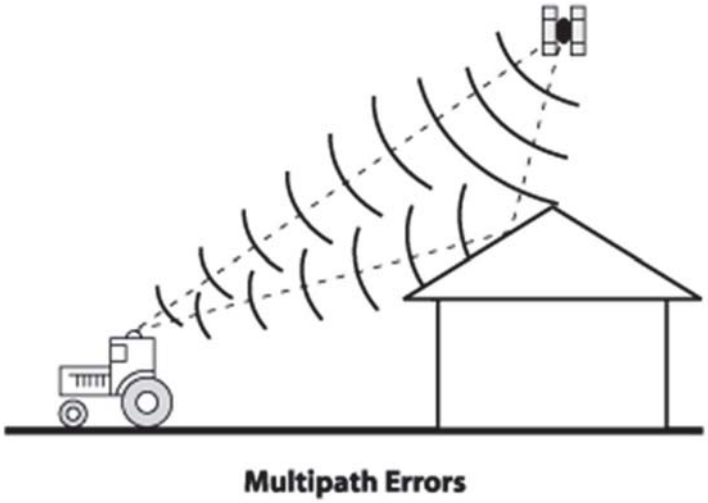

Figure 2-7: Multipath related errors

Even though all the errors should be considered, it appears that multipath (refer to Figure 2-7) may represent the most severe error source.

Typically, GPS satellites have rubidium clocks which are used to generate signals for the Doppler speed measurements. Any deviation of frequency in such clocks contributes to errors in speed measurements. However, such errors are typically much lower compared to multipath and the atmospheric errors. In addition, satellite velocity may not be constant and such errors would also influence the determination of Doppler shifts. Again, such errors are typically much lower compared to multipath and atmospheric errors (United States of America Department of Defence 2008).

GPS receiver errors related to frequency and phase shift determination are linked to the receiver's ability to operate as a frequency counter. The Doppler shift and the carrier phase are measured by first combining the received frequencies with the nominally constant reference frequency created by the receiver's oscillator. The difference between the two frequencies is the so-called beat frequency, and the number of beats over a certain timing interval is known as the Doppler count for that interval (John A Dutton e-Education Institute 2017). Since the beats can be counted much more precisely than their continuously changing frequency can be measured, most GPS receivers just keep track of the accumulated cycles, i.e. the Doppler count. The sum of the consecutive Doppler counts from an entire satellite pass is often stored, and the data can then be treated like a sequential series of biased range differences. In this process, the nominally constant reference frequency is generated within the GPS receiver and therefore its variations influence the magnitude of errors. However, modern GPS receivers usually have precise crystal oscillators as sources of such frequencies. Therefore, the errors due to multipath or atmospheric interference are much larger than errors caused by frequency variations in GPS receivers (Zhang 2007).

In this project, all receivers under test used the same method of speed determination, i.e. the Doppler derived method.

3 DESIGN OF A SPEED MEASUREMENT SYSTEM FOR GPS/GNSS TESTING

3.1 Analysis of existing speed measurement systems

Speed is typically measured as distance over time. A number of speed measurement devices and systems use this principle, although there are some devices which use completely different speed measurement techniques. Speed measurement systems may be classified as follows:

- Systems measuring distance covered by a test vehicle within a specific timeframe and subsequently calculating speed. The distance measurements are conducted via sensors installed on a test vehicle's wheel or some other rotating parts which move proportionally to speed. Such sensors do not belong to the vehicle's original electronics.
- Systems measuring distance based on optical technologies, for example, the Correvit-L400 (Corrys Datron Sensorsystems GmbH 2008), where such systems use their internal timing to calculate the speed output.
- Systems based on radar technologies.
- Systems receiving speed data from the existing speed / distance sensors already installed on a vehicle.

Each system has various advantages and disadvantages. Therefore, its suitability to test GPS receivers for speed accuracy may vary.

3.1.1 Speed via distance over time

Systems measuring speed via distance over time usually have sensors. These are often in the form of a Shaft Encoder (Encoder in further text), temporarily or permanently connected to a shaft of a vehicle's wheel (Eitel 2014; Viswanathan 2005). Such Encoders have been widely used in the automation industry for many years to measure the rotation of shafts installed on different machine tools at the manufacturing facilities. Typical examples of such applications can be found in Dyukov (1988, 1990). Shaft Encoders have also been used in the automobile industry. In speed applications, the Encoder effectively measures the ground distance which is then converted into speed by a microcontroller. The use of Encoders in such applications is common practice. For example, in Viswanathan (2005), the speed measurement system is described based on the Dynapar encoder producing 200 pulses per revolution of a wheel. As the wheel rotates, multiple pulses are produced by the Encoder and the number of pulses is directly proportional to the actual distance covered by the vehicle. A distance reading is recorded at specific timing intervals, e.g. every second.

The basic principle of the Encoder operation is shown in Figure 3-1. The Encoder is an electro-mechanical device that converts the angular position or motion of a shaft or axle to a digital code

or a series of pulses. There are two main types of Encoders: absolute and incremental (relative). The output of an absolute Encoder indicates the current position of a shaft, making it an angle transducer. The output of an incremental Encoder provides information about the motion of the shaft, which is typically further processed into information such as speed, distance, and position. In Figure 3-1, as the wheel rotates, the light from the light source is interrupted multiple times and therefore a photo detector produces a series of pulses. This number is then converted into speed because the timing intervals are known and the number of pulses produced by the encoder per one rotation is also known.

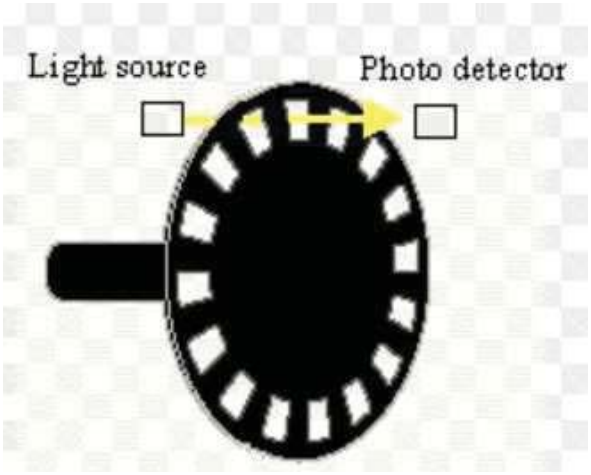

Figure 3-1: Basic principle of operation for the Encoder (Eitel 2014)

The main advantage of this method is that it is possible to synchronise the output speeds of the test vehicle with Universal Coordinated Time (UTC) once the microcontroller is synchronised with UTC. This, however, would typically require an in-house design because no commercial products are available which are capable to provide such synchronisation.

The disadvantage of this method relates to tyre pressure variations and the changing circumference as the tyres wear. These may cause less accurate readings or reference errors depending on the speed. Therefore, the test vehicle must be calibrated before the test and checked after the test to ensure that calibration was maintained. Also, the accuracy parameters of the test vehicle need to be well analysed and understood. This includes speed accuracy fluctuations depending on variations in tyre pressure.

3.1.2 Speed via optical technologies

Systems measuring speed via optical technologies are based on optical speed sensors. An example of such a system is the Correvit system (Corrys Datron Sensorsystems GmbH 2008) whose optical sensors are manufactured by Kistler Corrys Datron. Such speed sensors represent a major refinement in the evolution of measurement technology. Since the introduction of the

world's first optical speed and distance sensor in 1981, Corrys have worked continuously to bring increasingly high levels of accuracy and repeatability to non-contact measurement of dynamic variables including speed, distance, angle and height. An example of Correvit sensor is shown in Figure 3-2.

Technical Data

Performance Specifications		SFII	SFII-P
Speed range [1]	km/h	0,3 ... 250	
Distance resolution	mm	2,08	
Measurement accuracy [2]	%FSO	<±0,5	
Angle range	°	±40	
Angle resolution [3]	°	<±0,1	
Meas. accuracy angle [3]	°	<±0,5	
Meas. frequency	Hz	250	
Working distance and range	mm	180 ±50	

Signal Outputs		
Output Dig1 – IVI	pulses/m	1 ... 1 000/TTL
Output Dig2 – V_I	pulses/m	1 ... 1 000/TTL
Output Dig3 – V_q	kHz	0 ... 46/TTL
Output Dig4 – angle	kHz	0 ... 46/TTL
Output Ana1 – IVI	V	0 ... 10
Output Ana2 – V_I	V	0 ... 10
Output Ana3 – V_q	V	–10 ... 10
Output Ana4 – angle	V	–10 ... 10

Figure 3-2: Parameters of Correvit (Kistler 2014)

These optical sensors utilise a high-intensity light source to illuminate the measurement surface, while the optical sensor observes the stochastic microstructure of the surface via an objective lens. The acquired optical signal is then projected onto a periodic prismatic grating within the system, where it is multiplied as details of the surface microstructure move across the grating. Resultant spatial frequencies are integrated over the sensor field to generate a correlated average value.

A setup of the Correvit system can be seen in Figure 3-3 (Jankovic et al, 2012):

Figure 3-3: Installation of Correvit (Jankovic et al 2012)

The electronic signal-processing component of the system utilises tracking filters to determine the representative centre frequency. This is derived by calculating a mean value based on the variance in the frequency spectrum. The representative centre frequency allows reliable counting of signal periods, which are directly proportional to the distance that the observed surface has travelled.

The advantage of speed measurement systems based on optical sensors is their high accuracy of measuring speed with typical errors less than 0.5% of the actual speed value. The second advantage is that the speed error does not depend on tyre pressure.

The disadvantage of such speed measurement systems is that they measure speed autonomously based on their own timing and output speed measurement either through RS232 or by other means. Therefore, there is no synchronisation with UTC timing. Secondly, and more importantly, calibration of such systems is very complex and requires special facilities and methodologies (Lopez, Solva & Ruiz 2014). Considering that the speed tests in this research were to be conducted multiple times, it was not feasible to calibrate the Correvit system externally several times a year or build a calibration facility. Lastly, such devices as the Correvit are very complex and cost more than $20,000 to purchase.

3.1.3 Speed via radar technologies

Speed measurement systems based on radar technologies are well known. They work on the principle of reflected radar waves from the ground while a vehicle is moving (Dybedal 2013). Ground speed sensor Radar II from Dickey-John Corporation is an example of a radar based sensor, see Figure 3-4:

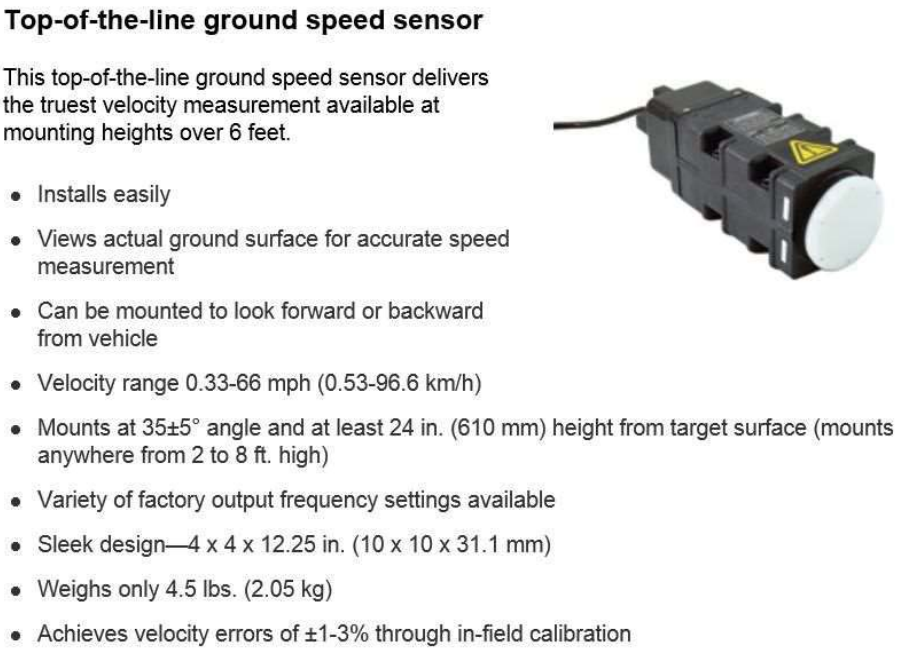

Figure 3-4: Speed sensor Radar II (Dickey John Corporation 2014)

These sensors operate using the Doppler principle when the generated and transmitted microwaves are reflected with a frequency shift. This shift occurs due to movement between the transmitter / receiver installed on a test vehicle and the target object, which is the ground in this instance. The difference between the transmitted and the reflected frequencies is known as the Doppler effect. The sensor then determines the frequency of the reflected signals and compares it with that of the generated signal. The difference is proportional to the vehicle speed.

The Doppler frequency can be calculated as shown:

$$F_d = (2V\cos\theta)/\lambda \qquad (3.1)$$

where

- F_d is the Doppler frequency (Hz);
- V is velocity of the vehicle (miles per second);
- λ is wavelength of the transmitted signal (miles);
- θ is an angle between the ground and the sensor (degrees).

The Dickey-John Radar II, for example, works on a 24.125 GHz ± 25 MHz microwave frequency with micro power level of 5 mW. The second example is the Stalker Pro II Speed Sensor Radar (Applied Concepts 2016) which operates at 34.6 GHz frequency and provides speed measurement accuracy of ±0.3%, as claimed by the manufacturer.

All speed measurement systems based on radar technology have either Personal Computer (PC) applications available for configuration and data downloading capabilities or ports like an RS232 to download the data in real time.

The disadvantages of radar based systems are:

- The accuracy depends on the surface on which a vehicle is travelling.
- Maintaining the mounting angle is critical to their accuracy (Viswanathan 2005).
- The speed output is not synchronised with UTC. Therefore, the synchronisation should be conducted at the PC level. In this case, the PC will obtain GPS data from the receivers under test plus the speed records data from the radar and then record them simultaneously. Such synchronisation, however, poses questions about the traceability of the results. This is because the PC will obtain several data streams which are not synchronised with each other.

3.1.4 Systems using embedded vehicle sensors

Systems measuring speed using existing speed sensors installed in vehicles are well known and represent digital speedometers. Such speedometers obtain data from sensors already installed in the vehicles. These sensors typically produce a certain number of pulses proportional to the actual speed. For example, the SDS detector (Ballinger Technology 2015) is produced in Australia and is a digital speedometer used by the police departments nationally (see Figure 3-5).

Figure 3-5: SDS detector (Ballinger Technology 2015)

The SDS detector has a four-digit LED speed readout and a status indicator which is visible in direct sunlight. The speed lock switch allows checked speeds to be locked into the display. Alternatively, the speed values can be transmitted to a PC.

The specified accuracy of such devices is about ±2 km/h. The SDS detectors conduct measurements over a 2 second period with a 0.5 second display update rate. One second update rate optional.

The SDS detector can be calibrated on a pre-surveyed straight section of the road, in which the distance is accurately pre-determined. Alternatively, a calibration might be conducted on a Dynamometer. In the latter case, the wheels of a vehicle would be forcefully rotated at a known speed level and the frequency of rotation is proportional to speed and controlled.

The disadvantage of these systems is their low accuracy. With a speed accuracy of ±2 km/h, it is not possible to accurately test GNSS receivers for speed as the test vehicle should be at least as accurate as the GNSS receivers under test, or better. The second disadvantage is that the speed output is not synchronised with UTC. Therefore, the synchronisation should be conducted on a PC where GPS data from the receivers under test plus SDS detector data are recorded simultaneously. Again, this approach poses questions regarding metrological traceability of the results.

3.1.5 Selection of a system configuration for the research

Systems based on radar technology and existing speed sensors are not suitable to test GNSS receivers for speed accuracy. This is mainly because of accuracy issues and the un-reliability of the operation across multiple road surfaces.

Systems based on optical technologies are suitable to test GNSS receivers from the accuracy point of view. However, their cost is high as well as the calibration is costly and requires specific installations (Lopez, Silva & Ruiz 2014). Considering that calibration needed to be conducted before each test and not just annually, then the use of optical systems may not be viable. Lastly, these systems require synchronisation with UTC. This action may be achieved via a PC which downloads data from the speed measurement system and the GNSS receivers under test. Such synchronisation, however, is complex. In terms of the metrological traceability it requires a guarantee of an exceptional timing match between all speed records from all devices under test as well as the test vehicle.

Therefore, in this research it was decided to design and build an in-house speed measurement system based on the methodology of “speed via distance over time”.

3.2 Hardware components in the speed measurement system

3.2.1 Speed measurement system operating in speed mode

Modern GNSS chipsets which represent an integral part of GNSS receivers usually have a minimum sampling and processing rate of at least 1 Hz. Such output rate allows GNSS equipment

to determine and report speed almost continuously. This sampling rate poses a requirement on how the speed measurement system of a test vehicle should operate.

Firstly, speed records produced by the test vehicle should be time synchronised with UTC.

Secondly, GNSS receivers represent very accurate speed measurement devices based on manufacturer's specifications. Therefore, there is a challenge to create a speed measurement system that should be at least as accurate as the receivers, and preferably better. As the speed of the vehicle represents a reference speed for comparison purposes, the accuracy of the reference speed must be well estimated via appropriate UOM techniques. Also, the test vehicle should be calibrated and preferably driven with all GNSS receivers on the same day immediately after calibration; and subsequently checked at the end of the test on the same day.

To address the issue of synchronisation with UTC, the adopted speed measurement system of the test vehicle must obtain time synchronisation via UTC using National Marine Electronics Association (NMEA) data strings (NVS Technologies AG 2012) produced by a high end geodetic quality GNSS receiver. Timing synchronisation of a specific device or system with UTC is well known in principle (National Coordination Office for Space Based Positioning, Navigation and Timing 2014; Bies 2016; Zhao 2015). Based on this general approach, a specific electronic diagram was developed to synchronise the speed records of the test vehicle with UTC. Figure 3-6 represents the structure of the speed measurement system of the test vehicle working in speed measurement mode.

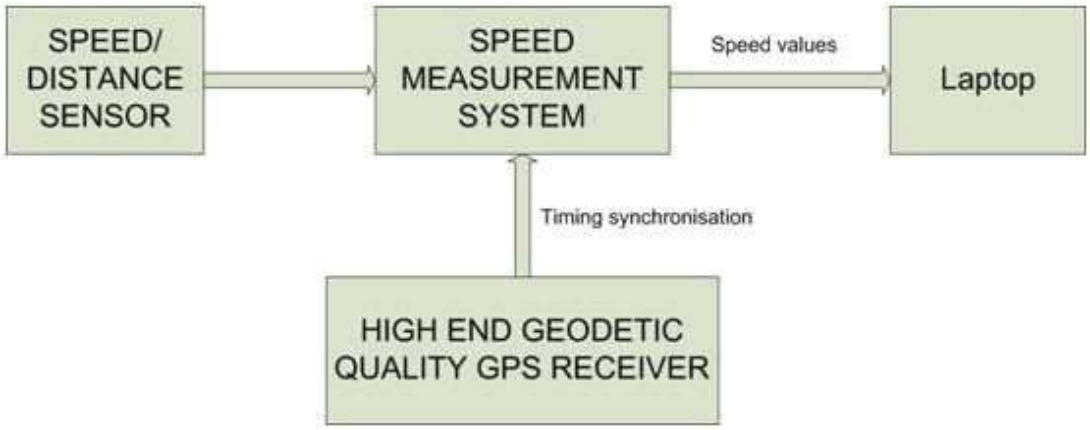

Figure 3-6: Speed measurement system working in speed mode

The principle of obtaining timing synchronisation by the speed measurement system is explained below.

A high end geodetic quality GNSS receiver produces data in NMEA format, where every $GPRMC string has UTC timing information. For example, the following string shows this timing in

yellow as 215035, which is equal to 21 hours 50 min 35 sec, then the next timing string shows 215036, which is equal to 21 hours 50 min 36 sec, and so on.

$GPRMC,215035.00,A,3741.1775371,S,14501.3474342,E,48.378,278.2,070795,0.0,E*76
$GPGSA,M,3,30,13,04,01,07,15,17,28,,,,,2.1,1.3,1.7*32
$GPGSV,3,1,10,28,65,166,49,13,55,260,48,17,55,001,48,30,50,080,49*7D
$GPGSV,3,2,10,15,22,228,45,07,21,066,44,11,20,117,,01,17,096,45*7C
$GPGSV,3,3,10,04,10,124,41,05,00,300,*79
$GPGGA,215036.00,3741.1757,S,14501.3306,E,1,08,1.3,105.94,M,5.37,M,,*42
$GPRMC,215036.00,A,3741.1757014,S,14501.3306458,E,48.521,277.8,070795,0.0,E*74
$GPGSA,M,3,30,13,04,01,07,15,17,28,,,,,2.1,1.3,1.7*32
$GPGSV,3,1,10,28,65,166,49,13,55,260,48,17,55,001,48,30,50,080,49*7D
$GPGSV,3,2,10,15,22,228,45,07,21,066,43,11,20,117,,01,17,096,43*7D
$GPGSV,3,3,10,04,10,124,41,05,00,300,*79
$GPGGA,215037.00,3741.1739,S,14501.3137,E,1,08,1.3,105.84,M,5.37,M,,*4A
$GPRMC,215037.00,A,3741.1738602,S,14501.3137255,E,48.751,277.3,070795,0.0,E*78

The task of the microcontroller of the speed measurement system is to determine the presence of each $GPRMC string and derive the timing from the string. This timing would then be used by the speed measurement system to output a previous speed reading and to start the next speed measurement cycle. In this way, the speed records of the test vehicle would then also be in synchronisation with UTC and the receivers under test.

The above approach enables synchronisation of the speed measurement system with NMEA records produced by the GNSS receivers. It is important to note that if GNSS signals are totally unavailable, NMEA messages from a high end geodetic quality GNSS receiver would be generated based on the internal clock of the receiver. Therefore, the measurements would not be interrupted. In any case, the speed measurement system obtains a string of NMEA data every second and the logging interval is determined by this time. At the start of every second the speed measurement system immediately completes the previous speed measurement and then starts the logging interval for the next measurement. Within the logging interval the speed measurement system counts pulses from the Encoder installed on a wheel. In this research, the Encoder is represented by an industrial shaft encoder WDG 58H manufactured by German company Wachendorff Automation GmbH & Co (Wachendorff Automation GmbH & Co 2013). This Encoder produces 2048 pulses per revolution of the rear wheel. Installation of the Encoder is shown in Figure 3-7 where the Encoder is visible. Before each test the Encoder itself has been covered to protect it from the direct sunlight and rain.

Figure 3-7: Installation of the Encoder WGD 58H on Mazda 3

The speed measurement system uses an internal calibration coefficient to convert the number of pulses from the Encoder into speed records. These are produced every second in synchronisation with UTC. A screenshot of an example of the logged speed records of the test vehicle is shown in Figure 3-8.

```
TIME 224437.0   SPEED 85.7 km/h
TIME 224438.0   SPEED 83.8 km/h
TIME 224439.0   SPEED 82.9 km/h
TIME 224440.0   SPEED 83.4 km/h
TIME 224441.0   SPEED 84.2 km/h
TIME 224442.0   SPEED 85.0 km/h
TIME 224443.0   SPEED 85.4 km/h
TIME 224444.0   SPEED 85.7 km/h
TIME 224445.0   SPEED 86.0 km/h
```

Figure 3-8: Format of speed records

As a result, the speed measurement system, based on a microcontroller, also has a sampling rate of 1Hz. The various GNSS receivers under test generally have the same sampling rate or higher and are therefore fully synchronised with the test asset. This approach addresses the issue of synchronising the speed records between the speed measurement system and the GNSS receivers under test.

The Speed / Distance data logger represents a laptop with the software to download the data from the speed measurement system. The software is called *Terminal* (Terminal 2013). This software works with an RS232 port and is a freeware package available from the Internet. The Terminal's screenshot is shown in Figure 3-9.

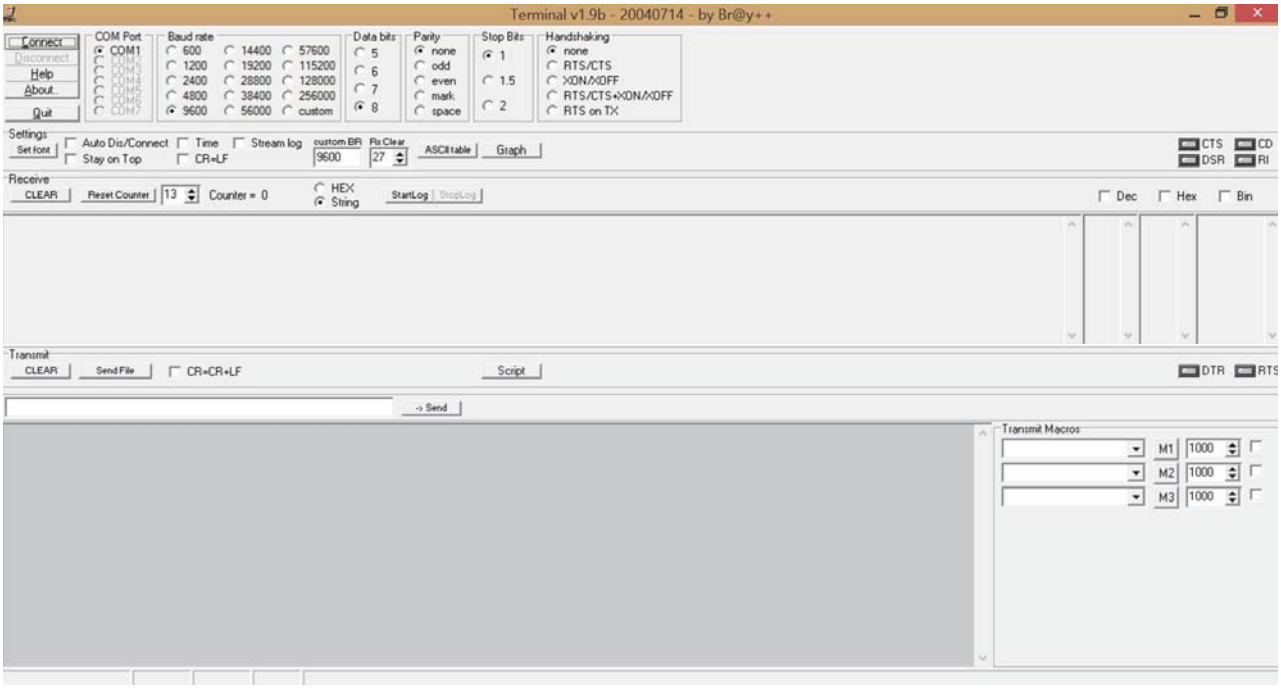

Figure 3-9: Terminal software screenshot

This software was used for downloading both speed records from the speed measurement system and the NMEA data from the GNSS receivers under test. The receivers had either an RS232 or a USB port. In the case of using a USB, a converter was required. In addition, this software was used to issue commands to the speed measurement system and load the Calibration Factor plus other parameters into the speed measurement system.

The speed over ground is determined by the speed measurement system as follows. The Encoder, which is robustly connected to a wheel, sends pulses to the microcontroller of the speed measurement system. The number of pulses is 2048 per revolution of the wheel. This number of pulses is then required to be converted into distance measurements and subsequently to speed measurements. The real ground speed is determined by applying the following calculation:

$$Speed\ (km/h) = 3.6\ Speed\ (m/sec) = (3.6 * (pulses\ per\ sample) * (samples\ per\ sec)) / (Calibration\ Factor) \quad (3.2)$$

The Calibration Factor is represented in pulses per meter generated by the Encoder. Equation (3.2) was adopted considering a conversion of speed from km/h into m/sec plus representing m/sec via pulses per sample and the Calibration Factor. In (3.2), the pulses per sample parameter is the number of pulses calculated by the speed measurement system for a sample timing interval in seconds. It should be noted that for one second interval, a value of (pulses per sample)*(samples per second) is equal to pulses per second, i.e. frequency of the Encoder's signal.

Therefore, speed in m/sec can be presented as

$$\frac{Frequency\ (\frac{pulses}{\sec})}{Calibration\ Factor\ (\frac{pulses}{m})} \quad (3.3)$$

Then, (3.2) for speed can be transformed into:

$$Speed\ (km/h) = 3.6\ Speed\ (m/sec) = 3.6 * Frequency/(Calibration\ Factor) \quad (3.4)$$

The Calibration Factor is a constant in the firmware of the microcontroller for the speed measurement system. This constant can be changed during calibration before the test to adjust the output to the right speed. Essentially the Calibration Factor is a divider of pulses from the Encoder. The Calibration Factor is measured in pulses per meter.

In this project, a Mazda 3 vehicle was used. Mazda 3 typically has 195/65 R15 tyres and the tyre circumference was specified to be equal to 1993 mm, i.e. 1.993 m or 0.001993 km. Therefore, for the specific Encoder installed on this vehicle the parameters specified in Table 3-1 would ideally apply if the tyre circumference was 1993 mm. It is highly unlikely that the real tyre circumference would be equal to 1993 mm. Therefore, the task of calibration was to determine a value of the Calibration Factor, which would correspond to the real tyre circumference for the testing date.

Table 3-1: Information to calculate the draft calibration factor

Encoder pulses per revolution	**Pulses per meter**	**Distance per pulse (depends on the wheel) for R15 tyre, m**
2048	948.90	0.0009733 m

Changes in tyre circumference are compensated during the calibration each time before the test so that the accuracy of the test vehicle remains at the highest standard. This process is described further below in this chapter and chapter 4 related to the UOM.

An example of using the Calibration Factor to calculate the actual speed:
During one second the Encoder produced 26546 pulses. With Calibration Factor of the Encoder equal to 922.4, the speed of the test vehicle would be calculated as,

$$V=3.6*26546/922.4 = 99.7\ km/h$$

The speed measurement system in speed mode operates in a way that for every second, which is in synchronisation with UTC, the number of pulses from the Encoder is counted. Thus, for each second the speed calculation is conducted using the Calibration Factor. The calculated speed is

transmitted to the output at the end of every second in synchronisation with UTC, and the next speed measurement starts immediately after such transmission.

3.2.2 The speed measurement system operating in calibration mode

It is important to maintain high accuracy of speed measurements for the test vehicle. This is addressed through a separate calibration of the distance and time measuring diagrams of the speed measurement system. Such calibration provides an assurance that the test vehicle meets the desired UOM parameters. Also, a thorough UOM analysis was conducted in this research to assess the magnitude of errors attributed to the speed measurement system.

3.2.2.1 Calibration of the distance measurement

In general, the calibration of test vehicles for speed can be conducted in two methods:

- The direct speed calibration when a speed dynamometer is used (Mainline 2014). With chassis dynamometers, the operator could manually set the desired speed and the vehicle will be held at that point regardless of throttle position. Such speed could be controlled in increments as small as 0.1 km/h. Getting frequent access to such calibration facilities for this research was challenging, particularly considering that calibration had to be conducted before each test drive and every visit would cost several thousand dollars.
- Conducting calibration of test vehicles through separate calibration of distance and time measurement diagrams. This method is widely used in engineering practice with differences seen in engineering solutions. Because of the advantages of this method, such as low cost, high calibration accuracy and many others, it was selected in this research.

The principles of distance calibration as a component of speed calibration are described in numerous sources. In Polar (2016), the calibration of a device was conducted using two surveyed points. In ASTM International Standards Worldwide (2010), a test method was described for speed and distance calibration of a fifth wheel. In Austroads (2012), a surveyed test strip of 500 m was used for road distance test with the results migrating into a road speed indicator test. In Queensland Police Service (2016), the calibration of speed detection devices via distance calibration bases was also described.

The calibrations of the distance measurement in this research were conducted before and after each test to ensure that the speed measurement system maintained the prescribed accuracy limit of the test. At the start of this research, a distance calibration site was surveyed. This site represented a straight section of a side road with a surveyed distance of 361.3 m as shown in Figure 3-10. This site was surveyed with an Electronic Distance Measurement device Leica FlexLine (Leica Geosystems AG 2013) provided by RMIT, to the accuracy better than 0.002 m. Two measurements were conducted during a survey to the above accuracy. However, a final distance value has been rounded to one decimal point. This is because the resolution of the

speed measurement system, when it operates during calibrations in distance measurement mode, equals 0.1 m. This would be shown in chapter 4.

The Leica FlexLine was calibrated with legal traceability to the national distance reference standards. This provided a chain of traceability for the speed measurement system with respect to distance measurements. The surveyed section of the road was located in the Noble Park area in Melbourne, Australia. It is parallel to Princess Hwy, has almost no traffic and represents a straight road (see Figure 3-11). The factors of a quiet and straight road are important in this instance, as it will be a challenge to conduct calibrations on busy streets. During the distance calibrations, the test vehicle was driven from one surveyed point A to the second surveyed point B with the speed measurement system working in calibration mode.

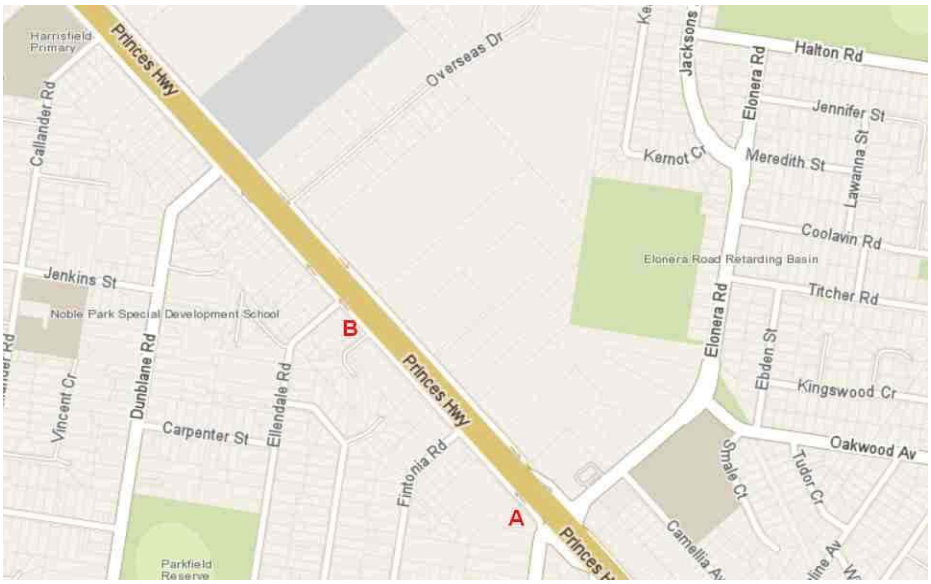

Figure 3-10: Calibration site

Figure 3-11: Calibration site view (Princess Hwy is to the right)

A diagram depicting the calibration mode for the distance measurements is shown in Figure 3-12.

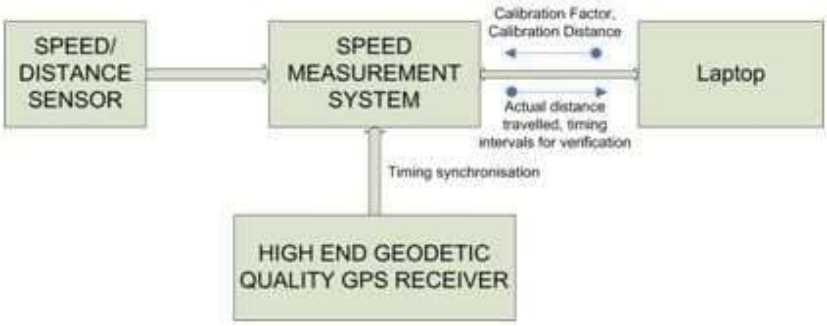

Figure 3-12: Speed measurement system in calibration mode

Before the field calibration, it was required to calculate an expected Calibration Factor. To do so, the following were considered:

- The driving distance for calibration is 361.3 meters and this distance was surveyed.
- The information from Table 3-1 about the number of pulses produced per meter and the distance travelled per pulse from the Encoder.
  It should be remembered that the Encoder produced 2048 pulses per revolution of a wheel.
- The information that the tyre circumference is 1.99334 meters for Mazda 3. Mazda 3 has 195/65R15 tyres and ideally their circumference can be determined based on Tyre Size Calculator (2014). It is required to know this value relatively precisely to establish a draft calibration factor before conducting calibrations.

Within the calibration procedure, the actual tyre circumference would be taken into consideration. At the start of the first calibration, an expected (draft) value of the Calibration Factor was used as input into the speed measurement system.

Considering that the distance was 361.3 m and the number of pulses produced by the Encoder per meter was 948.9, ideally the total number of pulses counted (N) for the calibration run should be,

$$N=\text{Distance} * \text{Calibration Factor} = 361.3 * 948.9 = 342837$$

Therefore, before the start of calibration a command to the speed measurement system was issued through the *Terminal* software, advising that the speed measurement system should start working in calibration mode. Subsequently, the speed measurement system uploaded via the *Terminal* software an expected Calibration Factor of 948.9 and the driving distance of 361.3 m.

Then, at point A (see Figures 3-10 and 3-13) of the calibration track, a command was issued to the speed measurement system from the laptop advising that the calibration drive was about to start, while the vehicle was in stationary mode.

Figure 3-13: Starting point of the distance calibration

The test vehicle was driven from the starting point A of the calibration site to the end point B. At point B, the test vehicle was stopped and a command issued through the *Terminal* software to the speed measurement system advising that the required distance was passed. During the drive from A to B the speed measurement system was working in the calibration mode and the pulses from the Encoder were counted. Then, the calculation of the distance was based on the expected Calibration Factor of 948.9 and the actual distance passed by the front wheel. At point B, where the front wheel reaches a specific mark on the ground the system, the test vehicle would be

stopped. At point B, therefore, the speed measurement system would calculate two values and send them back to the laptop:

- The calculated distance based on the Draft Calibration Factor.
  Each rotation of the wheel produced 2400 pulses per revolution and hence the distance was not measured down to single numbers but rather to numbers with decimal points.
- The correct (recommended) Calibration Factor, which shall be loaded into the system.
  This parameter was calculated by the speed measurement system based on the known distance of 361.3 meters and the actual measurement result shown by the speed measurement system for this distance.

The calculated distance was determined by the speed measurement system as,

$$D_{calc} = N / Draft\ Calibration\ factor \tag{3.5}$$

The recommended Calibration Factor was calculated based on the distance of 361.3 meters and the number of counted pulses N as,

$$Calibration\ Factor = N / D_{known} \tag{3.6}$$

Example 1.

The test vehicle was initially loaded with the Draft Calibration Factor of 948.9. Then a vehicle was driven from A to B and the microcontroller counted N=343900 pulses for the distance of 361.3 meters. At the end of the drive at point B the microcontroller would count the proposed correct Calibration Factor as,

Calibration Factor = 343900 / 361.3 = 951.8

This correct Calibration Factor would then be loaded into the speed measurement system through the Terminal software. A calibration drive then starts again to check the correctness of this Calibration Factor. If the recommended Calibration Factor was correctly calculated, the new calibration drive would show a better match of the distance covered. Generally, if the distance error was within 0.4 m (see chapter 4 for details as to why 0.4 m is the value selected as tolerance), then the calibration was complete. The recommended Calibration Factor was finally confirmed and permanently recorded in the EPROM of the microcontroller until the next calibration. This means that the recorded Calibration Factor was applied for the test run and this

also considers the actual tyre parameters, such as the tyre circumference and pressure, for the day of calibration and testing. This provided a higher accuracy of the test vehicle.

With this new Calibration Factor the speed was then determined in km/h as,

$$V=(3.6*N)/951.84 \quad (3.7)$$

where N is the number of pulses counted by the microcontroller within every 1 sec of measurements.

Example 2.

It was required to recalculate the correct Calibration Factor manually based on distance measured by the speed measurement system during a calibration drive.

A calibration drive was conducted for the Encoder producing 2048 Pulses Per Revolution (PPR) of a wheel and the actual distance of 361.3 meters. The system showed 362.5 meters measured with the Calibration Factor equal to 948.9 pulses per meter. It was required to determine the recommended Calibration Factor manually without the help of a microcontroller.

The following procedure could then be adopted:

- calculate a draft circumference of a wheel as,

  PPR / Calibration Factor = 2048 / 948.9 =2.158 m

- calculate the actual number of revolutions a wheel had during a calibration drive as

  Distance Measured / Draft Circumference = 362.5 / 2.158 =167.979 revolutions

- calculate a real circumference of a wheel using the same number of revolutions as

  Surveyed Distance / Actual Number of Revolutions = 361.3 / 167.979 =2.150 m

- calculate a recommended Calibration Factor as

  PPR / Real Circumference = 2048 / 2.15 = 952.5 pulses per meter.

Subsequently, it was required to upload the recommended Calibration Factor to the speed measurement system and repeat the drive to confirm that the value of Calibration Factor was correct.

Example 2 was not used in practice because the microcontroller of the speed measurement system calculated everything automatically following the procedure described in this example. This example simply demonstrated how the microcontroller normally handled this.

The distance calibration was traceable to national standards via surveyed distance measured with a calibrated surveying instrument such as Leica which was also verified through a distance calibration at a standard baseline.

In case of using any other EDM Unit, the calibration procedure still provides a complete traceability of distance calibration for the speed measurement system if such EDM Unit is traceable to national standards. For example, to provide a traceability to national standards, a different EDM Unit can be calibrated through any baseline which has such traceability. For example, the EDM might be calibrated by the National Measurement Institute (NMI) to the uncertainties as follows (National Measurement Institute 2015):

Calibration class 1.10 Survey and alignment equipment
Calibration subclass .08 Electronic distance measuring equipment
Electronic distance measuring instruments with least uncertainties of measurement of -
0.14 mm to 0.22 mm in the range 2 to 130 m;
0.25 to 0.49 mm in the range 20 to 650 m.

3.2.2.2 Calibration of the timing component of the speed measurement system

The timing calibration (verification) was conducted in this research with the use of a specific diagram as shown in Figure 3-14. This diagram was designed, assembled and implemented in this research.

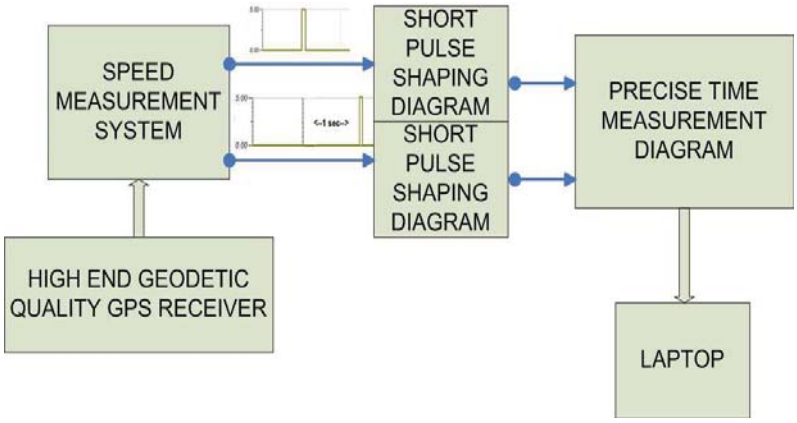

Figure 3-14: Timing calibration diagram

Even though the timing was obtained from NMEA messages received from a particular GNSS receiver, it was necessary to check the accuracy of timing. This was to ensure that the pulses from the Encoder were measured within the 1 sec interval ± an acceptable error. The value of this acceptable error can be described in the UOM. Even if timing in UTC is derived from a GNSS receiver and linked to UTC, there are processing delays present across the speed measurement system's schematic. Therefore, such calibration simply verifies that these delays are not outside the prescribed limits.

The speed measurement system in any mode, including calibration, outputs short pulses from the microcontroller. Such pulses constitute the start of the new measurement (Figure 3-14) and the end (Figure 3-14). The measurement cycle of the microcontroller to count the Encoder's pulses is shown in Figure 3-15. The cycle diagram was created using a website http://www.wavedrom.com.

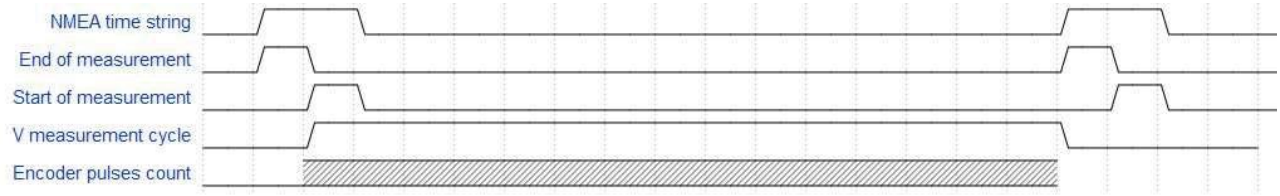

Figure 3-15: Measurement cycle

When a new NMEA, containing time, is received by the microcontroller, it initially completes a speed calculation for a previous measurement by launching a process upon a front of the "End of measurement" pulse (see Figure 3-15). The microcontroller also generates a corresponding short pulse on the relevant output. Subsequently, the microcontroller sends the calculated speed value to the output microchip of the microcontroller board and starts a new measurement upon the front of the "Start of measurement" pulse (see Figure 3-15). The same "Start of measurement" pulse launches a process of generating a corresponding short pulse on the relevant output. Therefore, the timing interval between the "Start of measurement" and "End of measurement" pulses should be close to 1 sec. This is because this interval is determined by the neighbouring NMEA data strings in synchronisation with UTC and a deduction of the microcontroller's time to count / output the result of a previous measurement. Thus, the timing interval between these two short pulses is used by the microcontroller to count high frequency pulses from the Encoder (see the V measurement cycle timing interval in Figure 3-15). Effectively, the same timing interval is measured during calibration to ensure that this interval sits within acceptable limits. This is because it determines the time used by the speed measurement system to count pulses from the Encoder.

A specific microchip called the Universal Frequency to Digital Converter (UFDC-1) was selected to conduct this time measurement. This microchip has a high accuracy in various modes of operation, including the time measurement mode (International Frequency Sensor Association 2004). The microchip interacted with a laptop via RS232 using the *Terminal* software to log these timing intervals in microseconds. The diagram of using the microchip UFDC-1 for time measurements is shown in Figure 3-16. A complete connection diagram for the UDFC-1 is shown in Appendix A.

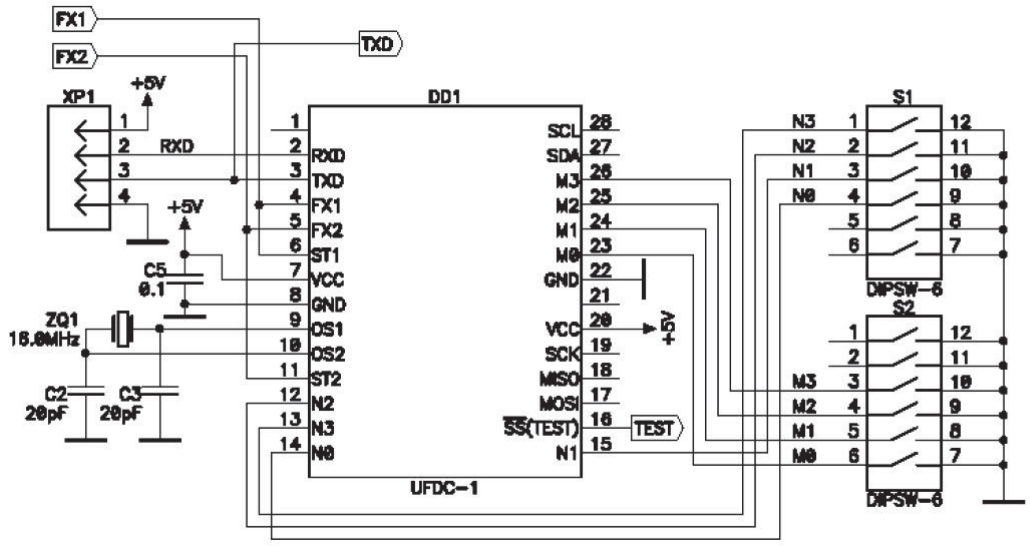

Figure 3-16: Typical UFDC-1 connection diagram (International Frequency Sensor Association 2004)

In the above diagram, inputs FX1 and FX2 were used for obtaining two timing signals which characterise the start and end of each 1 sec measurement. The UFDC-1 converted the time interval between these timing signals into digital data using mode 3 as shown in Figure 3-17.

M3	M2	M1	M0	Mode	Name	Mode No.
0	0	0	0	Frequency (channel 1), f_{x1}	FX1	0
0	0	0	1	Period (channel 1), T_{x1}	TX1	1
0	0	1	0	Phase-shift, φ_x	Fi	2
0	0	1	1	Time interval between start- and stop-impulse, τ_x	T	3
0	1	0	0	Duty-Cycle, *D.C.*	D.C.	4
0	1	0	1	Duty-Off Factor, *Q*	Q	5
0	1	1	0	Frequency difference with sign determination f_{x1}-f_{x2}	FD	6
0	1	1	1	Period difference with sign determination T_{x1}-T_{x2}	TD	7
1	0	0	0	Frequency ratio, f_{x1}/f_{x2}	FR	8
1	0	0	1	Period ratio, T_{x1}/T_{x2}	TR	9
1	0	1	0	Rotation speed (rpm), n_x	n	10
1	0	1	1	Pulse width, t_p	tp	11
1	1	0	0	Space interval, t_s	ts	12
1	1	0	1	Pulse number (events) count, N_x	N	13
1	1	1	0	Frequency (channel 2), f_{x2}	FX2	14
1	1	1	1	Period (channel 2), T_{x2}	TX2	15

Figure 3-17: Modes of operation for UFDC-1 (International Frequency Sensor Association 2004)

The timing interval values from the UDFC-1 would be transferred to a laptop via the RS232 converter microchip MAX232 series (see Appendix A). The unit of measurements for this conversion result is microsecond.

The timing calibration is achieved by verifying that the 1 sec timing interval of speed measurement is within the prescribed limit to maintain an appropriate UOM. This timing interval cannot be changed

through any settings as it depends on two factors: the 1 sec UTC from NMEA data strings and the speed of microcontroller's operation. However, verification of this timing interval is still required for metrological purposes and guaranteeing that the UOM of the speed measurement system is within the prescribed limits. Usually the measurement time sits within 0.999996 sec and 0.999998 sec because some time is lost when the microcontroller interrupts the measurement upon the NMEA data string, outputs the result of the previous cycle and then starts the new cycle of speed measurement.

As described by the International Frequency Sensor Association (2004), the measurement interval for timing for the UFDC-1 can vary between 2 microseconds and 250 seconds.

The assembled time calibration circuit based on the UFDC-1 microchip is shown in Figure 3-18.

Figure 3-18: Printed circuit board of the timing calibration circuit in the box

Figures 3-14 and 3-15 have previously shown that, in terms of methodology of timing calibration, the accuracy of time measurements depends on the microchip UFDC-1. This microchip typically uses a crystal of 16.0 MHz for the microchips' own operation and the Specification and Application Note for UFDC-1 (International Frequency Sensor Association 2004) confirms that the conversion error (E) in this mode depends on the converted values and can be calculated using the following equation:

$$E = \left(\frac{1}{16000000 * Time}\right) * 100\% \qquad (3.8)$$

where

- E is the conversion error;
- Time is the value of time measured.

Thus, for 1 sec, the conversion error is equal to 0.00000625% and so characterises a precise time measurement.

However, it is necessary to ensure that such measurements conducted by the UFDC-1 are traceable to national standards. In this instance, the accuracy of UFDC-1 measurements should be assessed against the devices having traceability to national standards via a chain of calibrations. For example, a calibrated pulse generator can be used to check the accuracy of the UFDC-1 time measurements. This is easily achievable with the use of an instrument such as the Agilent 81100 Pulse Generator which has two outputs with the capability to provide pulses with a calibrated known delay between them (Agilent 2009). Subsequently, this delay would be measured by the UFDC-1 and the results would demonstrate the error introduced by it in the time measurements.

The calibration diagram for the UFDC-1 itself as designed in this research is shown in Figure 3-19:

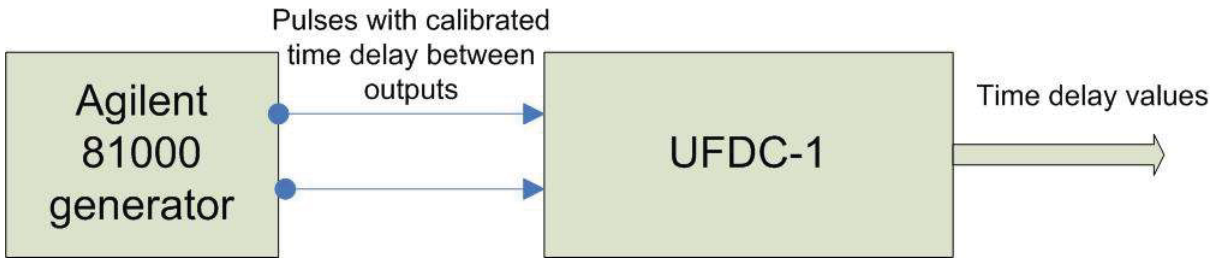

Figure 3-19: Calibration of UFDC-1 with traceability to national standards

Therefore, if the Agilent 81000 generator is calibrated with traceability to national standards, the timing calibration approach will also be.

Calibration of the speed measurement system for distance and time measurements provides an assurance that the test vehicle is accurate in terms of speed measurements. Calibration also provides a basis for the assessment of the UOM of the speed measurement system. This then ensures that it is capable to test GNSS receivers for speed measurement. See Appendix A for further information about the UFDC-1 microchip.

3.2.3 Microcontroller board

Speed measurement system is based on a Peripheral Interface Controller microcontroller (further PIC microcontroller as named by Microchip Technology which produces such microcontrollers) and is shown in Figure 3-20.

Note. This board was used in the tests.

Figure 3-20: PIC Microcontroller board

The microcontroller's Printed Circuit Board (PCB) represents a PICDEM HPC Explorer board based on PIC18F8722 microcontroller (Microchip Technology Inc 2006a). This microcontroller offers 128kBytes of flash program memory, together with 4kBytes of data memory or SRAM. The standard microcontroller feature includes two enhanced addressable Universal Asynchronous Receiver / Transmitter (UART) modules supporting RS232 interface, one of which is directly connected to RS232 socket installed on the board and the second may be utilised with a MAX232 microchip which is installed on this board by soldering it.

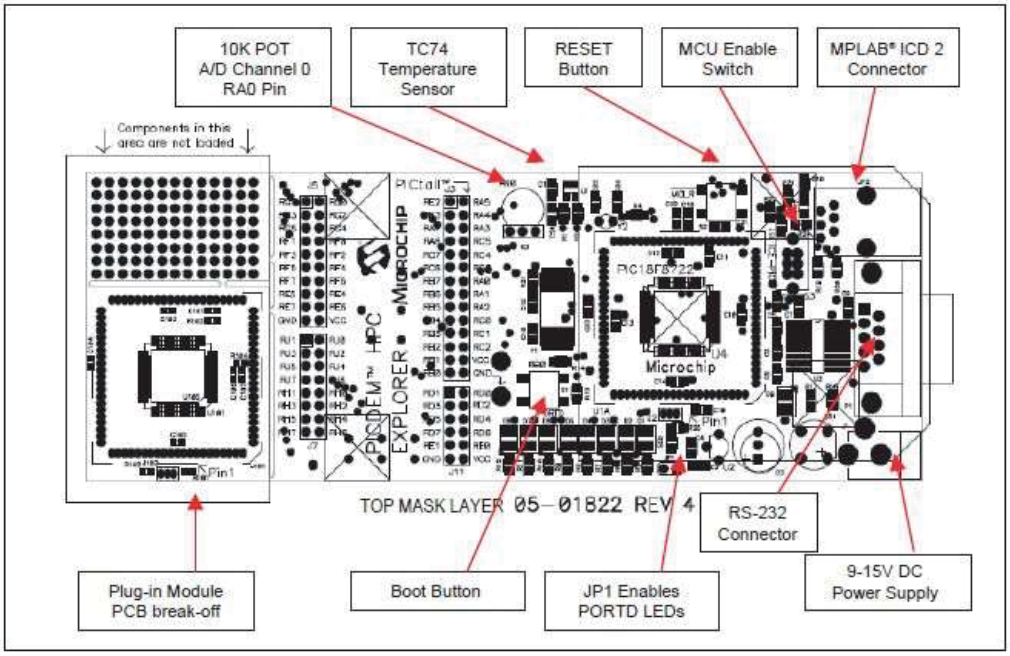

Figure 3-21: PCB parts placement diagram of the microcontroller (Microchip Technology Inc 2006a)

The PIC18F8277 PCB features an in-circuit program download for easy program modification and easy to use programming tools. The board has an MPLAB connector which allows a working program to be loaded into the microcontroller and kept in its Electrically Erasable Programmable

Read-Only Memory (EEPROM). A specific Run / Programming switch exists on the PCB and the Programming mode is selected to program the microcontroller. The programming mode is designed for high voltage programming mode for the PIC range of microcontrollers. Programming pins are then effectively isolated by switching the switch to RUN operation; the pins can then be used for inputs / outputs. Therefore, when a slide Switch position (PROG / RUN) is selected as PROG Position, the programming of the microcontroller occurs. Once the microcontroller is programmed, the switch can be moved to the RUN position and the microcontroller will commence to run the downloaded program. Programming of the microcontroller is conducted only at the stage of program development when the firmware embedded into the microcontroller is put in place and bugs are eliminated.

Basic features of the firmware are described below in section 3.3 of this thesis Firmware of the Speed Measurement System.

As soon as the program of the microcontroller works correctly, there is no need to use the PROG / RUN switch. Every time the power is on, the microcontroller's board would start its normal operation in a speed measurement mode.
The designed speed measurement system hardware diagram is shown in Figure 3-22.

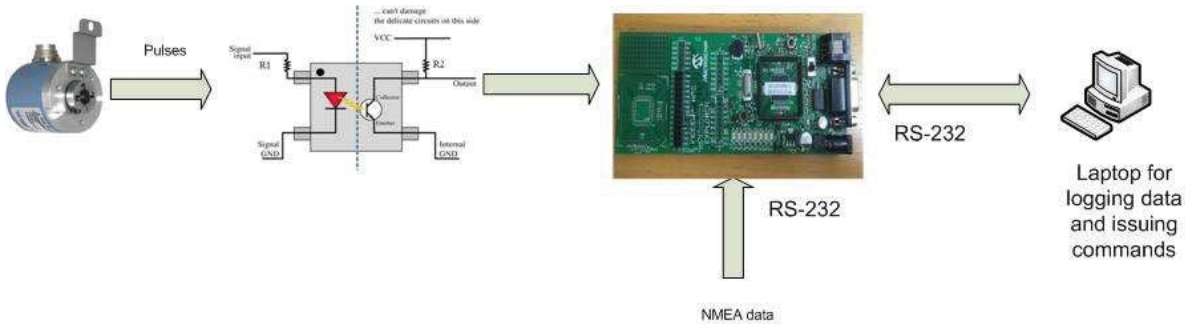

Figure 3-22: High level hardware diagram of the speed measurement system

In speed measurement mode, the Encoder installed on a wheel of Mazda 3 sends pulses through the optocoupler to the microcontroller. The number of pulses per second is proportional to speed and some other factors, such as the circumference of a wheel, the accuracy of the timing interval of 1 sec, etc., which are all taken into consideration in the Calibration Factor. The optocoupler (Vishay Semiconductors 2010) isolates the sensor from the microcontroller's diagram. This isolation is done for several reasons. The first reason is that the PIC microcontroller board has its internal own power supply and its ground is not the same ground as the ground of power feeding the board. The internal power supply on the PCB of the microcontroller itself has limited power and cannot provide power to the Encoder as a result. Therefore, the Encoder gets its own power from a separate power supply which has a separate ground as a result. Connecting the PCB's ground to the ground of the power supply of the Encoder would mean interfering with the PCB's

proper operation. Secondly, for devices staying apart from each other in an unknown electromagnetic environment, represented by the test vehicle and its wiring, it is safer to electrically isolate them from each other from the signal perspective and safety points of view. This is a good practice which is applied across many areas where electronic devices operate in electromagnetic environments. Electromagnetic noise is generated by numerous parts of a vehicle such as the ignition system, fuel pump, starter motor, spark plugs, battery charging circuit and many others. Such sources of electromagnetic noise are powerful enough to disturb electronic diagrams, which are not properly protected. The use of optocouplers is one of the methods to protect the speed measurement system from such electromagnetic noise.

The PIC microcontroller's PCB gets NMEA data via RS232 port from the geodetic quality GNSS receiver and derives timestamps from each $GPRMC string. For every 1 sec of speed measurements in synchronisation with UTC, the microcontroller counts the number of pulses from the Encoder and determines speed values based on the Calibration Factor. Such speed values are logged every second to a laptop using the Terminal software. The operator may interact with the PCB within calibration to send commands and receive calibration data. Communication with the PCB with the laptop is bi-directional, although in speed measurement mode the data would be sent only from the PCB to the laptop.

3.2.4 Encoder

The Encoder installed on the rear wheel of the test vehicle Mazda 3 was WDG 58H (Wachendorff Automation GmbH & Co 2013). It is a rugged industrial standard encoder which had a relatively high protection class IP65 and able to operate from -40^0C up until $+80^0$C. This Encoder is produced by Wachendorff Automation GmbH & Co in Germany.

The Encoder was fixed to a shaft, which was rigidly connected to a wheel, see Figures 3-23 and 3-24, and protected with a plastic case from rain and direct sunlight in a way shown in Figure 3-25.

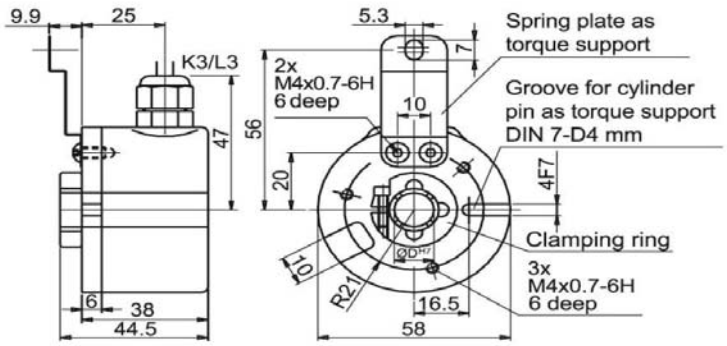

Figure 3-23: Dimensions and installation details of the Encoder (Wachendorff Automation GmbH & Co 2013)

Such types of encoders can produce up to 25000 pulses per revolution. However, the higher number of pulses is not necessarily translated in higher speed accuracy because the calibration accuracy depends on other factors, which will be detailed in chapter 4. Therefore, a particular modification of Encoder was selected with a capability to produce 2400 pulses per revolution. This represents a compromise between accuracy of speed measurements and errors due to high frequency signals distributed through a custom wiring.

Figure 3-24: Encoder WDG 58H (Wachendorff Automation GmbH & Co 2013)

Figure 3-25: Full installation of the Encoder on Mazda 3 with sunlight / rain protection

The plastic cover which protected the Encoder allowed some airflow inside so that the Encoder would not fail from high temperatures. Wiring for the Encoder included 5V power supply and output wires, which were fixed in a safe manner as per the above picture and followed to the cabin to be connected to the microcontroller of the speed measurement system.

3.3 Firmware of the speed measurement system

To load a working program into the microcontroller, it was required to connect the PCB of the microcontroller to a PC and use the specific proprietary software or Microchip's software MPLAB (Microchip Technology Inc 2006b). It is possible to develop programs in any language such as PIC Assembly, PicBasic Pro or C for the microcontroller. PicBasic Pro was used in this research (MicroEngineering Labs Inc 2005). Subsequently, the high-level program developed in PicBasic Pro was converted into a standard PIC hex code by MPLAB. The MPLAB is available as a free download from the Microchip website and allows writing and compiling the programs.

Once the code has been successfully compiled and no errors existed, the code was then downloaded to the microcontroller board. Figure 3-26 shows the operation of preparing a program in this research.

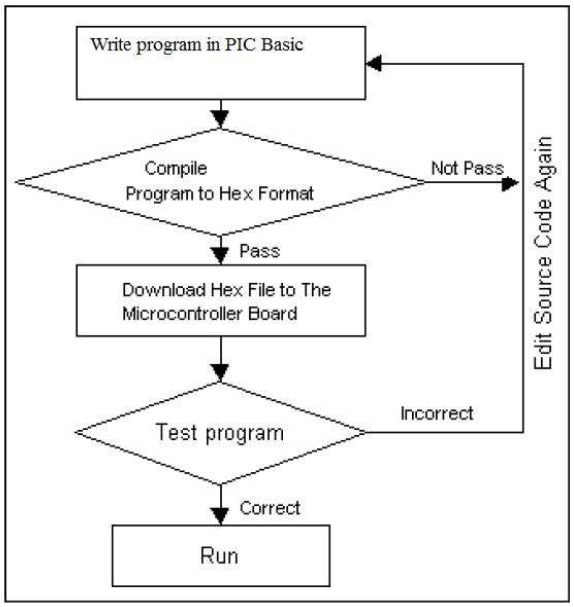

Figure 3-26: Creating a program

Algorithm of operation of the firmware in the designed speed measurement system is shown in Figure 3-27. This is the developed high-level algorithm, which was then translated into PicBasic commands of the actual program.

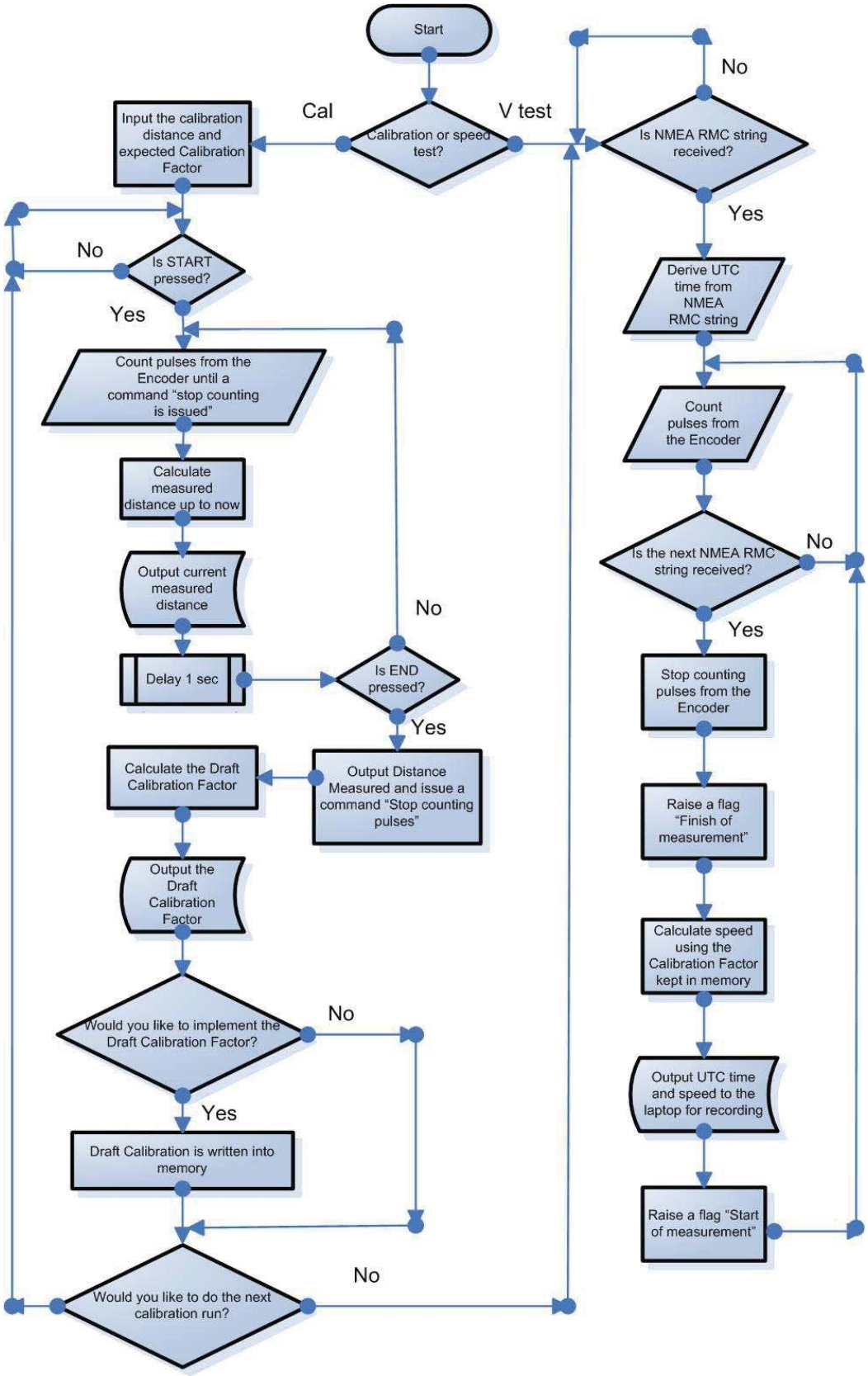

Figure 3-27: Algorithm of the firmware loaded into the microcontroller

The firmware can determine whether the speed measurement system is in calibration or speed measurement mode through an operator's response to this question.

When in calibration mode, the operator calculates and inputs a draft Calibration Factor and the calibration site distance, which equals 361.3 m in this research. The speed measurement system is hardcoded to use the Encoder with 2400 pulses per revolution and, therefore, as soon as the command START is issued when the test vehicle is at the start of the calibration track, the system starts counting pulses from the Encoder and outputting a current up to now distance as soon as the test vehicle keeps driving. At the same time, the system monitors if the operator issues a command END. Upon receiving the command END, the system knows that the test vehicle has reached a distance of 361.3 meters and stopped. At this point, the system displays the distance that was passed based on the draft Calibration Factor loaded earlier. If the result is suitable and within tolerance, the operator confirms that the Calibration Factor is correct and it is recorded and kept in microcontroller's memory. The operator still requires conducting the second run to ensure that the distance measured sits within the prescribed limits. If after the next run there is no need to change the Calibration Factor, the system goes into speed measurement mode getting a command from the operator. If the Calibration Factor is unsuitable, the operator would have several iterations in the process described above until the point when the test vehicle measures 361.3 meters with a suitable tolerance, which equals to 0.4 m (see chapter 4).

In the speed measurement mode, the microcontroller derives timing data from each NMEA $GPRMC string. As such strings are coming with a frequency of 1 sec, with each subsequent string the system stops counting pulses from the Encoder and then raises a flag "Finish of measurement". This flag represents a pulse equal to one working cycle of the microcontroller. Then the system calculates the speed based on the number of counted pulses within one second and Calibration Factor kept in microcontroller's memory. Immediately after that the speed measurement system outputs both the UTC and speed values to the laptop. Subsequently, the firmware raises a flag indicating the start of a new measurement. This measurement takes place until the next NMEA $GPRMC string comes in. The actions of speed calculation and outputting data take several cycles of the microcontroller's operation and effectively this is the time which provides a difference between the ideal 1 sec of measurements and the real measurement time. Considering that the microcontroller PIC18F8722 works with 10 MHz frequency oscillator, which is used with an internal PLL to provide 40 MHz of operational frequency, this time difference between the ideal 1 sec and the real measurement time is typically no more than 20 microseconds, providing a timing error of measurements no more than 0.002%. Obviously, the quicker the microcontroller operates, the smaller the timing error is; however, it is still taken into consideration in the UOM budget when a combined uncertainty of measurements for the test vehicle is calculated.

Therefore, in the speed measurement mode the system outputs UTC and speed data for every second and speed records are in full synchronisation with UTC.

Summary

This Chapter presented a detailed description of the following:

1. Detailed analysis of the existing methods and systems of the test vehicles used to measure speed.
2. Description of the designed speed measurement system, including its hardware and firmware components.
3. Technical solution for synchronising the microcontroller of the speed measurement system with UTC.
4. Determination of the Calibration Factor for the speed measurement system through the calibration process and the calibration site.
5. Calibration diagram and the processes of calibrating the speed measurement system for distance and timing.

4 UNCERTAINTY OF MEASUREMENTS OF THE SPEED MEASUREMENT SYSTEM

4.1 Background

Measured values are imperfect and the measure of imperfection is called Uncertainty. The UOM is a parameter, associated with the result of a measurement, that characterises the dispersion of the values that could reasonably be attributed to the measurand. The measurand is the particular quantity being measured, e.g. the speed of a vehicle.

The true value is a hypothetical quantity and is the value resulting from a perfect measurement. The error of a measurement is the difference between the measured value and the true value.

The UOM is the range, centered on the measured value, with an associated confidence level, which is often selected as 95%. This percentage means 5 chances in 100 that the true value is outside the range.

It is important not to confuse the terms ‘error’ and ‘uncertainty’. *Error* is the difference between the measured value and the ‘true value’ of the measurand. *Uncertainty* is a quantification of the doubt about the measurement result.

As the reference value of speed would be produced in this research by the speed measurement system, knowing the UOM for the speed measurement system is important for several reasons. The first is that GNSS speed records are expected to be accurate, therefore good quality measurements from the test vehicle are important. Secondly, making good quality speed measurements requires calibration of the speed measurement system and this is where the UOM is critical. Lastly, during the information processing stage, the UOM of the speed measurement system would be taken into consideration for making conclusions when the GNSS speed measurement is outside of the expected boundaries and subsequently the outliers are generated.

Uncertainties generally come from the following sources (Metrology Training International Pty Ltd 2005):

- The measuring instrument - instruments may have multiple sources of errors, such as: systemic errors, errors because of ageing, wear and tear, timing drift, noise and many others.
- The item measured may have random errors in the form of noise of the measured signal. It would be further shown that GNSS speed records also have random noise even in ideal static conditions.

- The measurement process can make it difficult to make a measurement. For example, if there is no full synchronisation of GNSS speed records with the test vehicle. This is a source of uncertainty associated with difficulties in measurement.
- ‘Imported’ uncertainties when calibration of an instrument has an uncertainty which is then embedded into the uncertainty of the actual measurements. Imported uncertainty is an uncertainty which typically comes from calibration sources. The calibration UOM of the speed measurement system would be imported as a parameter into speed measurement UOM when the actual speed tests are conducted.
- Operator skill**.** Some measurements may depend on the skill and judgement of the operator, particularly when measurements are conducted by non-digital equipment.
- Sampling issues. Measurements should be representative of the process under assessment.
- The environment**:** humidity, temperature, air pressure, etc.

In many measurements, often the values are more likely to fall near the average rather than further away. This is typical for a *normal* distribution. When the measurements are evenly spread between the highest and the lowest values, this would represent a *rectangular* distribution. More rarely, distributions may have other shapes, such as; triangular, M-shaped, etc. It is important to understand the types of distributions when it comes to individual UOM components.

4.1.1 Typical steps to calculate the uncertainty of measurements

To calculate the UOM, the sources of UOM must be first identified. Then, an estimation of the size of the uncertainty from each source should be conducted. Finally, the individual uncertainties are combined to give an overall value.

There are two approaches in estimating individual uncertainties: ‘Type A’ and ‘Type B’ evaluations (Metrology Training International 2006). In most measurement situations, uncertainty evaluations of both types are needed. Type A evaluations are uncertainty estimates using statistics, usually from repeated readings. Type B evaluations are uncertainty estimates from any other information. This could be information based on experience in conducting measurements, information derived from calibration certificates or manufacturer’s specifications, from published information or calculations and even from common sense.

Eight main steps are in place for the UOM evaluation (Metrology Training International 2005):
1. Decide what is needed to be determined from measurements and what measurements and / or calculations are required to produce the result.
2. Carry out the measurements required.
3. Make the UOM model using the UOM techniques.

4. Estimate the uncertainty of each individual component that feeds into the final UOM result and express all uncertainties in similar terms, i.e. calculate standard uncertainties.
5. Decide whether the errors of the input quantities are not connected to each other. If this is not the case, some extra considerations and assessments should be carried out.
6. Find the combined standard uncertainty from all the individual sources.
7. Express the uncertainty in terms of a coverage factor, together with a size of the uncertainty interval, and state a level of confidence.
8. Record the measurement result and the UOM.

4.1.2 Standard uncertainty

All contributing uncertainties should be expressed at the same confidence level, by converting them into standard uncertainties. A standard uncertainty is a margin whose size can be thought of as 'plus or minus one standard deviation'. The standard uncertainty describes the uncertainty of an average (not just about the spread of values). A standard uncertainty is usually shown by the symbol *u*, or *u(y)* (the standard uncertainty in *y*).

When a set of several repeated readings has been taken (for a Type A estimate of uncertainty), the mean, (*x)* , and the estimated standard deviation, (*s)*, can be calculated for the set. From these, the estimated standard uncertainty, *u*, of the mean is calculated using (4.1) (Cook 2002):

$$u = {}^{s}/_{\sqrt{n}} \qquad (4.1)$$

where *n* is the number of measurements in the set. The standard uncertainty of the mean is also called the standard deviation of the mean, or the standard error of the mean.

4.1.3 Combining standard uncertainties

Individual standard uncertainties calculated by Type A or Type B evaluations are typically combined by 'summation in quadrature', also known as 'root sum of the squares'. The result of this is called the combined standard uncertainty, shown by uc or uc(y).

4.1.4 Coverage factor k

Having scaled the components of uncertainty consistently, to find the combined standard uncertainty, re-scaling the result might be required. The combined standard uncertainty may be thought of as equivalent to 'one standard deviation', but it might be required to have an overall uncertainty stated at another level of confidence, e.g. 95%. This re-scaling can be done using a *coverage factor k.* Multiplying the *combined standard uncertainty, (uc)* , by a *coverage factor* gives a result which is called the *expanded uncertainty* (Cook 2002), usually shown by the symbol *U,* i.e.

$$U = k*uc \quad (4.2)$$

A particular value of the coverage factor gives a particular confidence level for the expanded uncertainty. Most commonly, the overall uncertainty is scaled by using the coverage factor k = 2, to give a level of confidence of approximately 95%. (k = 2 is correct if the combined standard uncertainty is normally distributed). This is usually a fair assumption, but it is worth noting this assumption. Some other coverage factors (for a normal distribution) are:

- k = 1 for a confidence level of approximately 68%;
- k = 2.58 for a confidence level of 99%;
- k = 3 for a confidence level of 99.7%.

4.1.5 Uncertainty budget

It is useful to summarise the uncertainty analysis or 'uncertainty budget' (Cook 2002). A simplistic example of such budget is shown in Figure 4-1 for the process of determination how long a piece of string is. As shown, the UOM budget shall have several components listed, such as: the sources of uncertainty and their respective values, types of distribution for each source with corresponding divisors and values of standard uncertainty for each component.

Source of uncertainty	Value ±	Probability distribution	Divisor	Standard uncertainty
Calibration uncertainty	5.0 mm	Normal	2	2.5 mm
Resolution (size of divisions)	0.5 mm*	Rectangular	√3	0.3 mm
String not lying perfectly straight	10.0 mm*	Rectangular	√3	5.8 mm
Standard uncertainty of mean of 10 repeated readings	0.7 mm	Normal	1	0.7 mm
Combined standard uncertainty		Assumed normal		6.4 mm
Expanded uncertainty		Assumed normal ($k = 2$)		12.8 mm

Figure 4-1: Example of the UOM budget (Bell 2013)

4.1.6 Compliance to data sheets

As highlighted previously, the majority of GPS/GNSS receivers have a number of parameters in their datasheets and one of them relates to speed accuracy. Strictly speaking, a statement of compliance against such data sheets in relation to speed accuracy should only be made if the ratio of the UOM of the test asset to the specified tolerance is reasonably small. If this is not the case, the UOM of the speed measurement system shall be taken into consideration when analysing the discrepancies between the speed data obtained from GNSS receivers and reference speed data records from the speed measurement system.

The key to the assessment of compliance is the concept of “decision rules”. These rules give a prescription for the acceptance or rejection of a product based on the measurement result, its uncertainty and the data sheet limits, considering the acceptable level of the probability of making a wrong decision. Based on the decision rules, an “Acceptance zone” and a “Rejection zone” are determined, such that if the measurement result lies in the acceptance zone the product is declared compliant. Alternatively, if in the rejection zone it is declared non-compliant. Four possible examples of decision rules are shown in Figure 4-2 (National Aeronautics and Space Administration 2010; Eurachem 2007):

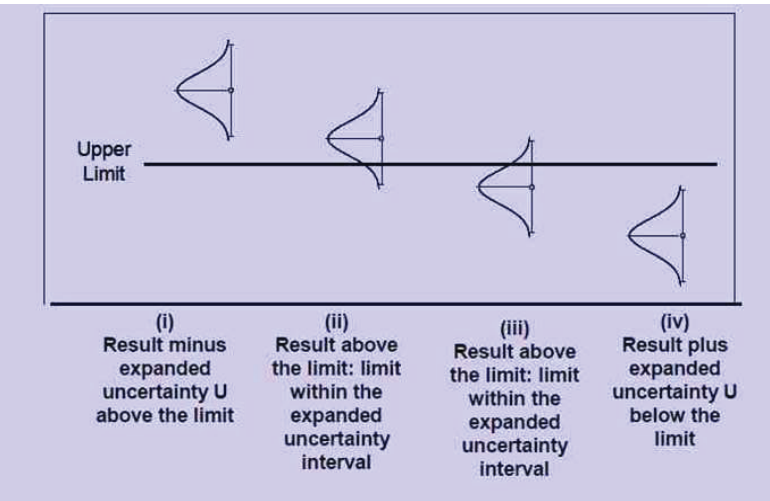

Figure 4-2: UOM and decision rules (Eurachem 2007)

The majority of manufacturers of GNSS receivers and chipsets claim that their products are accurate in speed measurements up to 0.2 km/h or better. On the other hand, the UOM of the speed measurement system used in testing might be worse than 0.2 km/h. Therefore, the best option is to apply the decision rule shown below in (4.3). This would mean that the UOM of the speed measurement system would be added to the maximum speed error claimed by the manufacturer and a combined figure would be compared against a speed error in any measurement. In this instance, the following approach is in place (Moscitta, Pianegiani & Petri 2004; Eurachem/Citac Guide 2011; Dobbert & Stern 2009):

$$CT = UOM + ME, \tag{4.3}$$

where

- CT is a compliance threshold;
- UOM is the uncertainty of measurement of the speed measurement system;
- ME – manufacturer’s speed error claimed in the datasheet.

If a measurement error sits outside CT, then such speed records would be considered as non-compliant with a high degree of probability, e.g. 95%. This rule is shown in Figure 4-3.

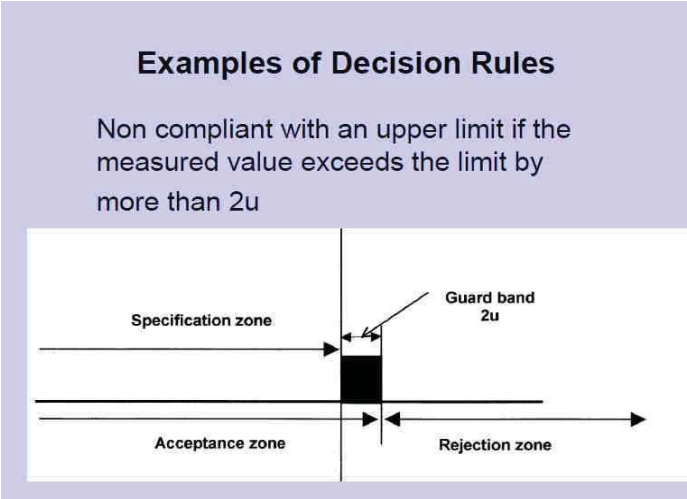

Figure 4-3: Decision rule used for testing (Eurachem 2007)

4.2 Supplementary data for uncertainty calculations

Before each speed test is conducted, the test vehicle is calibrated. Calibration is conducted through separate calibrations of distance and time measurement diagrams as described in chapter 3.

After each test, the same calibration process would follow in the form of verification of the performance of the distance and time measurement components of the speed measurement system. Such verification without conducting any re-calibrations must confirm that both the distance and time measurement components perform within the prescribed limits.

As explained previously, calibration for speed consists of distance and time calibrations. Within distance calibration, a few tolerances / errors are introduced which would influence the speed UOM. For example, when a vehicle is driven from A to B covering a surveyed distance of 361.3 m, it is not possible for the speed measurement system working in distance measurement mode to determine a covered distance precisely and there would be always a tolerance. This tolerance would obviously influence the speed UOM. Tolerances of initial positioning at points A and final positioning at point B would also influence the UOM. Therefore, it is important to understand the magnitude of such distance inaccuracies and how they influence the speed inaccuracy.

As an example, an influence of 1 m distance inaccuracy would be assessed for 1 km distance. Then, the assessment results would be applied to all other distances in the UOM budget, considering that the actual distance calibration is conducted using 361.3 meters.

Example.

During a distance calibration procedure, a vehicle is driven from A to B covering 1 km. A vehicle is placed at point A precisely with no error, then driven ideally in a straight line to point B. However, instead of stopping exactly at point B, it stopped 1 m before the point. It is required to estimate the impact of such 1 m inaccuracy in the distance calibration on speed accuracy.

One meter represents 0.1% of 1 km distance and therefore for any value of speed V it would cause a speed error of the magnitude equal to 0.1% of V, which means the actual speed error would be equal to (0.1*V)/100. Subsequently, 10 cm error of distance would cause a speed error which would be (0.01*V)/100 and so on.

If a similar distance calibration is conducted on a distance of 361.3 m with an error of 1 m, then the impact of this error on speed would be 2.7 times higher because the distance of 361.3 m is 2.7 times smaller than 1 km.

Table 4-1 illustrates speed error values caused by distance errors during calibrations for two scenarios. The first is if calibrations occur on 1 km distance which makes it easy to understand where the values are coming from; the second is if calibrations occur on a distance of 361.3 m, which is the real calibration distance used in this research. Data from this table would further be used in the UOM assessment.

Table 4-1: Speed error as a function of calibration distance error

Distance error	*Error in speed for 1 km distance*	*Error in speed for 361.3 m distance*
1 m	*0.1% of speed*	*0.27% of speed*
40 cm	*0.04% of speed*	*0.1% of speed*
30 cm	*0.03% of speed*	*0.081% of speed*
20 cm	*0.02% of speed*	*0.054% of speed*
10 cm	*0.01% of speed*	*0.027% of speed*
5 cm	*0.005% of speed*	*0.013% of speed*
4 cm	*0.004% of speed*	*0.011% of speed*
3 cm	*0.003% of speed*	*0.009% of speed*
1 cm	*0.001% of speed*	*0.005% of speed*

4.3 Calibration uncertainties

The UOM components for calibration are analysed below to establish their exact values and magnitude.

4.3.1 Resolution in distance measurement mode

The speed measurement system is designed such that it is capable to measure distances with the resolution of 10 cm when operating in calibration mode. Considering the information from Table 4-1 and the fact that calibration is conducted on a 361.3 m surveyed site, this resolution translates into (0.00027*V) km/h UOM component, where V is the actual speed of the vehicle.

4.3.2 Initial positioning

At the start of a calibration, the test vehicle is positioned at a surveyed point A. Due to inability to position the bottom of the wheel exactly at point A, an uncertainty of 3 cm is allocated based on practical experience. This uncertainty of 3 cm mainly relates to determination of the centre of a wheel.

Considering that calibration is conducted on a 361.3 m surveyed site and values mentioned in Table 4-1, the uncertainty of initial positioning translates into (0.00009*V) km/h UOM component.

4.3.3 Final positioning

During calibration, a test vehicle is driven from one surveyed point A to the second surveyed point B covering 361.3 m distance (see Figure 3-10). At point B, the test vehicle stops and its final position cannot be ideal. Therefore, the uncertainty of its final positioning is selected as 10 cm. This characterises the uncertainty of positioning of a vehicle's front wheel bottom exactly at the final surveyed point B. It must be emphasised that at this point it is not possible for the vehicle to move back and forth to reach a perfect match in positioning because the microcontroller counts pulses from the Encoder. Therefore, the UOM value of final positioning is higher than the one selected for initial positioning. Specifically, when a vehicle is positioned at the surveyed point A, its distance measurement system is not enabled in terms of counting pulses from a wheel sensor, and therefore a vehicle can be manoeuvred back and forth until a perfect match of the bottom of the wheel with the surveyed mark A is achieved. On the other hand, when a vehicle is about to reach the final surveyed point B, the distance measurement system is already enabled and counts pulses from a wheel's Encoder. As a result, it is not possible to conduct any movements back and forth to achieve a perfect match in the positioning of a wheel's bottom with the surveyed point B. In this instance, it is possible to miss the surveyed point and thus accept its final position without conducting further calibrations. However, this value of 10 cm is very conservative. In the reality, better positioning accuracy of the wheel could be achieved.

Considering that calibrations are conducted on a 361.3 m surveyed distance and information from Table 4-1, a calibration error due to this uncertainty factor equates to (0.00027*V) km/h.

4.3.4 Timing diagram

Timing calibration is conducted with the use of the microchip UFDC-1 working as a timing interval measurement device. Therefore, the error of the microchip UFDC-1 in time measurement mode is the value which might be used for further assessment of the time measurement uncertainty. This error according to UFDC-1 data sheet is determined using (eq.3.8). For the measured intervals of 1 sec which are used for time stamping of speed and distance measurements, the calculated error would be equal to 0.00000625% of the time stamp interval. This means that the UOM component related to timing uncertainty is negligible.

4.3.5 Surveying the baseline distance

Surveyed distance of 361.3 m was measured using the Leica FlexLine EDM unit. According to the brochure for this equipment (Leica Geosystems AG 2013), the accuracy of distance measurements sits within 1.5 mm (0.0015 m) for 361.3 m distance. Considering the magnitude of this value relative to other components mentioned earlier, its influence on speed errors would be negligible.

4.3.6 Driving straight

This UOM component relates to situations when a vehicle is not driven perfectly straight from A to B during calibrations.

To estimate the magnitude of this UOM component, a few practical experiments were conducted when a vehicle was driven through the calibration distance with the same tyre pressure and initial / final positioning points were maintained as precise as possible. Such approach is acceptable as far as there are no alternatives to estimate this UOM component. Through the number of experiments, it was determined that variations of 40 cm may occur between the runs when such runs seem to be identical. Therefore, 40 cm can be attributed to the uncertainty of driving straight factor, although, strictly speaking, this variation might be partially caused by the resolution of the distance measurement system of the test vehicle. According to Metrology Training International (2005), the error distribution for this component might be considered close to normal, if the number of tests conducted to determine this variation was more than 10.

Considering the information from Table 4-1, a final value of speed errors depending on this component equals to (0.001*V) km/h.

4.3.7 Tyre pressure

This uncertainty component is attributed to the error in tyre pressure measurements conducted by calibrated pressure gauges.

The tyre pressure gauge used in the experiments was Longacre 2" Digital Tire Pressure Gauge Longacre Part # 53036 (Longacre Racing Products 2016). This gauge has a measurement range of 0-100 Pounds per Square Inch (PSI) with a claimed accuracy of 0.8%. Considering that the nominal tyre pressure for Mazda 3 used in the experiments equals to 32 PSI, an expected error of tyre pressure measurements would equal (0.8*32)/100 = 0.25 PSI.

To determine the actual link between this error and the subsequent distance measurement error, a few experiments were conducted during this research (Dyukov 2016c). The test vehicle Mazda 3 was driven multiple times along the surveyed distance of 361.3 m with different tyre pressure values, resulting in slight differences in distance measurements. The experiments revealed the following data:

Table 4-2: Distance measurements as a function of tyre pressure

Tyre pressure, PSI	Average distance measured	Number of test drives
28	362.0	10
32 (Nominal)	361.3	10
35	361.2	10

It is evident from Table 4-2 that the tyre pressure variations influence the distance measurement error when the actual pressure goes down rather than up. Therefore, to assess the impact of this UOM component, a worst-case scenario is considered. Instead of an ideal 32.0 PSI tyre pressure, the value would be equal to 31.75 PSI because of the above-mentioned error 0.25 PSI in measurement.

Considering that a difference of 4 PSI in tyre pressure causes 0.7 m distance measurement error on a surveyed 361.3 m distance (see Table 4-2), it is possible to estimate that a tyre pressure error of 0.25 PSI may cause an error in distance measurement of approximately (0.25*0.7)/4 = 0.04 m (4 cm). This error, as per Table 4-1 would translate into (0.0001*V) km/h.

4.3.8 Allowable tolerance in distance measurements

When distance calibrations are conducted, it is highly unlikely that the distance measurement component of the speed measurement system would measure a surveyed distance with the

result, which exactly matches this distance. Therefore, the allowable tolerance in distance measurements is introduced. This is the tolerance when a calibration run is considered to be successful without a perfect match between the measured and surveyed distances.

Distance calibrations are conducted before each test. The purpose of distance calibrations is to determine a Calibration Factor of the speed measurement system for the test day. Considering the resolution of the speed measurement system in distance measurement mode (0.1 m as mentioned earlier), it is not practical to select the tolerance in distance measurements to be smaller than the resolution. Also, if a small allowable tolerance is selected, for example 20 cm, this may not be practical too because driving perfectly straight is not achievable in practice. Therefore, in this instance a high number of calibration runs might be conducted before the actual test trying to achieve the allowable tolerance. As a result, time would be spent on calibrations rather than testing. On the other hand, if the allowable tolerance is selected too high, this would increase errors in speed measurements.

Therefore, the tolerance was selected as 40 cm considering the practicalities of calibration and the above information. This would practically mean that calibration is considered to be successful if the actual distance measurement sits within the range of 360.9 m–361.7 m.

In this instance, considering the information from Table 4-1, the corresponding speed error equals to (0.001*V) km/h.

4.3.9 Calibration uncertainty spreadsheet

The Calibration UOM spreadsheet, created as per the recommendations described in Metrology Training International Pty Ltd (2005) takes into account all the above components and calculates the combined UOM attributed to the calibration activities. As shown above in sections 4.3.1 – 4.3.8, almost every UOM component depends on speed and therefore the combined Calibration UOM would also be speed dependant. Figure 4-4 and Figure 4-5 show two screenshots derived from the UOM spreadsheet for specific speeds of 60 km/h and 110 km/h. Considering that 110 km/h is the maximum allowable speed to conduct testing due to relevant traffic legislation in Victoria, the corresponding UOM related to this speed would subsequently be used when speed test UOM is counted. This calibration UOM equals to 0.16 km/h as per Figure 4-5.

O23

	A	B	C	D	E	F	G	H	I
1					Notes				
2	**Speed**	**60**							
3									
4	**Uncertainty Components**								
5	Resolution (Vr)	±	0.0162	km/h	10 cm resolution				
6	Uncertainty of initial positioning, Vip	±	0.0054	km/h	3 cm positioning				
7	Uncertainty of final positioning, Vfp	±	0.0162	km/h	10 cm positioning				
8	Uncertainty of timing diagram, Vt	±	0	km/h	Negligible				
9	Uncertainty of surveying of a calibrated distance	±	0	km/h	Negligible				
10	Uncertainty of driving straight, Vdr	±	0.06	km/h	Derived from experiments as 0.4 m for 361.3 m				
11	Uncertainty of tyre pressure while calibrating, Vtp	±	0.006	km/h	Derived from tyre pressure experiments				
12	Allowable tolerance of distance measurement, Vd	±	0.06	km/h	40 cm for 361.3 m is allowed				
13									
14									
15	Note: All Sensitivity Coefficients are equal to 1								
16	**COMPONENT**	**Range**	**Units**	**Distribution**	**diviser**	**ui**	**ci**	**uici**	**(uici)^2**
17	Vr	0.0162	km/h	Rectangular	1.73	0.0094	1.0000	0.0094	0.0001
18	Vip	0.0054	km/h	Normal	2.00	0.0027	1.0000	0.0027	0.0000
19	Vfp	0.0162	km/h	Normal	2.00	0.0081	1.0000	0.0081	0.0001
20	Vt	0	km/h	Normal	2.00	0.0000	1.0000	0.0000	0.0000
21	Vd	0	km/h	Normal	2.00	0.0000	1.0000	0.0000	0.0000
22	Vdr	0.06	km/h	Normal	2.00	0.0300	1.0000	0.0300	0.0009
23	Vtp	0.006	km/h	Normal	2.00	0.0030	1.0000	0.0030	0.0000
24	Vd	0.06	km/h	Normal	2.00	0.0300	1.0000	0.0300	0.0009
25								**SUM**	0.0020
26								**uc**	0.0444
27								**k=2**	2.0000
28								**U**	**0.0888**

Figure 4-4: Combined Calibration UOM for 60 km/h speed

C11 =PRODUCT(0.01,B2)/100

	A	B	C	D	E	F	G	H	I
1					Notes				
2	**Speed**	**110**							
3									
4	**Uncertainty Components**								
5	Resolution (Vr)	±	0.0297	km/h	10 cm resolution				
6	Uncertainty of initial positioning, Vip	±	0.0099	km/h	3 cm positioning				
7	Uncertainty of final positioning, Vfp	±	0.0297	km/h	10 cm positioning				
8	Uncertainty of timing diagram, Vt	±	0	km/h	Negligible				
9	Uncertainty of surveying of a calibrated distance	±	0	km/h	Negligible				
10	Uncertainty of driving straight, Vdr	±	0.11	km/h	Derived from experiments as 0.4 m for 361.3 m				
11	Uncertainty of tyre pressure while calibrating, Vtp	±	0.011	km/h	Derived from tyre pressure experiments				
12	Allowable tolerance of distance measurement, Vd	±	0.11	km/h	40 cm for 361.3 m is allowed				
13									
14									
15	Note: All Sensitivity Coefficients are equal to 1								
16	**COMPONENT**	**Range**	**Units**	**Distribution**	**diviser**	**ui**	**ci**	**uici**	**(uici)^2**
17	Vr	0.0297	km/h	Rectangular	1.73	0.0171	1.0000	0.0171	0.0003
18	Vip	0.0099	km/h	Normal	2.00	0.0050	1.0000	0.0050	0.0000
19	Vfp	0.0297	km/h	Normal	2.00	0.0149	1.0000	0.0149	0.0002
20	Vt	0	km/h	Normal	2.00	0.0000	1.0000	0.0000	0.0000
21	Vd	0	km/h	Normal	2.00	0.0000	1.0000	0.0000	0.0000
22	Vdr	0.11	km/h	Normal	2.00	0.0550	1.0000	0.0550	0.0030
23	Vtp	0.011	km/h	Normal	2.00	0.0055	1.0000	0.0055	0.0000
24	Vd	0.11	km/h	Normal	2.00	0.0550	1.0000	0.0550	0.0030
25								**SUM**	0.0066
26								**uc**	0.0814
27								**k=2**	2.0000
28								**U**	**0.1627**

Figure 4-5: Combined Calibration UOM for 110 km/h speed

4.4 Field speed measurement uncertainty

Field speed measurement uncertainty is the most important parameter which needs to be taken into consideration when assessing an individual GNSS receiver against its relevant datasheet for speed performance.

The UOM of the actual field speed measurement has its own parameters which should be individually assessed in a similar manner as it was done for the calibration UOM. These parameters are listed and analysed below, taking into consideration information in Table 4-1.

4.4.1 Resolution of speed measurement

The displayed speed is logged by the speed measurement system to one decimal place (see Figure 3-8). Therefore, the resolution component in the UOM is 0.1 km/h.

4.4.2 Uncertainty inherited from calibration

This component comes from the Calibration UOM spreadsheet and characterises an imperfection in calibration and how it influences the UOM when a vehicle is driven. The uncertainty inherited from calibration is selected at its maximum level, i.e. at a level corresponding to 110 km/h.

Considering the value of UOM in Figure 4-5, the uncertainty inherited from calibration is 0.16 km/h.

4.4.3 Time stamp random error

This error is caused by possible missing of a pulse from the speed sensor (Encoder) installed on a wheel during a sampling timing interval of 1 sec. This may occur because of random timing of pulses from the Encoder in relation to a sampling timing interval of 1 sec.

The Encoder produces 2048 pulses per one rotation of a wheel and such pulses are not in synchronisation with 1 sec time stamps produced by the microcontroller. Therefore, one pulse of the Encoder might be missed at either the start of count or the end.

The missing of a pulse from the speed sensor in each measurement causes a distance measurement error of 0.0009733 m (see Table 3-1). This error is negligible compared to other UOM factors and therefore not taken into consideration in the UOM spreadsheet.

4.4.4 Tyre pressure error due to non-ideal initial tyre pressure

Implementation of the incorrect tyre pressure causes speed errors when a vehicle is driven during speed tests. Such errors and their influence on speed error are fully described in paragraph 4.3.7 and Table 4-1. Therefore, a value of (0.0001*V) could be used to describe a speed error caused by initial non-ideal tyre pressure.

4.4.5 Speed error caused by changes in tyre pressure

When conducting a speed test, the tyres are subject to friction and increased temperature. Therefore, their circumference may change because of increased tyre pressure. There are currently no reviews on how hot tyres can increase tyre pressure for specific vehicles. Therefore, experiments were conducted in this research to understand the link between the driving speed and

tyre pressure (Dyukov A 2016c). In such experiments, a vehicle Mazda 3 was used with 195/65 R15 tyres.

To determine the speed error caused by tyre pressure, the following steps were taken:

- Determination of possible changes in tyre pressure while a vehicle is driven with different speeds;
- Determination of changes in distance measurement by the speed measurement system of the test vehicle depending on tyre pressure; and
- Estimation of speed errors depending on tyre pressure.

The first step was to reveal how hot tyres might change the tyre pressure. To achieve this, an experiment was conducted when the test vehicle Mazda 3 was driven using several speeds with the specific tyre pressure gauges installed on each wheel. Such gauges have Radio Frequency (RF) transmitters embedded in each gauge that could transmit tyre pressure values remotely to the Instrument Panel (Advantage Enterprises 2014). Figures 4-6 and 4-7 show the actual installation of the RF tyre pressure gauges and the Instrument Panel (monitor) getting the RF pressure signals. Figure 4-8 shows the principle of operation and the devices used during the experiment.

Figure 4-6: Tyre pressure gauge with the RF transmitter installed on Mazda 3 tyre

Figure 4-7: Instrument Panel to receive, indicate and record tyre pressure values

The system consisted of four RF tyre pressure sensors installed on the wheels of Mazda 3 (see Figure 4-8). Such sensors were capable of measuring tyre pressure on the move and transmit the results through the RF to the Instrument Panel. The latter displayed pressures in sequence for each wheel or logged pressure values to a laptop via RS232 port embedded to the Instrument Panel. These systems are produced by Advantage Enterprises, Inc in the United States and sold under the trademark PressurePro^{TM}. In this research, the 10-wheel Monitor Part #ALTGPM10 was used as the Instrument Panel **(**Advantage PressurePro LLC 2014) with software package for logging called enTIRE Pressure Agent provided by the same company**.**

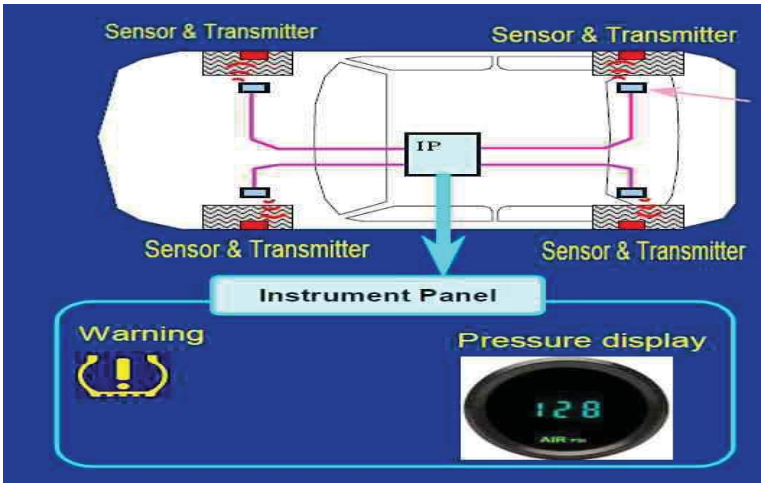

Figure 4-8: Tyre pressure monitoring on the move

In this experiment, the test vehicle Mazda 3 was driven from 0 km/h up to 110 km/h with an initial and nominal tyre pressure of 32 PSI implemented before driving. Further analysis of the tyre pressure log-file depending on speed values recorded during an experiment, revealed that at 0 km/h the tyre pressure was at 32 PSI; and at 100 km/h, the tyre pressure was 34 PSI. This is because the temperature of the tyres increases as the speed increases. This change essentially means that pressure increased by about 6% from its original nominal value. Quantifying the actual

changes in tyre pressure depending on how fast the test vehicle moved, allowed estimation of potential errors in speed measurements caused by changes in tyre pressure.

To understand how hot tyres contribute to distance measurement errors and consequently speed errors, an experiment was conducted with a number of drives along the surveyed distance of 361.3 m with different tyre pressures: nominal 32 PSI, below nominal 28 PSI and above nominal 35 PSI. Such variations would cover possible tyre pressure increase while driving at high speed.

The results for different tyre pressures were shown earlier in Table 4-2 and the main outcome was as follows: an increase of tyre pressure from 32 PSI to 35 PSI changes a measured distance from 361.3 m to 361.2 m. It appears that inner plies of a tyre, particularly for a belted tyre, would not stretch or compress a lot in this circumstance. This is probably because the steel belt of a tyre remains the same regardless of air pressure. When a tyre is under-inflated, a tyre thread is deformed to be flat against the ground and the tyre flat spot, or footprint, increases with reduction of air pressure. Therefore, as the tyre thread is deformed to be flat against the ground, the outermost part is slightly compressed to be shortened to the same length as the steel belt over the length of the flat area. This then accounts for the slightly reduced travel distance in relation to the tyre circumference. As a result, under-inflation causes a larger error than over-inflation as shown in Dyukov (2016c). Therefore, maintaining a nominal initial tyre pressure is very important. If this condition is met, subsequent distance measurement error caused by even 10% tyre pressure increase might be about 10 cm or so for a distance of 361.3 m. This would translate into speed errors of 0.01% of the actual speed, i.e. 0.0001*V as shown in Table 4-1. For example, at 100 km/h, an increase by 10% in tyre pressure may cause a speed error up to only 0.01 km/h.

Considering that during the experiments the tyre pressure increased by 6% at speeds equal to 110 km/h, such changes in tyre pressure would cause a speed error of approximately 0.006 km/h as a result. This result is taken into consideration in calculating the relevant UOM component in the uncertainty budget.

4.4.6 Noise of the GNSS receiver under test

This parameter is determined to be 0.33 km/h based on field experiments conducted with stationary GNSS receivers. This is the most convenient way of verifying the noise of the receivers for speed measurements. Details of the field experiments will be provided in chapter 6. However, to keep the UOM budget conservative, the worst results of 0.33 km/h were selected.

4.4.7 Uncertainty of field speed measurements

A combined UOM for speed measurements was calculated based on the individual UOM components described above. Below are two screenshots derived from the Speed UOM spreadsheet for specific speeds of 60 km/h and 110 km/h. Considering that the speed of 110 km/h

is the maximum allowable speed to conduct testing because of relevant traffic legislations in Victoria, the corresponding UOM of 0.4 km/h related to this speed would subsequently be used in all assessments. Normally the test asset should be more superior in terms of accuracy compared to the device under test. However, considering the speed accuracy claimed by the manufacturers of GNSS receivers, providing such a superiority represents a challenge. More importantly, the GNSS speed outliers investigated in this thesis would be far beyond the UOM of a test vehicle.

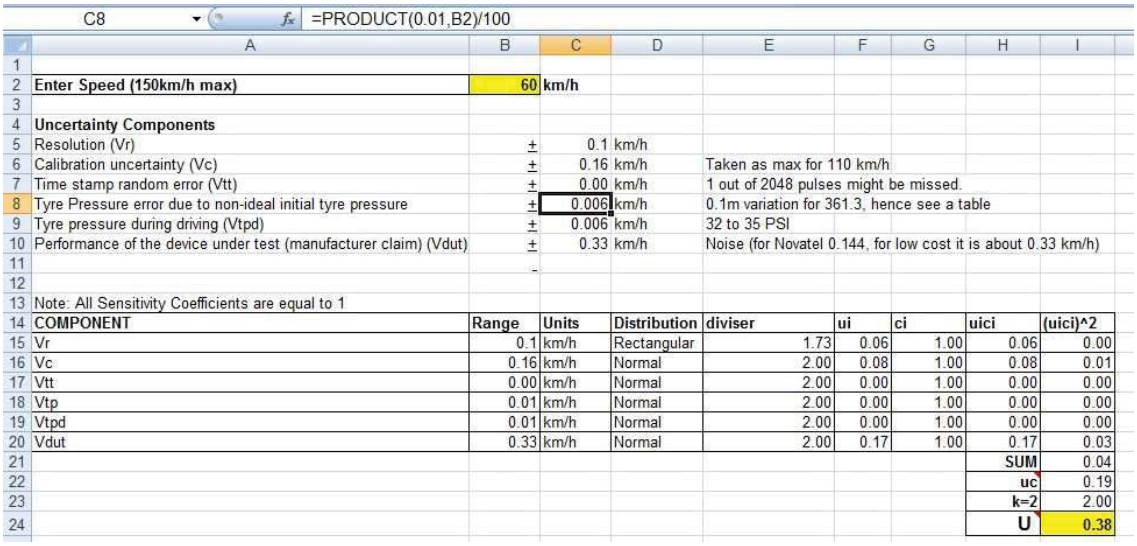

C8 =PRODUCT(0.01,B2)/100

	A	B	C	D	E	F	G	H	I
1									
2	**Enter Speed (150km/h max)**	60	km/h						
3									
4	**Uncertainty Components**								
5	Resolution (Vr)	±	0.1	km/h					
6	Calibration uncertainty (Vc)	±	0.16	km/h	Taken as max for 110 km/h				
7	Time stamp random error (Vtt)	±	0.00	km/h	1 out of 2048 pulses might be missed.				
8	Tyre Pressure error due to non-ideal initial tyre pressure	±	0.006	km/h	0.1m variation for 361.3, hence see a table				
9	Tyre pressure during driving (Vtpd)	±	0.006	km/h	32 to 35 PSI				
10	Performance of the device under test (manufacturer claim) (Vdut)	±	0.33	km/h	Noise (for Novatel 0.144, for low cost it is about 0.33 km/h)				
11		-							
12									
13	Note: All Sensitivity Coefficients are equal to 1								
14	**COMPONENT**	**Range**	**Units**	**Distribution**	**diviser**	**ui**	**ci**	**uici**	**(uici)^2**
15	Vr	0.1	km/h	Rectangular	1.73	0.06	1.00	0.06	0.00
16	Vc	0.16	km/h	Normal	2.00	0.08	1.00	0.08	0.01
17	Vtt	0.00	km/h	Normal	2.00	0.00	1.00	0.00	0.00
18	Vtp	0.01	km/h	Normal	2.00	0.00	1.00	0.00	0.00
19	Vtpd	0.01	km/h	Normal	2.00	0.00	1.00	0.00	0.00
20	Vdut	0.33	km/h	Normal	2.00	0.17	1.00	0.17	0.03
21								**SUM**	0.04
22								**uc**	0.19
23								**k=2**	2.00
24								**U**	**0.38**

Figure 4-9: Speed UOM for 60 km/h driving speed

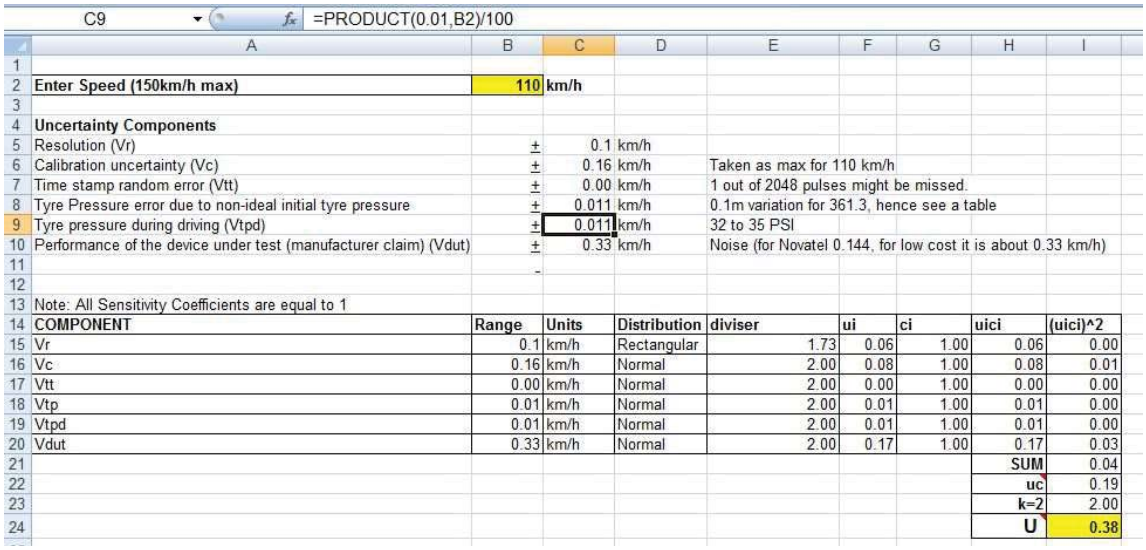

C9 =PRODUCT(0.01,B2)/100

	A	B	C	D	E	F	G	H	I
1									
2	**Enter Speed (150km/h max)**	110	km/h						
3									
4	**Uncertainty Components**								
5	Resolution (Vr)	±	0.1	km/h					
6	Calibration uncertainty (Vc)	±	0.16	km/h	Taken as max for 110 km/h				
7	Time stamp random error (Vtt)	±	0.00	km/h	1 out of 2048 pulses might be missed.				
8	Tyre Pressure error due to non-ideal initial tyre pressure	±	0.011	km/h	0.1m variation for 361.3, hence see a table				
9	Tyre pressure during driving (Vtpd)	±	0.011	km/h	32 to 35 PSI				
10	Performance of the device under test (manufacturer claim) (Vdut)	±	0.33	km/h	Noise (for Novatel 0.144, for low cost it is about 0.33 km/h)				
11		-							
12									
13	Note: All Sensitivity Coefficients are equal to 1								
14	**COMPONENT**	**Range**	**Units**	**Distribution**	**diviser**	**ui**	**ci**	**uici**	**(uici)^2**
15	Vr	0.1	km/h	Rectangular	1.73	0.06	1.00	0.06	0.00
16	Vc	0.16	km/h	Normal	2.00	0.08	1.00	0.08	0.01
17	Vtt	0.00	km/h	Normal	2.00	0.00	1.00	0.00	0.00
18	Vtp	0.01	km/h	Normal	2.00	0.01	1.00	0.01	0.00
19	Vtpd	0.01	km/h	Normal	2.00	0.01	1.00	0.01	0.00
20	Vdut	0.33	km/h	Normal	2.00	0.17	1.00	0.17	0.03
21								**SUM**	0.04
22								**uc**	0.19
23								**k=2**	2.00
24								**U**	**0.38**

Figure 4-10: Speed UOM for 110 km/h driving speed

Summary

This Chapter presented a detailed description of the following:

1. Principles of decision making when assessing GNSS receivers for compliance to speed accuracy parameters from their datasheets.
2. The analysis of the UOM components for calibration and speed measurement.
3. Experimental results which help to calculate individual UOM components.

5 GPS/GNSS RECEIVERS UNDER TEST AND TRIAL TESTS

This chapter describes all GPS/GNSS receivers tested in this research and preliminary trial testing. Trial testing was conducted because it was anticipated that difficulties may occur while the long test drives are conducted. The main goal was to become familiar with the speed measurement system's reliability parameters and to assess the mechanical parts of the speed measurement system for robustness, as well as the ability to record the speed data from multiple sources to a PC.

5.1 GPS receivers under test

Table 5-1 summarises the GNSS receivers tested in this research.

Table 5-1: GNSS receivers tested

Parameter	*Columbus*	*G-Log*	*V-Box Sport*	*Garmin GPS 72H*	*NovAtel ProPak-V3-L1*	*NovAtel OEM6*
Classification	Consumer grade	Consumer grade	Medium range	Medium range	Geodetic quality	Geodetic quality
GPS antenna	Internal	Internal	Internal External	External	External	External
Data logging	SD card 50 million records, CSV file	Via USB NMEA 0183 v.3.01	SD card	Via RS232	Via RS232 NMEA 0183 v.3.01	Via RS232 NMEA 0183 v.3.01
GPS chipset	MTKII	MTKII	Unknown	SiRFIII	OEM3	OEM6
Number of channels	66	66	Unknown	Unknown	72	72
Sensitivity	-165dBm	-165dBm	Unknown	-159dBm	Unknown	Unknown
Frequency	L1	L1	Unknown	L1	L1	L1
Data update	1 Hz	1 Hz	0.01 Hz	0.5 Hz	1 Hz	1 Hz
Internal battery	Yes 13-15 hours	No	Yes	Yes	No	No
Mask angle	Unknown	Unknown	7°	Unknown	5° - 15°	15°
Claimed speed accuracy	N/A	0.36 km/h	0.1 km/h	0.36 km/h	0.1 km/h	0.1 km/h

It should be noted that GNSS receivers mean not only the devices showing GNSS data on their display, but also the devices capable of data logging either on Secure Digital (SD) cards or via any

output ports, for example, RS232 or USB. Such devices are widely available to the general public and researchers nowadays.

The first group of GNSS receivers was classified as consumer grade primarily because of their simplicity and limited set of functions and capabilities. This group originally consisted of three receivers: Columbus (Victory Co Ltd 2011), Canmore (CanMore Electronics Co Ltd 2013) and G-Log (Transystems Inc 2011). However, the performance of the Canmore GPS receiver was inconsistent as multiple records were missing. This behaviour was discovered during the trial tests and confirmed during subsequent speed tests. Therefore, only Columbus and G-Log receivers were tested in speed tests (see Table 5-1) and their performance analysed. Consumer grade receivers often do not allow the operator to change their settings. Also, such receivers are priced up to $100 and they all use internal GPS antennas. Therefore, such receivers can only be installed inside a test vehicle on a dashboard as per manufacturer's recommendations. In terms of data logging the following parameters were logged by Columbus to its own SD card: date, time, latitude, longitude, altitude, speed, direction, voice, Position Dilution of Precision (PDOP), HDOP, Vertical Dilution of Precision (VDOP). Columbus uses the Doppler derived methodology for speed determination and this principle was confirmed by the manufacturer through email.

Figure 5-1: Columbus GPS receiver

One of the features of Columbus was that the speed output was hardcoded by the manufacturer to produce by default the integer speed values with no option to change. The manual for Columbus has no information about the speed accuracy (Victory Co Ltd 2011). However, considering that Columbus V-990 uses MTK 3329 GPS chipset, it may be assumed that the estimated speed accuracy is around 0.36 km/h (Mediatek Inc 2010).

The second low cost consumer grade receiver tested in this research was a recreational GPS receiver G-Log 760 (Transystems Inc 2011).

G-Log is a low-cost GPS recorder which allows a route to be logged by setting the interval of time / distance / speed. It has a rechargeable battery and several indicators of the receiver's operation. In this research the receiver was configured to log GPS data with 1 sec timing intervals.

Figure 5-2: G-Log GPS receiver

The second group of GPS receivers was classified as medium range primarily because of their increased complexity, functionalities and cost compared to low cost consumer grade receivers. This group consisted of two receivers: VBox Sport and Garmin GPS 72H. Medium range receivers generally do not allow the operator to change their internal settings, but their cost varies from $200 to $500. Such receivers typically use active external GPS antennas. This allows optimisation of GPS signal strength when external antennas could be placed on the roof of the test vehicle.

The first medium range GPS receiver was VBox Sport. This receiver comes with an option of using the internal and external antenna (Racelogic 2013). It is is produced by Racelogic in the United Kingdom.

Figure 5-3: VBox GPS receiver

During initial experiments (prior to October 2015) this receiver was tested with its internal antenna. An external antenna was purchased on 10 Oct 2015 and subsequently used for experiments. The receiver does not have an option of adjusting a mask angle which has been hardcoded by the manufacturer. Therefore, the default angle was 7°. As per Racelogic (2013), the receiver should provide speed measurements accurate to 0.1 km/h. However, the operating conditions when such accuracy could be guaranteed, are not specified. The speed measurements are made using the Doppler method. This receiver is specifically designed for use in sport racing applications where speed is measured with high frequency and then acceleration / deceleration and speed accuracy parameters are analysed.

Unfortunately, very little is known about the parameters of the GPS chipset of VBOX. In addition to the information provided above, the following might be of interest. The VBOX Sport is officially certified by Apple. It can connect to an iPhone™, iPod™, or iPad™ via a wireless Bluetooth connection and work with the popular application such as Harry's Lap Timer. Racelogic's own performance test application is also available from the Apple App Store, providing increased functionality and immediate feedback for performance testing.

As well as using VBOX Sport for motorsport, it can be employed as an enhancement for GPS reception on iOS devices, or for adding GPS functionality to those that do not have it already.

The limitations of this receiver for testing purposes related to the non-generation of records when the receiver was in stationary mode. In addition, the receiver generated records every 0.01 sec when a vehicle was moving. This complicated the data matching process with other receivers and the speed measurement system, as well as prevented comparison when the receiver was stationary. The third disadvantage of VBox was that this receiver generated latitude and longitude in VBox's own format and this format was non-standard.

The second medium range GPS receiver was Garmin GPS 72H (Garmin Corporation 2009).

Figure 5-4: Garmin GPS 72H receiver

Garmin GPS 72H is very popular among marine navigators. The reasons for this is that the receiver is water-proof and it can float on water. The second reason is that it can save coordinates of up to 500 favourite places in its internal memory. Originally this receiver was priced at about $200 but with time its price dropped to about $130-$140.

Geodetic quality GPS / GNSS receivers tested in this research were NovAtel products with advanced configuration functions, multi-GNSS capability and specialised external GPS / GNSS antennas (NovAtel Inc 2015). The cost of these receivers varies between $5,000 and $7,000 depending on their complexities and functions.

The first geodetic quality receiver was NovAtel ProPak-V3-L1 (further in text ProPak-V3-L1) (NovAtel Inc 2007; NovAtel Inc 2013; NovAtel Inc 2014a).

Figure 5-5: Novatel ProPak-V3-L1 GPS receiver

Up to three Novatel ProPak-V3-L1 receivers were tested during this research simultaneously. To address the research objectives the receivers had different elevation cut off angles: 5°, 10° and 15°. ProPak-V3-L1 receivers were equipped with external GPS antennas and configured by the commands sent via RS232 port to output speed records every second with four NMEA data strings: $GPGGA, $GPGSA, $GPRMC and $GPGSV. These NMEA records contained all

information required, such as UTC date and time, speed, HDOP, number of satellites tracked and the satellites parameters, such as SNR and satellite elevation angle. These parameters were used to address the research objectives.

NovAtel receivers use Doppler based methods in conducting speed measurements. This was confirmed through NovAtel Inc (2014a).

The second geodetic grade GNSS receiver tested in this research was NovAtel OEM6 (NovAtel Inc 2014b; NovAtel Inc 2014c), (see Figure 5-6). It represents the next generation of NovAtel receivers capable of operating with all existing and emerging GNSS constellations. In addition, the receiver is also Satellite-Based Augmentation Systems (SBAS) capable. The details of the specific NovAtel OEM6 model used in this research are outlined in Table 5-1.

Figure 5-6: Novatel OEM6 GNSS receiver

5.2 Typical test setup

Depending on the constraints and availability of GNSS receivers during the research, the number of receivers tested during each test were different. However, Figure 5-7 and Figure 5-8 show a typical test setup covering the most extensive configuration when all receivers were tested simultaneously. Figure 5-7 shows the data flow, while Figure 5-8 shows the power connections. This test configuration could be narrowed during a specific test if the number of receivers under test has been smaller than shown on Figure 5-7 and Figure 5-8.

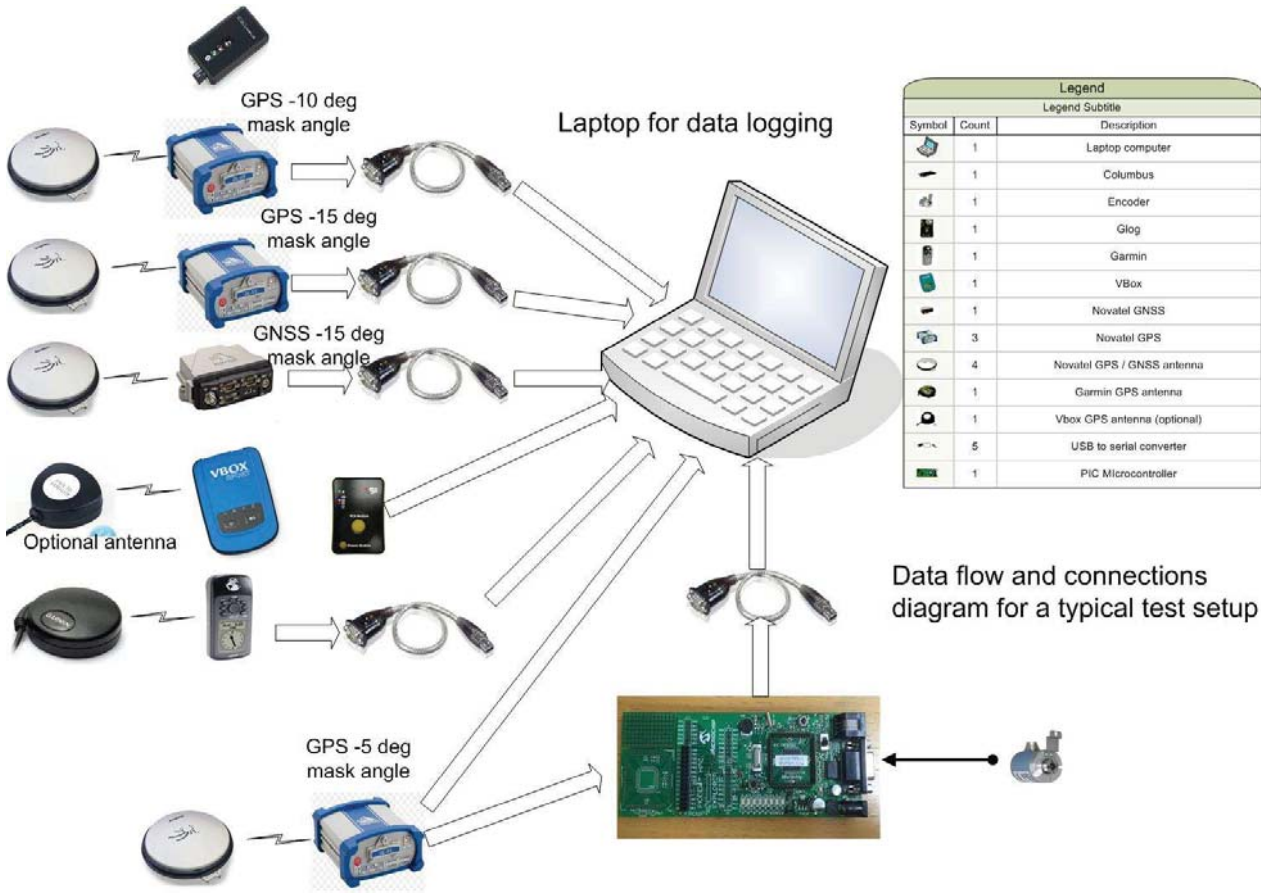

Figure 5-7: Data flow for a typical test setup for all tests

Figure 5-7 shows the data flow diagram for a typical test setup. Three NovAtel receivers ProPak-V3-L1 were configured to operate with 5°, 10° and 15° elevation cut-off angle, respectively. They were connected to their respective GPS antennas and sent NMEA data through USB-to-Serial converters to the laptop for logging. While only one RS232 output in the receivers with higher elevation cut-off was used to send the data to the laptop, the ProPak-V3-L1 with the lowest cut-off angle of 5° had its second RS232 port connected to the microcontroller board to send NMEA data used for time stamps detection. G-Log GPS receiver had direct connection to the USB port of the laptop, whereas both VBox and Columbus logged GPS data to their own SD-cards. Each test further below would mention explicitly whether VBox used its internal or external antenna, because this antenna has been received not at the start of the research.

USB-to-Serial converters represented an off-the-shelf product and their task was to convert signals from RS232 ports to USB format. The laptop used in the tests had one RS232 port available and this port was always connected to one of the ProPak-V3-L1 receivers directly (on Figure 5-7 this is ProPak-V3 with the lowest cut-off angle).

The Encoder installed on the back wheel of the test vehicle was connected to the microcontroller's input for counting pulses, whereas the output of the microcontroller sent time stamps with corresponding speeds to the laptop via the USB-to-Serial converter.

Figure 5-8 shows the research test setup with power connections, i.e. how power was supplied to the equipment.

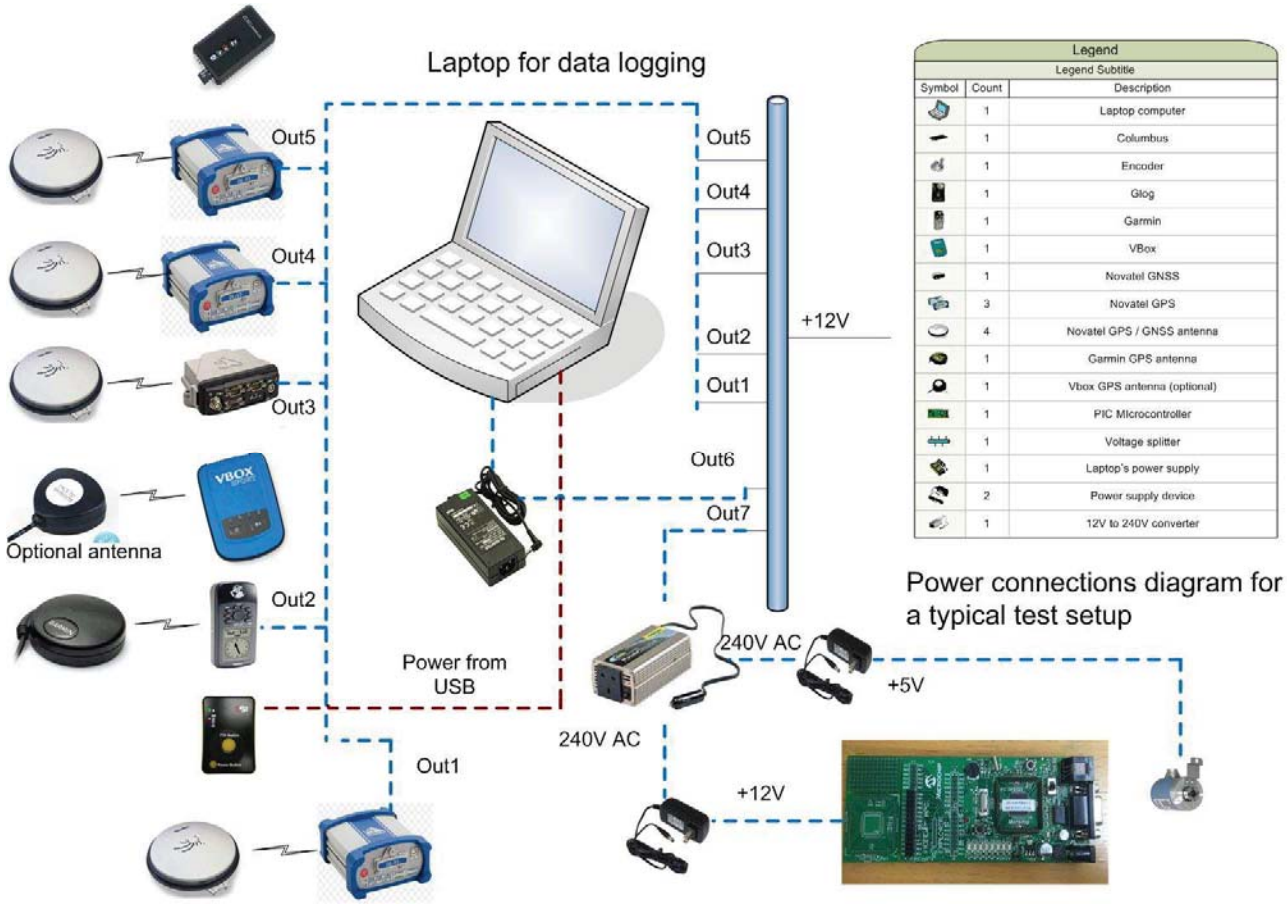

Figure 5-8: Typical test setup for power connections in all tests

All NovAtel receivers and Garmin got their power supply +12V from a splitter connected to a cigarette lighter of the vehicle. Columbus and VBox GPS receivers used their internal batteries. G-Log GPS receiver used a USB interface to obtain power directly from the laptop, whereas the laptop itself had its own power supply converter providing the right power for the laptop from 12V. Finally, the microcontroller board and Encoder obtained +12V and +5V power supply voltages respectively from separate power supply devices connected to the 12V DC –to- 240V AC converter. This converter produced 240V AC from +12V DC obtained from a splitter.

The power supply connections to the microcontroller and Encoder provided their electric isolation from each other.

Figure 5-9 and Figure 5-10 show examples of the receivers' setup in the test vehicle.

Figure 5-9: Installation of GPS receivers on a dashboard

Figure 5-10: GPS receivers and speed measurement system in the boot

Figure 5-10 demonstrates the installation of two Novatel ProPak-V3-L1 receivers, VBox and Garmin. Also, a laptop for logging data is to the right. Behind the laptop is the microcontroller box. GPS antenna cables were linked from the luggage compartment to the roof where the antennas were installed; see two examples in Figures 5-11 and 5-12.

Figure 5-11: GPS antennas on the roof

Figure 5-12: Test vehicle with antennas on the roof during a trial test

5.3 Trial test for the speed measurement system

The goal of a trial test was to confirm the operation of the typical setup and the speed measurement system. Typically, it is important to determine whether new test assets are appropriate for conducting the tests. Trial tests are used to determine what has 'worked', or can be fixed and improved. The goal of this test was not to collect experimental data from the receivers to make a conclusion about their speed accuracy, but rather to validate all technical solutions used in designing the speed measurement system.

At the time of trial testing, not all receivers used in this research for kinematic testing described in chapter 6 were available and therefore a limited number of them were used in the test. On the other hand, the main goal of the test was to practically check the performance of the speed measurement system and its reliability during a long drive. In particular, the mechanical fixing of a speed sensor to a wheel was the main area of concern.

The receivers tested were:

- NovAtel ProPak-V3-L1 receiver with 15° elevation mask operating in GPS mode only;

- NovAtel OEM6 GNSS receiver with 15° elevation mask working in GPS + GLONASS mode;

- VBOX Sport operating with an internal GPS antenna; and

- Columbus and Canmore.

5.3.1 Test route

The test was conducted in February 2015 with the test vehicle driven from Melbourne to Echuca. The route consisted of different environments: freeways with many overpasses, suburban areas, countryside roads with tree canopies and long open sky sections; and the distance covered was approximately 250 km. Considerable parts of the test route are represented in Appendix B.

To eliminate any potential causes of systematic errors which might be experienced by all receivers on the day, the following measures were put in place:

a/ Space weather reports were analysed to confirm that there were no events which could potentially impact the performance of the receivers under test;

b/ GPS Notice Advisory to NAVSTAR Users (NANU) Reports and GLONASS advisories were analysed to confirm that the integrity of the GPS and GLONASS constellations can be maintained for the duration of the test;

c/ An analysis was conducted with help of the GPS planning software to confirm the satellites availability in Victoria and HDOP for the duration of the test.

The above assessments were conducted for the trial test and any subsequent test described in this thesis.

Figures 5-13, 5-14 and 5-15 show the results from the GPS planning software for the area where the test was conducted.

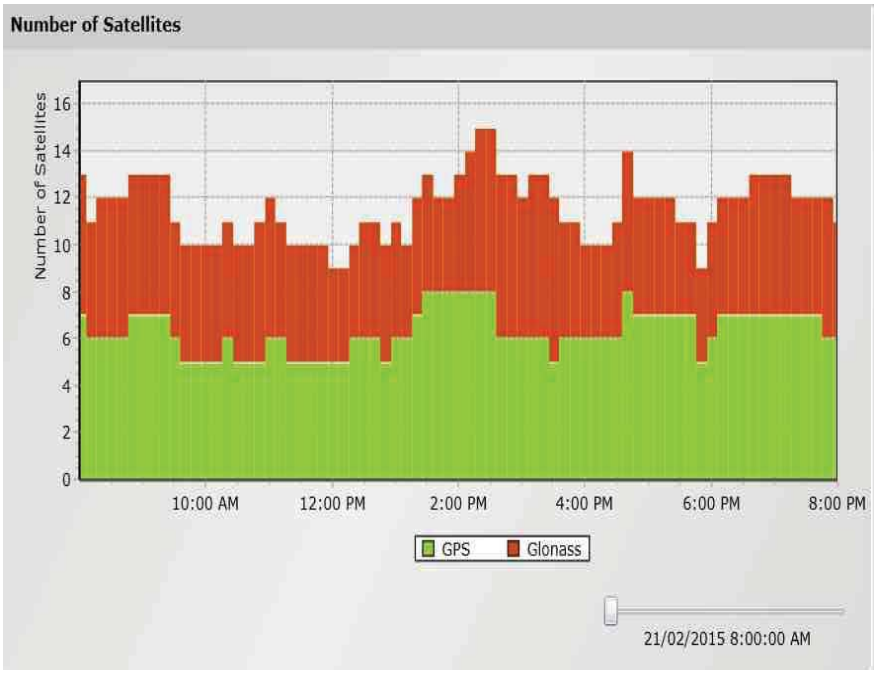

Figure 5-13: Number of GPS + GLONASS satellites during the test period

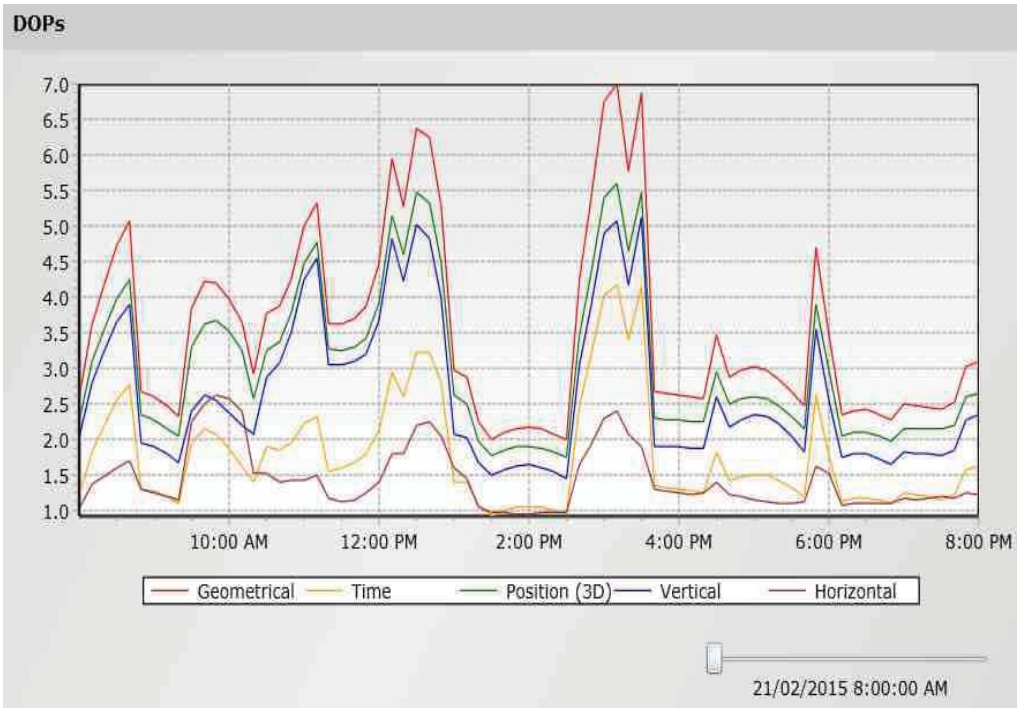

Figure 5-14: GPS DOP values during the test period

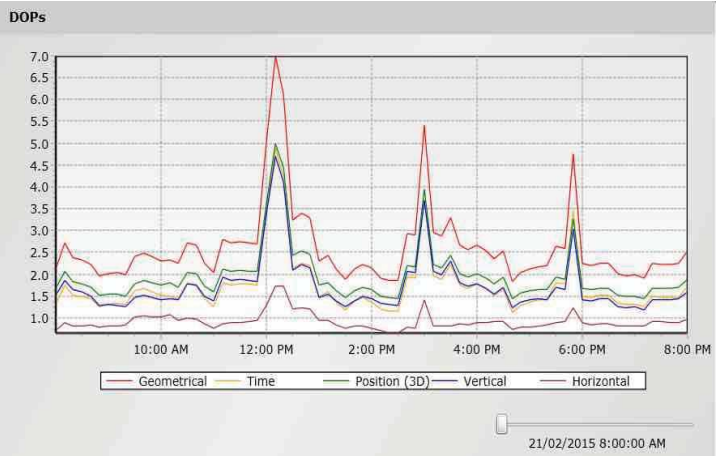

Figure 5-15: GPS and GLONASS DOP values during the test period

It is visible from the above plots that for GPS only receivers the number of predicted satellites in open sky conditions varied from five to eight. For GPS +GLONASS receivers, the number of satellites varied between nine to 15. Also, the predicted HDOP for GPS only receivers was no more than 2.5 and for GPS+GLONASS receivers was no more than 1.75 (refer to the lowest graph in Figure 5-15). All the above demonstrates that GNSS availability in the area was sufficient for conducting speed tests.

5.3.2 Statistical results from the trial test

Statistical analysis of the speed differences between the speed measurement system and GPS/GNSS receivers from a trial test is provided in Table 5-2.

Table 5-2: Statistical performance of GPS/GNSS receivers in kinematic conditions

Parameter	NovAtel ProPak-V3-L1	Novatel OEM6	VBox	Columbus
Mean, km/h	-0.1	-0.1	-0.1	0.4
Standard deviation, km/h	0.3	0.3	0.7	0.5
Maximum negative speed difference, km/h	-3.5	-2.8	-11.3	-3.1
Maximum positive speed difference, km/h	3.1	3.9	6.5	4.0

To understand how the measured values of the speed measurement system correlated with GPS speed records, the Pearson's correlation assessment (paired t-test) was conducted (Shier 2004). A paired t-test is typically used to compare two population means where there are two samples in which observations in one sample can be paired with observations in the other sample. One of the examples of where this might occur is a comparison of two different methods of measurements where the measurements were applied to the same subjects. This is exactly our case where speed measurements were conducted with the test vehicle and they were compared against a number of GPS speed measurements.

Evans (1996) suggests that according to the Pearson's assessment the strength of correlation highlights the following:

- 0.00 – 0.19 is considered as very weak correlation;
- 0.20 – 0.39 is considered as weak correlation;
- 0.40 – 0.59 is considered as moderate correlation;
- 0.60 – 0.79 is considered as strong correlation; and
- 0.80 – 1.00 is considered as very strong correlation.

Table 5-3 shows the results obtained from the Pearson's correlation assessment conducted using the trial test data.

Table 5-3: T-test paired two samples for means

	Test vehicle	**Novatel GPS ProPak-V3-L1**
Observations	3269	3269
Pearson Correlation		0.9999
	Test vehicle	**Novatel GPS+GLONASS OEM6**
Observations	4927	4927
Pearson Correlation		0.9998
	Test vehicle	**VBox**
Observations	5409	5409
Pearson Correlation		0.9991
	Test vehicle	**Columbus**
Observations	3305	3305
Pearson Correlation		0.9996

Results shown in Table 5-3 highlight that some GPS receivers are more conservative than the others, considering the number of records generated by each receiver.

More importantly, measurements from the test vehicle and GPS receivers demonstrated very strong correlation with the t-test result no less than 0.9991.

Figures of Appendix C demonstrate speed difference distributions for the receivers under test during a trial test. Such distributions represent the number of speed records of the GPS/GNSS receivers corresponding to the specific speed errors. Speed errors were measured as differences between the calibrated test vehicle speed records and the relevant speed records of the receivers. Such distributions were put in place considering smooth driving records of the test vehicle only. Smooth driving records represented only those records of the test vehicle when the speed difference between neighbouring 1 sec records was less than the UOM of the test vehicle. This means that sharp accelerations and decelerations of the test vehicle were excluded and only those records processed when the speed difference between neighbouring ones did not exceed 0.4 km/h. Also, speed outliers generated around overpasses were eliminated from the assessment as they are separately analysed in the next paragraph 5.3.3. Finally, speed records

when the test vehicle was stationary were also eliminated from the assessment as they may change the statistical performance dramatically due to differences in static measurements caused by rounding in the Columbus GPS receiver. This means that Columbus always produced 0 km/h speed when a vehicle was stationary, while other receivers produced speed around 0 km/h with no perfect match because of a GPS speed noise.

5.3.3 Speed outliers

An outlier is defined herein as a measurement that is distant from other measurements. As GNSS receivers are generally very precise in speed measurements, any GNSS speed measurement with an error of several kilometers per hour is considered to be an outlier.

Table 5-4 outlines the magnitude and the number of speed outliers generated by the receivers during a trial test only around overpasses. Also, an example of a location where speed outlier was generated is shown in Figure 5-16 for NovAtel ProPak-V3-L1. More examples for different receivers are provided in Appendix D.

Table 5-4: Average GNSS speed spikes for overpasses only and the number of spikes during the test

	Novatel ProPak-V3-L1	Novatel OEM6	VBox	Columbus
Average speed difference between the test vehicle and the receiver, km/h	5.3	4.7	10.7	10.5
Number of outliers	7	10	30	23

Figure 5-16: Example of the environment where an outlier was generated by Novatel ProPak-V3-L1

For the trial test it was calculated that the amount of outliers represented 0.09% for Novatel ProPak-V3-L1 and 0.08% for Novatel OEM6 from the total number of valid speed records.

In addition to the outliers generated around overpasses, VBox only generated 122 outliers in the countryside on road sections where some tree foliage environments were present. The average magnitude of such outliers was equal to 3.8 km/h. Trees can potentially be a significant source of GNSS signal loss and GPS speed accuracy degradation. However, this topic would be further discussed in chapters 6 and 7.

Despite all receivers used Doppler based method to determine speed, their statistical results demonstrated significant performance differences. Considering the standard deviation of speed errors produced by different receivers as shown in Table 5-2 and relevant speed error distributions (see Appendix C), it is possible to derive a preliminary conclusion that the reported speed sits within 0.6 km/h from the true speed (two standard deviations) for geodetic quality receivers. For medium range receiver VBox and low-grade receiver Columbus, speed records are within 1.4 km/h and 1 km/h from the true speed, respectively. It is likely that the statistical performance of Novatel receivers complies to the datasheets. This is because when combined with the UOM of the test vehicle (0.4 km/h), the total UOM is ±0.5 km/h, compared to ±0.6 km/h as reported from the test.

Unlike Novatel receivers, the receiver VBox was potentially non-complaint to its specified speed accuracy parameter. The receiver's speed values were ±1.4 km/h from the true speed. In the worst situation, the combined UOM of the test vehicle is 0.4 km/h and the speed noise of VBox receivers is expected to be 0.1 km/h. The total speed error is expected to be up to 0.5 km/h, which significantly differs from ±1.4 km/h range of speed errors.

It is to note that the above conclusions are only preliminary. Further experiments will validate the

performance of the GNSS receivers, particularly in challenging environments.

Despite the fact that all receivers use the Doppler based method to determine speed, the performance of geodetic quality receivers was considerably better compared to medium range and low-grade receivers both in terms of the number of outliers and their magnitude. Around overpasses, Novatel receivers produced either good or blank records indicating unreliable speed measurement with only several outliers, i.e. seven and 10 respectively for Novatel ProPak-V3-L1 GPS receiver and Novatel OEM6 GPS + GLONASS receiver for the entire run. VBox and Columbus produced more outliers than Novatel receivers despite sufficiently higher number of satellites in speed records.

The use of GLONASS in the Novatel OEM6 receiver did not significantly improve the performance in terms of both speed accuracy and the number of outliers. However, it increased the number of valid speed records in general (see Table 5-3). The average speed error for Novatel OEM6 outliers was 4.7 km/h compared to 5.3 km/h for Novatel ProPak-V3-L1. This improvement is marginal, considering that Novatel OEM6 is the next generation of Novatel receivers. It is to highlight that the number of outliers, i.e. seven and 10 produced by geodetic quality receivers ProPak-V3-L1 and OEM6 for the entire test, was still relatively high in magnitude (see Table 5-4). The average speed errors of 5.35 km/h and 4.74 km/h are generally not expected from geodetic quality receivers.

For medium range (VBox) and low grade (Columbus) receivers the speed accuracy around overpasses is worse. These receivers had average speed errors of 10.7 km/h and 10.5 km/h (see Table 5-4). The number of outliers was also relatively high. These preliminary results highlighted that the use of speed records, when produced around overpasses and narrow pedestrian crossing bridges (see Figure 5-17), cannot be justified. Also, VBox produced 122 outliers when measuring speed on road sections with tree canopies. The average error for this group of outliers was 3.8 km/h. Such magnitude of speed error highlighted that the measurements from VBox may not be trusted in such environments.

Summary

This chapter presented a detailed description of the following:

1. The GNSS receivers tested in the research.
2. Typical test setup used in the experiments.
3. Planning of experiments for each test date to confirm that the test results would not be adversely affected by the GNSS availability in the area where the test was conducted.
4. Analysis of results of the trial test.

6 VALIDATING THE ACCURACY OF GPS/GNSS SPEED MEASUREMENT

6.1 Tests overview

Static and kinematic tests were conducted to evaluate the performance of GNSS receivers in different environments. Static tests were conducted in two environments, e.g. ideal open sky and non-ideal environment. In the static tests, the receivers were stationary.

The next group of tests represented several kinematic tests where a test vehicle was driven through a number of specific GNSS environments. All static and kinematic tests are summarised in the Table 6-1. As the test environments were becoming more complex with each subsequent kinematic test, the goal of each test was to get the statistical performance of the speed error and compare the test results against each other to determine the environment representing the biggest challenge.

Table 6-1: Summary of tests

Test No	Environment
	Static tests
1	Ideal open sky environment
2	Non-ideal open sky environments with good GNSS visibility
	Kinematic tests
1	Predominantly open sky with limited number of trees (Narre Warren – Drouin - Warragul)
2	Predominantly open sky with limited number of trees (number of trees is higher compared to the kinematic test No1)
3	Freeway with a number of overpasses (Monash Fwy in Melbourne)
4	Tree foliage environment (Berwick – Upper Beaconsfield – Emerald – Berwick)
5	Tree foliage environment (Berwick – Emerald – Nangana - Woori Yallock)

In all kinematic tests No1 – No5 shown in Table 6-1, the VBox GPS receiver was tested with an external GPS antenna located on the roof of the test vehicle.

In the following sections, the results from the static and kinematic tests will be explained in more detail.

6.2 Static speed tests

Before commencing kinematic tests, the receivers were tested for their static performance to ensure their speed errors are known in ideal environmental conditions. The first static test (refer to Table 6-1) represented the open sky ideal environment where the receivers were stationary having good GNSS visibility with no trees or any other structures around. The duration of this test was 24 hours and thousands of speed records were collected from each receiver. Speed test results from the static test No1 were also required to assess the speed noise parameter, which was subsequently used in UOM calculations described in chapter 4. Then, the receivers were tested in non-ideal static conditions when the receivers were also stationary, but located at different locations (refer to Table 6-1, static test 2). For example, such locations could represent situations when the test vehicle was stationary at traffic lights or emergency lanes off roads. The duration of this test comprised several hours with times when the GPS visibility dropped. Therefore, test results from the static test No2 would demonstrate how simple, non-dynamic changes in the environments could affect the speed accuracy parameter.

During such static tests, the receivers reported minor variations in speed values and their statistical speed difference parameters are shown in Tables 6-2 and 6-3.

Table 6-2: Speed errors for the static test No1

Parameter	Novatel ProPak-V3-L1 GPS receiver	Novatel OEM6 GPS + GLONASS receiver	VBox GPS receiver	Columbus GPS receiver	G-Log GPS receiver	Garmin GPS Receiver
Mean, km/h	0	0	N/A	0	0	0
Standard deviation, km/h	0.02	0.02	N/A	0	0.01	0.02
Maximum negative speed difference, km/h	0	0	N/A	0	0	0
Maximum positive speed difference, km/h	0.2	0.16	N/A	0	0.31	0.33

Considering that in the static test No1 the test vehicle was not present, it was decided to use the worst values from this environment as a GPS speed noise. The worst performer in this instance was Garmin with a noise value of 0.33 km/h. This value was used in the UOM analysis as described in chapter 4.

It should be noted that VBox GPS receiver did not produce static speed records because of the internal accelerometer preventing the receiver to produce records in stationary conditions. Columbus GPS receiver produced very good static results, simply because the receiver does not generate speed records with decimal points. Therefore, all speed values were rounded to zero for Columbus. Novatel ProPak-V3-L1 used 15° cut off elevation angle in such experiments.

Table 6-3: Speed errors for the static test No2

Parameter	Novatel ProPak-V3-L1 GPS receiver	Novatel OEM6 GPS + GLONASS receiver	VBox GPS receiver	Columbus GPS receiver	G-Log GPS receiver	Garmin GPS receiver
Mean, km/h	0	0	N/A	0	0.02	0
Standard deviation, km/h	0.04	0.04	N/A	0	0.03	0.04
Maximum negative speed difference, km/h	-0.3	-0.4	N/A	0	0	0
Maximum positive speed difference, km/h	0	0	N/A	0	0.7	0.74

As can be seen from the results in Tables 6-2 and 6-3, the geodetic quality Novatel receivers complied with the manufacturers specifications. At the same time, it was noticed that for Novatel receivers the occasional speed records in the static test No2 were outside the datasheet boundaries. In such instances Novatel receivers produced occasional outliers of up to 0.3 km/h and 0.4 km/h respectively, while errors of the test vehicle were eliminated as it was stationary. The number of outliers sitting beyond the boundaries prescribed in the datasheets was 113 for the Novatel ProPak-V3-L1 and 66 for Novatel OEM6 for the test data covering several hours of operation.

Garmin and G-Log GPS receivers were the worst performers in stationary speed tests as shown from Tables 6-2 and 6-3.

One important consideration relates to the comparative performance of receivers. While their speed inaccuracies are different, it is not possible to guarantee that the consumer grade or medium range receivers performed very differently against the geodetic quality receivers. This is seen from the standard deviation values of the speed error. This highlights the fact that potentially in the ideal environments, it would be hard to distinguish the differences in speed measurement performance between various receivers.

6.3 Kinematic speed tests in a predominantly open sky environment

The goal of the kinematic tests No1 and No2 (refer to Table 6-1) was to collect kinematic speed records from all GNSS receivers in predominantly open sky environment. Test results will be compared to those collected in challenging environments. This comparison would help to assess the impact of such challenging environments on speed accuracy.

6.3.1 Test routes

The test routes were mainly on the Australian countryside roads. Unfortunately, in a real-world environment when collecting thousands of speed records, it is challenging to select a test route with absolutely no trees or obstacles causing obscuration to GNSS signal. However, the test routes for the tests No1 and No2 were selected so that the vast majority of GNSS speed records would be generated in the open sky environments. Also, the routes were selected so that only occasional trees would be present but no buildings. The kinematic test No1 contained less trees along the road compared to the kinematic test No2. In the kinematic test No1 several overpasses were present, but speed records around them were carefully filtered out for all receivers under test. Filtering was conducted with a buffer of several seconds around each overpass.

The route for kinematic test No1 is shown in Figure 6-1. Figure 6-2 shows the route for the kinematic test No2.

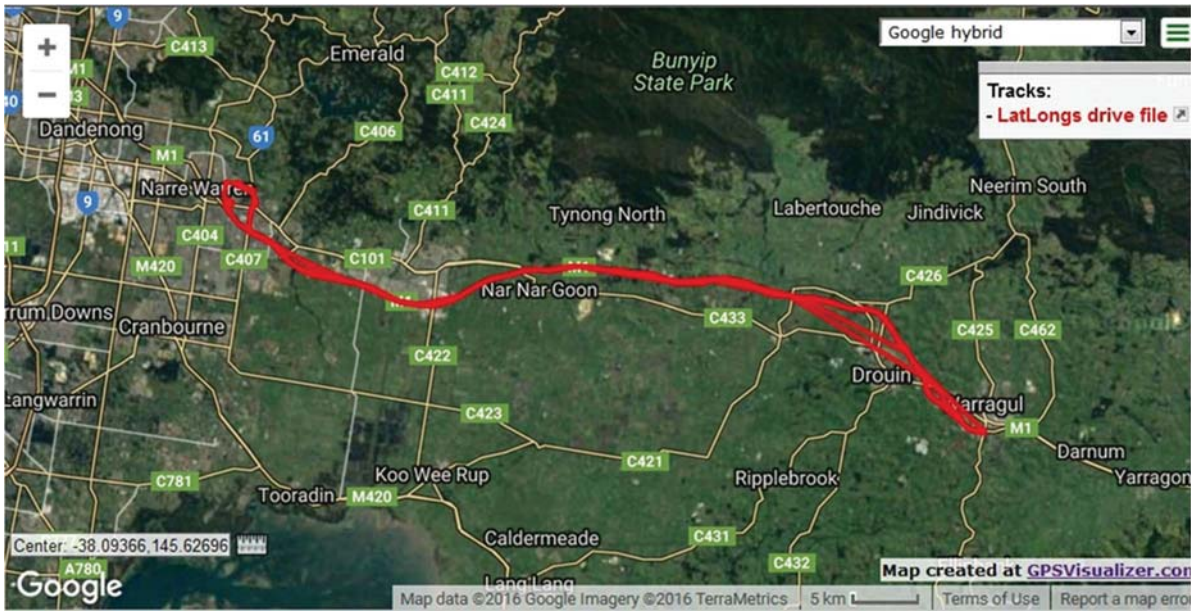

Figure 6-1: Test route for the kinematic test No1

Figure 6-2: Test route for the kinematic test No2

6.3.2 Comparative test results

Comparative test results for the speed error for the kinematic tests No1 and No2 are shown in Tables 6-4 and 6-5, respectively.

Table 6-4: Practical performance in speed measurement for the kinematic test No1

Parameter	Novatel GPS ProPak-V3-L1 with 5º cut-off angle	Novatel GPS ProPak-V3 with 10º cut-off angle	Novatel GPS ProPak-V3 with 15º cut- off angle	Novatel OEM6 GNSS	VBox	Garmin	Columbus	G-Log
Mean, km/h	-0.05	-0.06	-0.05	-0.06	0.00	-0.03	0.48	0.00
Standard deviation, km/h	0.19	0.20	0.25	0.19	0.31	0.16	0.34	0.25

Table 6-5: Practical performance in speed measurement for the kinematic test No2

Parameter	Novatel GPS ProPak-V3-L1 with 5^{o} cut-off angle	Novatel GPS ProPak-V3 with 10^{o} cut-off angle	Novatel GPS ProPak-V3 with 15^{o} cut- off angle	Novatel OEM6 GNSS	VBox	Garmin	Columbus	G-Log
Mean, km/h	-0.02	-0.02	-0.04	-0.04	0.10	-0.14	0.54	0.01
Standard deviation, km/h	0.64	0.45	0.31	0.35	0.59	0.30	0.45	0.52

In open sky environment, all GNSS receivers tested had similar performance. Hence, it was not possible to conclude that geodetic quality receivers performed better.

Looking at the results shown in Tables 6-4 and 6-5, it is possible to make the following conclusions. First, for the kinematic test No1 in ideal environments, all receivers were within the prescribed limits. Second, not all the receivers were compliant to their specifications in kinematic

test No2 as more trees were present along the route. Such conclusions can be made considering two factors: one is the UOM of 0.4 km/h of the speed measurement system; second is the manufacturer's data sheets where the speed accuracy parameter is stipulated. For the kinematic test No1 two standard deviations of the speed difference is generally no higher than the sum of the UOM and the speed measurement error expressed in the datasheet for each receiver (refer to Table 6-6). This is however not the case for a number of receivers tested in the kinematic test No2. Nevertheless, considering the results from Table 6-6, it is premature to make conclusions without further testing of the receivers in the real challenging environments.

Table 6-6: Test results versus datasheets information

Receiver	Datasheet speed accuracy, km/h	UOM of the speed measurement system, km/h	Compliance threshold, km/h (Sum of two previous columns)	Practical error (two standard deviations) for kinematic test No1	Practical error (two standard deviations) for kinematic test No2
Novatel GPS ProPak-V3 with 5^{o} cut-off mask	0.1	0.4	0.5	0.38	1.28
Novatel GPS ProPak-V3 with 10^{o} cut-off mask	0.1	0.4	0.5	0.40	0.9
Novatel GPS ProPak-V3 with 15^{o} cut-off mask	0.1	0.4	0.5	0.50	0.62
Novatel OEM6 GNSS	0.1	0.4	0.5	0.38	0.7
VBox	0.1	0.4	0.5	0.62	1.2
Garmin	0.04*	0.4	0.44	0.32	0.6
Columbus	N/A*	0.4	N/A	0.68	0.90
G-Log	0.36	0.4	0.76	0.50	1.04

It should be noted that Columbus' speed accuracy parameter is not specified in the datasheet.

It should also be noted that having no challenging GNSS environments in kinematic tests No1 and very limited challenges in the kinematic test No2, the receivers still generated some speed outliers. The number and magnitude of outliers, though, were relatively minor. Figures 6-3 to 6-7 mention the outliers for the kinematic test No1 for each GPS receiver with the speed errors greater than 2 km/h when compared to the test vehicle. The corresponding GPS parameters for

every outlier are also indicated. All speed values and speed differences in Figures 6-3 to 6-7 are indicated in km/h.

UTC	Latitude	Longitude	HDOP	Number of satellites	GPS speed	Vehicle time	Vehicle speed	Speed difference
010638	-38.07788	145.68198	3.4	4	99.52	10638	102.7	3.1
010957	-38.06901333	145.62135	2.2	6	100.165	10957	98	-2.1

Figure 6-3: Speed outliers generated by Novatel GPS ProPak-V3-L1 with 5° mask angle

UTC	Latitude	Longitude	HDOP	Number of satellites	GPS speed	Vehicle time	Vehicle speed	Speed difference
004554	-38.1306017	145.877092	2	5	107.232	4554	104.9	-2.3
010321	-38.0789283	145.743452	23.8	4	93.718	10321	95.9	2.1

Figure 6-4: Speed outliers generated by Novatel GPS ProPak-V3-L1 with 10° mask angle

UTC	Latitude	Longitude	HDOP	Number of satellites	GPS speed	Vehicle time	Vehicle speed	Speed difference
4424	-38.11127	145.8599	1.4	6	108.4827524	4424	105.3	-3.2
10844	-38.07104	145.6438	2.2	6	102.326702	10844	99.3	-3.0
10943	-38.06982	145.6255	2.2	5	94.86129324	10943	96.9	2.0
10945	-38.06961	145.6249	4.5	5	102.9749062	10945	97.5	-5.5

Figure 6-5: Speed outliers generated by Novatel GPS ProPak-V3-L1 with 15° mask angle

Number of satellites	UTC	Latitude	Longitude	GPS speed	Vehicle time	Vehicle speed	Speed difference
9	1606	-2283.39	-8721.87	89.37	1606	91.5	2.1
9	1612	-2283.46	-8721.93	91.11	1612	93.5	2.4
10	1758	-2284.32	-8723.4	89.54	1758	92.2	2.7
10	4514	-2287.3	-8752.2	102.05	4514	105.9	3.9
10	4617	-2288.12	-8752.91	101.3	4617	105.1	3.8
8	10632	-2284.71	-8741.03	99.69	10632	102.5	2.8
9	10641	-2284.66	-8740.87	100.07	10641	102.5	2.4
8	10850	-2284.23	-8738.52	96.99	10850	100.5	3.5
8	10854	-2284.22	-8738.45	97.84	10854	100.9	3.1
8	10944	-2284.18	-8737.51	94.99	10944	97.2	2.2
8	10947	-2284.17	-8737.46	94.62	10947	97.3	2.7

Figure 6-6: Speed outliers generated by VBox

UTC	Latitude	Longitude	HDOP	Number of satellites	GPS speed	Vehicle time	Vehicle speed	Speed difference
001758	-38.0721	145.3906	0.74	11	89.896	1758	92.2	2.3

Figure 6-7: Speed outliers generated by G-Log

Garmin GPS receiver had no outliers during the kinematic test No1 and the maximum / minimum speed differences for this receiver were equal -0.8 km/h and 0.7 km/h respectively.

Columbus GPS receiver had no outliers for the kinematic test No1 and the maximum / minimum speed differences for this receiver were equal -1.0 km/h and 1.6 km/h respectively.

During this test and all the subsequent kinematic tests, it was noticed that the consumer grade receivers reported GPS visibility over-optimistically. On the other hand, the geodetic quality receivers were more conservative. This is visible from the reported number of satellites and HDOP.

After careful examination of each outlier generated in kinematic test No1, it was determined that almost every outlier was generated in areas where there were single trees or groups of trees

along the road, except for G-Log. Also, it was noticed that outliers were generated at different times for different receivers, which makes it highly unlikely that the speed measurement system of the test vehicle caused them.

Lastly, it is worth mentioning that in the kinematic test No1 there were two occasions when VBox GPS receiver generated duplicate speed records for the same time but provided different speed values (see Figure 6-8). Two records instead of one were generated for 00:18:38 UTC with different speed values and the same problem was seen for 00:18:39 UTC. Such occurrences may compromise the performance of a particular type of receiver and raise doubts in relation to its integrity, although during this test and the subsequent tests this event did not happen anymore.

Number of satellites	UTC	Latitude	Longitude	GPS speed	Vehicle time	Vehicle speed
10	1830	-2284.43	-8723.93	99.04	1830	98.3
10	1831	-2284.44	-8723.95	99.33	1831	98
10	1832	-2284.44	-8723.97	98.63	1832	97.9
10	1833	-2284.44	-8723.99	98.21	1833	98
10	1834	-2284.44	-8724	97.8	1834	98.3
10	1835	-2284.45	-8724.02	98.06	1835	98.7
10	1836	-2284.45	-8724.04	98.01	1836	99.3
10	1837	-2284.45	-8724.06	98.63	1837	99.9
10	1838	-2284.45	-8724.08	99.09	1838	100.6
10	1839	-2284.46	-8724.1	99.66	1839	101.2
10	1838	-2284.46	-8724.11	100.51	1840	101.6
10	1839	-2284.46	-8724.13	100.95	1841	101.8
10	1840	-2284.47	-8724.15	101.46	1842	102
10	1841	-2284.47	-8724.17	101.85	1843	101.8

Figure 6-8: Duplicate speed records generated by VBox

6.4 Speed tests in challenging environments

6.4.1 Freeways with overpasses

The main tasks of this test, which is represented by the kinematic test No3 (refer to Table 6-1), were as follows:

- To investigate if high GPS receiver mask angle can improve the speed measurements accuracy and reduce the number of speed outliers and/or their magnitude.
- To assess the performance of consumer grade, medium range and high end geodetic quality GPS / GNSS receivers in terms of generation of outliers, specifically in the environments where overpasses are present.
- To assess if the GPS + GLONASS solution provides improved speed measurement performance compared to GPS only in case of driving through overpasses.

To address the above tasks, kinematic test No3 (see Table 6-1) was conducted along Monash Fwy in Melbourne where there were a lot of overpasses between Narre Warren and Chadstone. The route for this test is shown in Figure 6-9. The challenge of this route was that the receivers passed

through many overpasses causing the multipath and obstruction of the GPS signal to occur. It is important to note that only those speed records where multipath caused issues in speed measurement would be further investigated. Such records demonstrated good GPS visibility considering such parameters as HDOP and number of satellites.

Overpasses mainly represented bridges for traffic or narrow pedestrian bridges. For the entire route there were 40 overpasses. In addition, several road gantries or wide metal signs, crossing over Monash Freeway were also presented. It was expected (see chapter 1) that the geodetic quality receivers under test whose mask angle might be configured to higher degrees would generate several speed outliers with the magnitude and frequency dependent on the mask angle. In this instance, it was expected that the best performer would be the GNSS receiver Novatel OEM6 as it had the highest mask angle of 15° and used two GNSS constellations, i.e. GPS and GLONASS. Subsequently, the second-best performer was expected to be the GPS receiver ProPak-V3-L1 with the highest elevation mask of 15°, followed by the GPS Novatel receivers with 10° and then 5° elevation masks. The expectation was based on the fact that the receivers had completely identical GPS/GNSS settings except the mask angle. In addition, ProPak-V3-L1 receivers were of the same type. Finally, the expectation was based on the fact that higher elevation masks would filter potential multipath occurrences as described in chapter 1 (Zhang 2007; Roberts 2015; Abd-Elazeem, Farah & Farrag 2010).

In addition, all medium range and consumer grade receivers were also tested; however, no expectations could be formulated in advance in relation to their comparative performance to each other and to geodetic quality receivers.

This test was conducted at speeds between 80 km/h and 100 km/h with no cruise control.

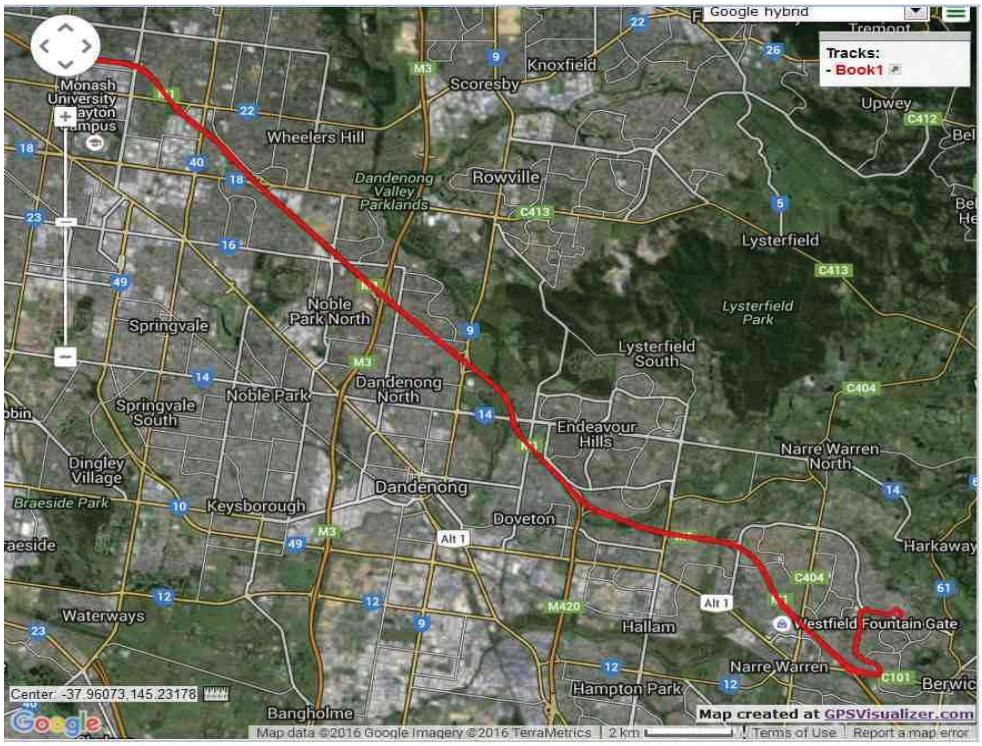

Figure 6-9: Test route along Monash Fwy

After processing the data, the statistical parameters for speed errors from geodetic quality Novatel receivers are presented in Table 6-7.

Table 6-7: Statistical parameters for speed errors from GPS/GNSS Novatel receivers for the kinematic test No3

	Novatel GPS ProPak-V3-L1 with 5° mask angle	Novatel GPS ProPak-V3-L1 with 10° mask angle	Novatel GPS ProPak-V3-L1 with 15° mask angle	Novatel OEM6 GPS + GLONASS with 15° mask angle
Mean, km/h	-0.11	-0.15	-0.10	-0.09
Standard deviation, km/h	0.3	1.0	0.3	0.4
Minimum speed difference, km/h	-2.1	-27.9	-0.9	-1.0
Maximum speed difference, km/h	5.5	4.1	4.6	9.8

Speed difference distributions for Novatel receivers for this test are shown in Appendix E.

The results for four geodetic quality GPS/GNSS receivers having different mask angles demonstrate the following:

- All geodetic quality Novatel receivers demonstrated occasional significant speed errors.
- Despite theoretical approaches that higher mask angles would lead to better speed accuracy results because of elimination of outliers caused by multipath, this is not always the case in practice. The worst performer was Novatel with 10° mask angle for both generation of outliers and standard deviation of the speed error. Also, there was no significant difference in performance between GPS receivers having 5° and 15° mask angles. It is possible that differences in electronic components of the receivers and antennas, despite the fact that the antennas are the same and receivers are identical with the same settings, may play a bigger role in the performance than the masking angle.
- Lastly, the newer and more modern GPS+GLONASS OEM6 Novatel receiver with 15° mask angle performed no better than Novatel GPS only receivers having the same mask angle or even 5° mask angle. This highlights the fact that adding GLONASS to GPS may

not improve the performance in terms of generation of speed outliers. Possibly, adding Galileo may improve speed accuracy in the future.

The other four GPS receivers tested during this test expressed the results shown in Table 6-8.

Table 6-8: Statistical parameters for speed errors from consumer grade and medium range GPS receivers for the kinematic test No3

	VBox	Garmin	Columbus	G-Log
Mean, km/h	-0.06	-0.16	0.35	-0.07
Standard deviation, km/h	0.64	0.87	1.06	0.39
Minimum speed difference, km/h	-3.22	-10.52	-13.0	-2.37
Maximum speed difference, km/h	11.52	2.04	13.4	2.00

Speed difference distributions for the medium range and consumer grade receivers for this specific test are shown in Appendix E.

The results for medium range and consumer grade GPS receivers demonstrate the following:

- Geodetic quality receivers on average performed better compared to medium range and consumer grade receivers;
- Despite the average performance, G-Log consumer grade receiver performed equally to the geodetic quality ones (refer to G-Log standard deviation parameter).
- G-Log consumer grade GPS receiver demonstrated good performance around overpasses.

To further analyse how many outliers were generated by each receiver during this test a specific assessment was conducted with a focus on the number of outliers and their magnitude. Table 6-9 illustrates the number of records where the GPS speed differs from the true speed by more than 2 km/h, 3 km/h and 10 km/h for each receiver. Such number of records characterises how many speed outliers were generated by each GPS/GNSS receiver under test because of the overpasses along a freeway.

Table 6-9: Number of records where GPS speed errors are higher than specific thresholds

Speed error	**Novatel ProPak-V3-L1 GPS receiver with 5° mask angle**	**Novatel ProPak-V3-L1 GPS receiver with 10° mask angle**	**Novatel ProPak-V3-L1 GPS receiver with 15° mask angle**	**Novatel GPS + GLONASS OEM6 receiver with 15° mask angle**	**VBox**	**Garmin**	**Columbus**	**G-Log**
>2 km/h	3	9	1	2	11	5	19	2
>3 km/h	1	5	1	2	5	3	14	0
>10 km/h	0	2	0	0	1	1	3	0

It is to note that Garmin receiver measures speed at every two seconds.

Table 6-9 shows the following:

- The worst receivers (Columbus, VBox and Garmin) belong to consumer grade and medium range ones. It should be noted that Garmin was included in this group because it generated speed records every two seconds rather than every one second. Therefore, despite the fact that the number of outliers generated by Garmin is less compared to Columbus or VBox, the dataset of Garmin's speed records is half as much compared to Columbus or VBox. The number of speed outliers generated by Columbus and VBox is very significant and considering that only 40 overpasses were present, every second overpass for Columbus and every forth for VBox triggered a speed outlier. This is not what a general consumer may expect from such receivers.
- There was no one receiver which did not generate speed outliers.
- Adding GLONASS to GPS constellation did not reduce the number of speed outliers around overpasses (refer to the results of Novatel OEM6 receiver versus ProPak-V3-L1 with 5° and 15° mask angles).
- Receivers in all groups generated speed outliers with very high magnitude (>10 km/h). It is important to highlight that all outliers were having good GPS data, including the number of satellites and HDOP. This means that the receivers have not seen a problem with the GPS, while generating such speed records. Again, this is not what average consumers and even researchers may expect to see.

- There is no correlation between the mask angle of Novatel GPS receivers and the number of outliers. The expectation was that the receiver with 5° mask angle would be the worst performer, while the receiver with 15° the best and the receiver with 10^0 in between. In practice (refer to Table 6-9), a specific receiver with 10° mask angle having all other GPS settings identical was the worst performer, while the receivers with 5° and 15° mask angles did not differ too much from each other.
- It was observed from the data that in the majority of instances around overpasses the Novatel receivers produced either good records or blank records indicating unreliability of speed measurement. At the same time, in such instances VBOx and Columbus produced more outliers. More importantly, such outliers reported good GPS quality indicators looking at number of satellites and HDOP in the relevant speed records.
- It was noticed that some receivers produced speed spikes not only around overpasses but also near narrow pedestrian bridges above the road or road gantries.

Figure 6-10 shows an example of the environment where the outlier was generated by Novatel GPS receivers. Further examples for different receivers are provided in Appendix F.

Figure 6-10: An outlier generated by Novatel with 5° elevation mask (Speed error = 2.2 km/h, Number of satellites in view = 9, HDOP = 1.2)

Looking at the data from each outlier from this test proved that almost all outliers were generated by GPS/GNSS receivers around overpasses or road gantries except for G-Log. G-Log generated two outliers and both were in the areas where some trees were observed about 10 meters from the freeway (see Figure 6-11). Therefore, G-Log and the majority of geodetic quality receivers proved to be relatively accurate receivers for speed measurements in the vicinity to the overpasses compared to the rest of the receivers under test. However, it was observed that the

performance of all receivers in this challenging environment degraded compared to open sky environment in kinematic tests No1 and No2.

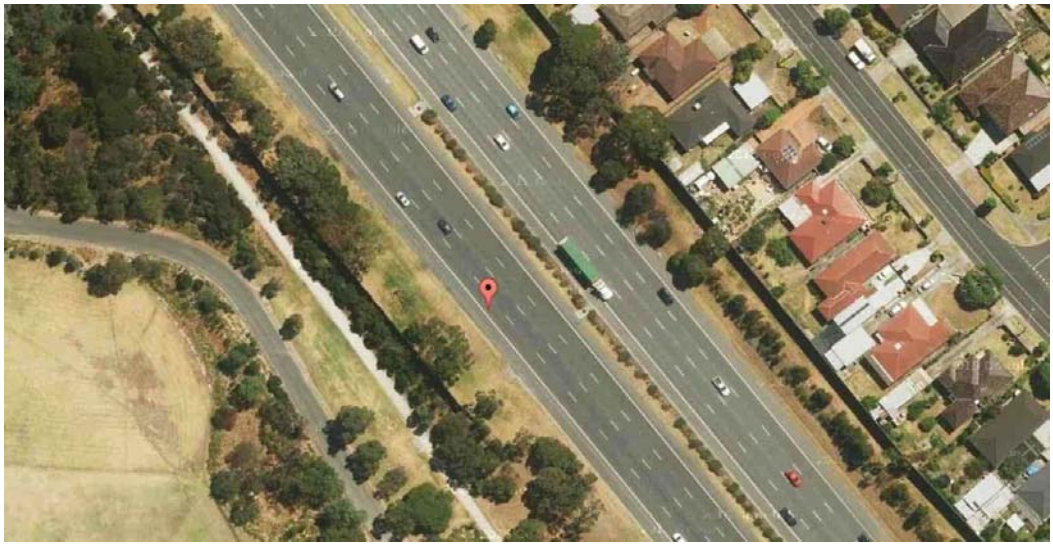

Figure 6-11: An outlier generated by G-Log (Speed error = 2.0 km/h, Number of satellites in view = 11, HDOP = 0.85)

6.4.2 Roads with tree canopies

Tests along roads with tree canopies are represented by the kinematic tests No4 and No5 (refer to Table 6-1). Kinematic test No4 represented a test along the route: Berwick- Upper Beaconsfield – Emerald – Narre Warren East – Harkaway – Berwick as shown in Figure 6-12. This specific route was selected as it has a high percentage of tree-lined roads with 5 m to 20 m high evergreen trees.

Kinematic test No5 represented a test along the route: Berwick – Emerald – Nangana – Woori Yallock and back as shown in Figure 6-13. This specific route was selected as it was longer than the route No4 and also had a high percentage of tree-lined roads with 5 m to 20 m high evergreen trees.

The main goal of the tree canopies environment tests was to assess if tree foliage environments represent a bigger challenge for GNSS receivers compared to overpasses in terms of generation of speed outliers. Obviously, the remaining research objectives mentioned in chapter 1 had to be addressed too.

The driving speed in both tests varied between 50 km/h and 90 km/h. Also, the mask angle of the top of the trees varied and sometimes reached 90°. This means that occasionally trees completely prevented GNSS signals to be received or significantly reduced the GNSS signal's power.

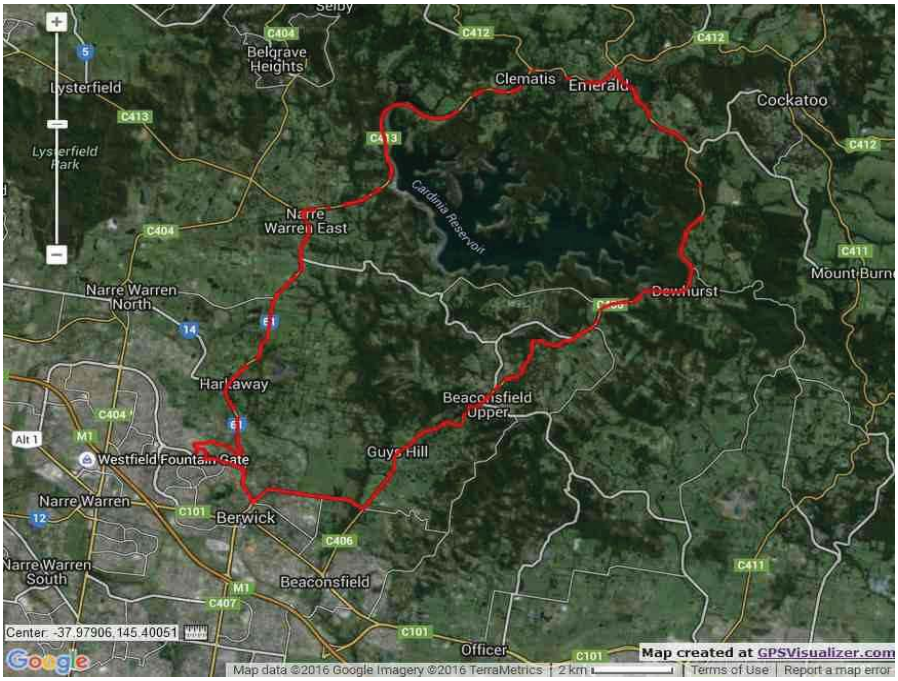

Figure 6-12: Kinematic test No4, tree foliage environments

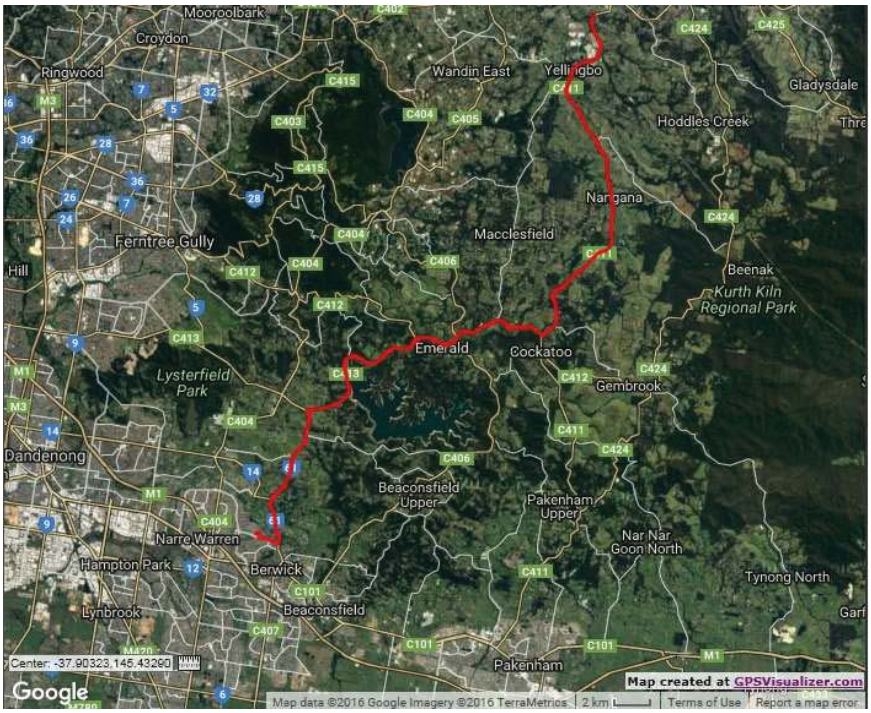

Figure 6-13: Kinematic test No5, tree foliage environments

Statistical performance of Novatel GPS/GNSS receivers for the kinematic tests No4 and No5 is shown in Table 6-10 and Table 6-11, respectively. Statistical performance of the consumer grade and medium range GPS receivers for the kinematic tests No4 and No5 is demonstrated in Table 6-12 and Table 6-13, respectively.

Table 6-10: Statistical speed difference parameters for geodetic quality receivers in tree foliage environment for the kinematic test No4

	Novatel ProPak-V3-L1 GPS receiver with 5° mask angle	**Novatel ProPak-V3-L1 GPS receiver with 10° mask angle**	**Novatel ProPak-V3-L1 GPS receiver with 15° mask angle**	**Novatel GPS + GLONASS OEM6 receiver with 15° mask angle**
Mean, km/h	0.16	0.17	0.19	0.02
Standard deviation, km/h	0.5	0.7	0.6	0.9
Minimum speed difference, km/h	-2.2	-4.8	-3.0	-9.1
Maximum speed difference, km/h	2.9	6.0	2.5	15.2

Table 6-11: Statistical speed difference parameters for geodetic quality receivers in tree foliage environment for the kinematic test No5

	Novatel ProPak-V3-L1 GPS receiver with 5° mask angle	**Novatel ProPak-V3-L1 GPS receiver with 10° mask angle**	**Novatel ProPak-V3-L1 GPS receiver with 15° mask angle**	**Novatel GPS + GLONASS OEM6 receiver with 15° mask angle**
Mean, km/h	0.0	0.0	0.03	0.21
Standard deviation, km/h	1.11	0.5	0.46	1.1
Minimum speed difference, km/h	-24.0	-6.1	-6.1	-5.6
Maximum speed difference, km/h	6.3	2.6	3.2	24.3

Table 6-12: Statistical speed difference parameters for medium range and consumer grade receivers in tree foliage environment for the kinematic test No4

	VBox	Garmin	Columbus	G-Log
Mean, km/h	0.97	0.22	0.74	0.18
Standard deviation, km/h	1.73	0.60	0.71	0.82
Minimum speed difference, km/h	-7.46	-5.54	-4.60	-3.46
Maximum speed difference, km/h	15.36	2.39	6.20	5.42

Table 6-13: Statistical speed difference parameters for medium range and consumer grade receivers in tree foliage environment for the kinematic test No5

	VBox	Garmin	Columbus	G-Log
Mean, km/h	0.23	0.07	0.80	0.10
Standard deviation, km/h	6.11	0.50	1.14	1.20
Minimum speed difference, km/h	-176.9	-2.5	-6.3	-6.2
Maximum speed difference, km/h	16.6	2.7	8.0	8.0

The following conclusions can be made from information presented in Tables 6-10 to 6-13:

- Almost all GPS/GNSS receivers performed worse in tree foliage environment compared to a test No3 along a freeway with overpasses. This is derived from the comparative values of standard deviation of speed error and maximum / minimum speed differences for tree foliage environment (refer to Tables 6-10 to 6-13) versus overpasses (refer to Tables 6-7 to 6-8).
- In tree foliage environment, high end geodetic quality GPS or GNSS receivers generally performed better than the medium and low cost receivers.
- The addition of GLONASS satellites did not improve the performance of the GNSS OEM6 Novatel receiver compared to its GPS Novatel ProPak-V3-L1 counterparts.
- The use of high mask angles did not improve the performance of GPS receivers in tree foliage environment.

To investigate the number of outliers and their relative magnitude, a separate assessment was completed for two tests conducted in tree foliage environment with results presented in Table 6-14 and Table 6-15.

Table 6-14: Outliers generated in tree foliage environment during kinematic test No4

Speed error	**Novatel ProPak-V3-L1 GPS receiver with 5° mask angle**	**Novatel ProPak-V3-L1 GPS receiver with 10° mask angle**	**Novatel ProPak-V3-L1 GPS receiver with 15° mask angle**	**Novatel GPS + GLONASS OEM6 receiver with 15° mask angle**	**VBox**	**Garmin**	**Columbus**	**G-Log**
>2 km/h	3	14	9	10	167	3	31	34
>3 km/h	0	4	2	6	88	1	9	13
>10 km/h	0	0	0	2	6	0	0	0

Table 6-15: Outliers generated in tree foliage environment during kinematic test No5

Speed error	**Novatel ProPak-V3-L1 GPS receiver with 5° mask angle**	**Novatel ProPak-V3-L1 GPS receiver with 10° mask angle**	**Novatel ProPak-V3-L1 GPS receiver with 15° mask angle**	**Novatel GPS + GLONASS OEM6 receiver with 15° mask angle**	**VBox**	**Garmin**	**Columbus**	**G-Log**
>2 km/h	14	7	6	29	209	5	162	150
>3 km/h	3	1	0	9	90	0	80	51
>10 km/h	1	0	0	0	8	0	0	0

During the kinematic test No5 VBox GPS receiver generated five large outliers with the values shown in Figure 6-14:

Number of satellites	UTC	Latitude	Longitude	VBox speed	Vehicle time	Vehicle speed	Speed difference
3	62755	-2275.48	-8728.58	141.34	62755	60.3	-81.04
4	70911	-2275.61	-8727.13	191.77	70911	67.4	-124.37
4	70912	-2275.61	-8727.12	244.74	70912	67.8	-176.94
4	70914	-2275.6	-8727.1	147.41	70914	65.9	-81.51
6	71706	-2276.86	-8723.03	112.58	71706	88.4	-24.18

Figure 6-14: Large speed outliers of VBox during the kinematic test No5

From Tables 6-14 to 6-15 and Figure 6-14, the following conclusions can be made:

- It is clearly visible that almost all GPS/GNSS receivers performed worse in tree foliage environment (refer to Table 6-14 and Table 6-15) compared to a test conducted on a freeway with overpasses (refer to Table 6-9).
- In tree foliage environment, geodetic quality GPS or GNSS receivers generally performed better compared to other types of receivers.
- VBox GPS receiver generated a substantial number of speed outliers (167 for the kinematic test No4, and 209 for the kinematic test No5). The second worst performer was G-Log, followed by Columbus.
- G-Log performed well when it was tested around overpasses (refer to Table 6-9). However, tree foliage environment represented a bigger challenge for this receiver. This is evident from 34 and 150 outliers generated by G-Log in tree foliage environments with a speed difference of more than 2 km/h (refer to Tables 6-14 to 6-15). An important conclusion can be made from here: a GPS receiver may perform differently in different challenging environment. A particular environment, such as trees, may represent a bigger challenge for a specific receiver compared to a different challenging environment. This highlights the fact that it is important to test a receiver in a variety of environments to uncover its true behaviour.
- The use of GLONASS did not improve the performance of the OEM6 Novatel receiver when compared to the GPS Novatel ProPak-V3-L1. In fact, the OEM6 GNSS receiver was the worst performer amongst geodetic quality receivers.
- The use of high mask angles did not improve the performance of GPS receivers in terms of generation of outliers.
- Generation of five large speed outliers by VBox highlighted that tree foliage environments might be exceptionally challenging for certain types of GPS receivers.

An example of the environment where a speed outlier was generated by the Novatel ProPak-V3-L1 receiver during the test in tree foliage environment is shown in Figure 6-15. Additional examples are shown in Appendix G:

Figure 6-15: Street view for an outlier of Novatel ProPak-V3-L1 with 10° mask angle (Speed error = -4.87 km/h, Number of satellites in view = 4, HDOP = 7.6)

From Figure 6-15 and all figures represented in Appendix F it can be noted that outliers were generated in the environments represented by typical Victorian countryside roads. This means that full reliance on GPS receivers when driving along such roads can be compromised. Also, HDOP and number of satellites for outliers revealed that in the majority of instances all the receivers reported good GPS visibility.

The speed difference distribution graph for the kinematic test No4 for VBox is shown in Figure 6-16. Additional examples are presented in Appendix H.

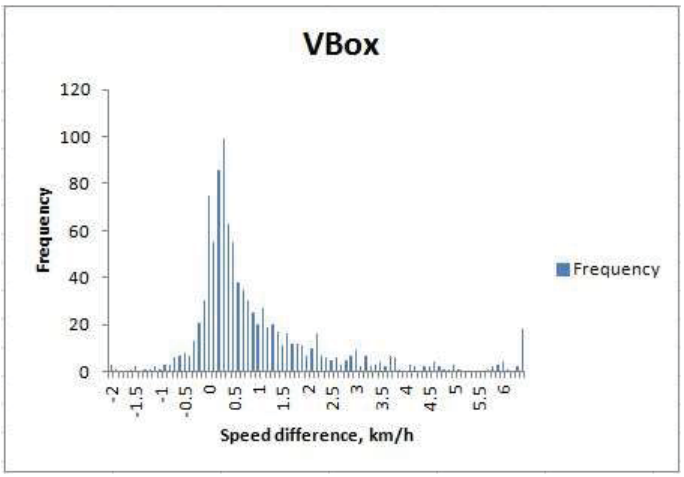

Figure 6-16: Speed difference distribution for VBox

Speed difference distribution graphs from the kinematic test No4 (refer to Figure 6-16 and Appendix H) demonstrate the following:

- Speed difference distribution for VBox is significantly asymmetric (see Figure 6-16). For VBox this is only noticed for tree foliage environment. Again, as with G-Log, this

demonstrates that GPS receivers should be tested in a variety of environments separately to reveal their true performance in speed measurements for specific environments.

- Speed difference distributions for test No3 with overpasses (see Appendix E) and test No5 in the tree foliage environment (see Appendix H and Figure 6-16) are completely different. In the tree foliage environment, the receivers perform worse considering the shape of distribution graphs.
- The worst performers are different in test No3 with overpasses versus tests No4 and No5 in tree foliage environment. This highlights that different receivers are capable to handle specific types of challenging environments differently. Therefore, it is important to test each receiver in different environments separately. Such tests would reveal their true performance in each specific environment. Then, this performance should be compared against the receivers' specifications. For test No4 and No5, the receivers are non-compliant to their specifications, considering the speed distribution graphs, speed error statistical parameters and outliers.
- Mask angle is not a speed error contributor in both tree foliage and overpasses environments. For example, the GPS receiver Novatel ProPak-V3-L1 with 5° mask angle in theory was expected to be the worst performer. However, in practice this receiver was not the worst. The result highlights the fact that possibly the differences in electronic components of the receivers, even in case the receivers are of the same type, might play a bigger role than expected. Indeed, all three Novatel ProPak receivers had their GPS settings and firmware versions identical, except the mask angle. Therefore, it is likely that the parameters of RF channels of these receivers played a bigger role in speed errors than expected. Such parameters may include sensitivity of the RF componentry of the receivers, amplification, actual crystal oscillator parameters with phase noise and some others.
- GPS+GLONASS solution did not improve the speed accuracy parameter in tree foliage environment.
- In tree foliage environments, geodetic quality receivers performed better compared to medium range and consumer grade receivers in terms of number of speed outliers and their magnitude. On the other hand, it is not possible to conclude that medium range receivers performed better than consumer grade receivers.

7 ANALYSIS OF FILTERING METHODS FOR GPS / GNSS SPEED OUTLIERS

Chapter 6 provided examples of instances when GNSS receivers generated speed outliers in challenging environments. Therefore, it is important to investigate whether it is possible to filter such outliers. It is to note that filtering should preferably be conducted based on GPS parameters provided by the majority of GNSS receivers. These parameters are mainly the number of satellites and HDOP. For more advanced receivers, such as Novatel, the SNR parameter may be considered.

To address the research objectives of filtering outliers based on HDOP, number of satellites and SNR, further assessment was conducted. The results of this assessment are described in this chapter.

7.1 Horizontal dilution of precision as a possible quality indicator to filter the speed outliers

Generally, it is considered that more satellites used in calculating a position provide a greater level of accuracy. As the GNSS satellites orbit around the Earth, the number of satellites in view varies. With just three satellites it is possible to determine the location. In practice, a fourth satellite is required to improve accuracy because of errors in measuring the precise time by the receiver. Generally, more satellites provide better HDOP. One of the research objectives, therefore, is to determine if HDOP values can be used to filter unreliable speed records.

HDOP is a measure of the geometric quality of a GNSS satellite configuration in the sky. The smaller the HDOP number, the better the geometry. HDOP is calculated mathematically from the positions of the satellites.

For position determination, the location of satellites in the sky is one of the factors that determines the accuracy of positioning, see Figure 7-1.

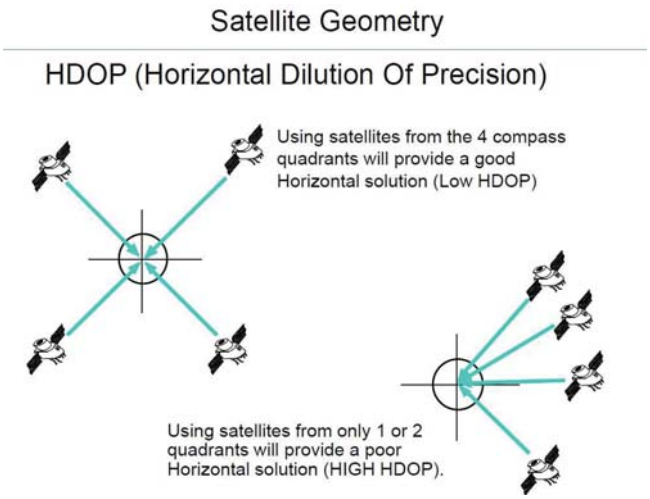

Figure 7-1: Satellite geometry and HDOP (Texas Tech University 2015)

While for positional accuracy the dependency of it on HDOP is clear, for speed accuracy this dependency needs to be investigated. When using triangulation techniques for calculating a position, the distance from known points is used to determine the position of the target point. The known points are the ones where the GPS satellites are located. The optimum positional accuracy is achieved when the angles to the known points are near right angles to each other (see Figure 7-1). Where the satellites are close together (refer to the right picture in Figure 7-1), the distance lines intersect with a small angle and it is more difficult to determine the exact point of intersection. HDOP is related to the volume formed by the intersection of the points of the user satellite vectors, with the user at the centre of the sphere. However, for speed accuracy parameter the relationship between HDOP and the Doppler frequencies assessed by GPS receivers on the ground is not so clear. At the same time, it might be possible that the geometric configuration of satellites, characterised by HDOP, could influence the accuracy of speed determination. This is because the Doppler frequency shift is dependent on the angle of the satellite's movement against the GPS receiver (Borio, Sokolova & Lachapelle 2009).

For positional determination, it is generally considered that if DOP values, including HDOP, are less than one, the GNSS situation for the receiver is ideal. When HDOP is more than one but less than 2, the situation is excellent (Texas Tech University 2015). In Texas Tech University (2015) one of the tables classifies GNSS reception for positional determination depending on DOP ranges in a way as follows:

DOP Value	Rating	Description
<1	Ideal	This is the highest possible confidence level to be used for applications demanding the highest possible precision at all times.
1-2	Excellent	At this confidence level, positional measurements are considered accurate enough to meet all but the most sensitive applications.
2-5	Good	Represents a level that marks the minimum appropriate for making business decisions. Positional measurements could be used to make reliable in-route navigation suggestions to the user.
5-10	Moderate	Positional measurements could be used for calculations, but the fix quality could still be improved. A more open view of the sky is recommended.
10-20	Fair	Represents a low confidence level. Positional measurements should be discarded or used only to indicate a very rough estimate of the current location.
>20	Poor	At this level, measurements are inaccurate by as much as 300 meters with a 6 meter accurate device (50 DOP × 6 meters) and should be discarded.

Figure 7-2: Positional accuracy and HDOP (Texas Tech University 2015)

The United States of America Department of Defence (1996), which is one of the fundamental documents on GPS, mentions that the expected velocity accuracy of GPS receivers on the ground, although not guaranteed, might be 0.4 m/sec (1.44 km/h) for 95% of measurements. However, this document does not mention how such accuracy might depend on GPS constellation parameters, multipath and other real life environmental factors. The US. Department of Defence (2008), which is the subsequent fundamental document on GPS, is more cautious about speed accuracy of GPS receivers on the ground and does not specify this parameter in km/h. However, this document specifies the horizontal speed error as follows:

$$UHVE=UERRE * HDOP, \quad (7.1)$$

where

- UHVE is the User Horizontal Velocity Error;
- UERRE is the User Equivalent Range Rate Error; and
- HDOP is Horizontal Dilution of Precision.

The above equation emphasises that the speed error would depend on HDOP. It also highlights that, ideally, i.e. if the receivers are of the same complexity with the same errors, it might be possible to derive a certain HDOP threshold when speed measurements are becoming unreliable.

In addition, in Clark (2015) it is also emphasised that the speed error generally depends on HDOP

and theoretical estimations are conducted on what the ideal speed accuracy of the receivers might be. The GPS signal carrier wavelength is ~20 cm and with a reasonable SNR the PLL inside the receiver can measure the carrier phase to about 1 cm. Therefore, for one second speed measurement intervals ~1 cm/sec of velocity error for a given satellite might be (in theory) achieved, which is equal ~0.04 km/h. To factor in the geometry and the fact that multiple satellites are observed, this error for horizontal speed should be multiplied by HDOP as recommended by Clark (2015). Since HDOP for the majority of records is typically less than three, this means that the "system" speed error is rarely (in theory) expected to be less than ~0.12 km/h. In practice, due to multipath around overpasses and sharp changes in SNR in the tree foliage environment, HDOP values calculated by the receivers might be misleading and hence errors could grow. If a receiver moves and a satellite is suddenly blocked by a tree, a receiver may not output a correct value of HDOP depending on time of blocking of a particular satellite versus a sampling rate. With rapid changes of the GPS reception around trees and one second rate of HDOP updates, the output HDOP values may not correspond to the reality. The effect of an addition or loss of a visible satellite (or different visible satellite for the situation when the total number of visible satellites remains the same) on HDOP depends on angular separation between that satellite and the rest of the visible satellites used for speed computation. If none of the remaining visible satellites were near that satellite, the effect of seeing or losing sight of the additional satellite would make a disproportionally big difference to the HDOP value. Therefore, rapid changes of the GNSS environment may provide incorrect HDOP reporting if such changes occur faster than the reported frequency, e.g. 1 Hz. However, considering the above information, the task of this investigation is to determine HDOP thresholds with the goal to try to filter out potentially unreliable speed records. Of course, because the GPS receivers have different magnitudes of errors, this HDOP threshold might be specific for each type of receiver.

Ideally, the task of further investigation is to consider if it is possible to put a similar table for GNSS speed records as shown in Figure 7-2 for positional accuracy depending on HDOP.

For a start, the speed data records from Feb 2015 drive from Melbourne to Echuca (described in chapter 5.3) were used to understand if individual speed outliers may be filtered out based on HDOP. Two geodetic quality receivers tested during this run were Novatel GPS ProPak-V3-L1 with 15° mask angle and Novatel OEM6 GPS + GLONASS with the same mask angle. The consumer grade receiver capable to output HDOP and used during this test was Columbus. All receivers under test generated a number of speed outliers mainly around overpasses on Eastlink Freeway and Eastern Freeway. Tables 7-1 to 7-3 represent each individual outlier with GPS parameters derived from NMEA data for Novatel receivers and Excel log-file for Columbus.

Table 7-1: GPS parameters for speed outliers produced by the GPS Receiver NovAtel ProPak-V3-L1

HDOP	Number of Satellites	Speed Difference, km/h
1.6	7	5.3
2.1	6	5.4
2.2	6	2.5
4.8	4	6.1
7.4	4	4.3
9.3	4	-6.0
26.3	4	7.6

Table 7-2: GPS parameters for speed outliers produced by the GPS + GLONASS Receiver NovAtel OEM6

HDOP	Number of Satellites	Speed Difference, km/h
0.9	12	2.5
1.1	11	2.7
1.1	12	6.0
1.2	8	-2.9
1.2	11	9.6
1.6	7	-2.7
7.2	6	3.8
9.2	6	5.8

Table 7-3: GPS parameters for the selected* speed outliers produced by GPS receiver Columbus

HDOP	Number of Satellites	Speed Difference, km/h
1.1	N/A	-12.0
1.1	N/A	-10.3
1.1	N/A	28.0
1.1	N/A	13.7
1.1	N/A	22.2
1.1	N/A	-10.0
2.1	N/A	-14.0

It should be noted that Columbus produced more speed outliers than shown in Table 7-3 for this run and only selected outliers are presented in Table 7-3. It is to note also that the Columbus GPS receiver does not record the Number of Satellites parameter in its log-file.

It is seen from the above Tables 7-1 to 7-3 that speed records with high values of HDOP might be used to potentially indicate a problem in speed accuracy. However, some records represent speed outliers while having low values of HDOP. Considering that equation (7.1) has been always correct, this means that the receivers could provide incorrect HDOP due to multipath around overpasses or tree foliage environments. Therefore, from an integrity point of view, it is safe to exclude speed records around overpasses from the assessment rather than rely on them even in case if HDOP values do not indicate a problem.

Tables 7-4 to 7-10 show the outliers with the respective GNSS parameters produced by all receivers under test during a kinematic test No3 described in 6.4.1. It should be noted that VBox receiver does not output HDOP in the log-file.

Table 7-4: GPS parameters for speed outliers produced by the GPS Receiver Novatel ProPak-V3-L1 with 5° mask angle on Monash Fwy

HDOP	Number of Satellites	Speed Difference, km/h
1.2	9	2.2
1.3	9	5.5
2.2	7	-2.1

Table 7-5: GPS parameters for speed outliers produced by the GPS Receiver Novatel ProPak-V3-L1 with 10° mask angle on Monash Fwy

HDOP	Number of Satellites	Speed Difference, km/h
1.4	8	2.5
1.6	4	4.0
2.0	7	2.0
2.1	6	-8.7
2.5	7	2.9
3.2	5	-2.2
3.5	5	-12.5
11.3	5	-27.9
50.0	4	3.3

Table 7-6: GPS parameters for speed outliers produced by the GPS Receiver Novatel ProPak-V3-L1 with 15° mask angle on Monash Fwy

HDOP	Number of Satellites	Speed Difference, km/h
1.4	7	4.6

Table 7-7: GPS parameters for speed outliers produced by the GPS + GLONASS Receiver Novatel OEM6 with 15° mask angle

HDOP	Number of Satellites	Speed Difference, km/h
1.1	11	3.1
9.9	7	9.7

Table 7-8: GPS parameters for speed outliers produced by the GPS receiver Garmin on Monash Fwy

HDOP	Number of Satellites	Speed Difference, km/h
0.8	11	-9.1
0.8	11	-4.6
0.8	11	2.0
1.0	10	-2.6
1.6	7	-10.5

Table 7-9: GPS parameters for speed outliers produced by the GPS receiver G-Log on Monash Fwy

HDOP	Number of Satellites	Speed Difference, km/h
0.8	11	2.0
0.8	11	-2.3

Table 7-10: GPS parameters for speed outliers produced by the GPS receiver Columbus on Monash Fwy

HDOP	Number of Satellites	Speed Difference, km/h
0.8	N/A	-5.3
0.9	N/A	3.0
0.9	N/A	4.1
0.9	N/A	3.2
0.9	N/A	-3.9
0.9	N/A	-11.6
1.0	N/A	-6.0
1.0	N/A	-3.0
1.1	N/A	-3.7
1.1	N/A	13.4
1.1	N/A	3.0
1.2	N/A	-9.1
1.3	N/A	4.6
1.3	N/A	2.5
1.3	N/A	2.3
1.4	N/A	-3.8
1.5	N/A	-8.4
1.7	N/A	-13.0
1.8	N/A	-10.1

Several examples are also given for the kinematic test No5 where the receivers were driven along roads with tree canopies.

In Figures 7-3 to 7-5 the outliers are shown for the respective receivers under test with corresponding satellite visibility parameters and/or HDOP.

UTC	Latitude	Longitude	HDOP	Number of	GPS speed	Vehicle time	Vehicle speed	Speed difference
061914	-37.9389	145.4025	2	5	89.157	61914	91.2	2.0
064113	-37.8368	145.518	3.9	4	72.848	64113	70	-2.8
065213	-37.8157	145.508	6.2	4	68.148	65213	66.1	-2.0
065233	-37.8188	145.5059	55.2	4	101.4	65233	77.4	-24.0
065234	-37.819	145.5059	55.2	4	71.311	65234	77.7	6.4
070423	-37.9283	145.4924	1.3	6	26.009	70423	28.4	2.4
070424	-37.9283	145.4923	6	4	25.372	70424	28.4	3.0
070448	-37.9263	145.4902	18.7	4	68.268	70448	63.7	-4.6
070449	-37.9262	145.49	18.9	4	61.814	70449	64.1	2.3
071444	-37.935	145.4066	26.5	4	78.76	71444	81.5	2.7
072330	-37.9985	145.344	8.7	4	76.352	72330	78.4	2.0
072654	-38.0175	145.3351	1.1	7	24.574	72654	26.6	2.0
072732	-38.0152	145.3333	1.1	7	19.414	72732	17.4	-2.0

Figure 7-3: Outliers generated by Novatel ProPak-V3-L1 with 5° mask angle for the kinematic test No5

UTC	Latitude	Longitude	HDOP	Number of satellites	GPS speed	Vehicle time	Vehicle speed	Speed difference
061432	-37.964423	145.36277	9.9	5	75.296	61432	73	-2.3
061648	-37.954567	145.38438	4.1	5	86.48	61648	83.8	-2.7
062001	-37.933588	145.41174	6.5	5	59.597	62001	74.8	15.2
062123	-37.929332	145.42496	7.5	5	58.406	62123	62.2	3.8
062439	-37.926212	145.44772	3.6	6	51.759	62439	54	2.2
062555	-37.924058	145.45991	4.2	5	54.426	62555	57.3	2.9
062622	-37.923027	145.46524	6.4	5	49.281	62622	54.4	5.1
062632	-37.921822	145.46568	3.7	5	58.532	62632	56.3	-2.2
063416	-37.903317	145.50813	9.9	5	76.322	63416	78.4	2.1
063536	-37.893308	145.52194	5.1	5	74.72	63536	78.9	4.2
063719	-37.878307	145.53143	3.7	6	86.492	63719	84.2	-2.3
064006	-37.846955	145.52632	4.5	5	75.165	64006	77.3	2.1
064143	-37.831592	145.51502	2.6	6	76.257	64143	78.3	2.0
064437	-37.806938	145.51653	3.1	7	85.858	64437	83.2	-2.7
064518	-37.804132	145.52399	3	7	78.667	64518	76.3	-2.4
064625	-37.79195	145.52146	1.2	9	80.876	64625	78.8	-2.1
065129	-37.809335	145.51106	1.9	8	65.288	65129	62.6	-2.7
065335	-37.82992	145.51392	3.7	5	87.518	65335	85.4	-2.1
065346	-37.83195	145.51535	1.3	8	79.1	65346	81.7	2.6
065741	-37.875072	145.53222	1.3	9	79.528	65741	81.6	2.1
065828	-37.884168	145.5319	5.3	5	74.565	65828	72	-2.6
065945	-37.894628	145.52018	7.3	5	75.976	65945	80.5	4.5
065949	-37.895207	145.51947	5.1	6	81.521	65949	78.5	-3.0
065950	-37.895372	145.51942	7.4	5	80.806	65950	78.7	-2.1
070423	-37.928308	145.49243	1.1	10	25.74	70423	28.4	2.7
070424	-37.928283	145.49235	1.1	10	25.318	70424	28.4	3.1
070503	-37.924915	145.48818	4.1	6	54.696	70503	50.5	-4.2
070626	-37.924658	145.47648	1.6	8	59.452	70626	57.2	-2.3
070627	-37.924803	145.4763	7.6	6	66.401	70627	57.3	-9.1

Figure 7-4: Outliers generated by Novatel OEM6 GPS + GLONASS with 15° mask angle for the kinematic test No5

Number of satellites	UTC	Latitude	Longitude	GPS spee	Vehicle time	Vehicle speed	Speed difference
8	65810	-2272.84	-8731.88	74.93	65810	81.2	6.3
8	65828	-2273.05	-8731.91	67.72	65828	72	4.3
8	65836	-2273.13	-8731.92	68.44	65836	70.7	2.3
8	65839	-2273.17	-8731.92	65.74	65839	69.1	3.4
7	65908	-2273.44	-8731.67	82.4	65908	84.6	2.2
8	70053	-2274.18	-8730.51	74.18	70053	77	2.8
8	70059	-2274.24	-8730.45	70.71	70059	77.8	7.1
7	70100	-2274.25	-8730.44	74.81	70100	77.7	2.9
5	70124	-2274.43	-8730.2	59.81	70124	62.6	2.8
6	70141	-2274.48	-8730.02	65.17	70141	62.2	-3.0
6	70150	-2274.55	-8729.98	54.01	70150	60.5	6.5
3	70151	-2274.55	-8729.97	68.21	70151	60.6	-7.6
6	70152	-2274.56	-8729.97	52.62	70152	60.8	8.2
6	70154	-2274.58	-8729.97	58.05	70154	60.6	2.6
5	70155	-2274.59	-8729.97	64.07	70155	60.7	-3.4
6	70156	-2274.6	-8729.96	57.82	70156	61	3.2
7	70221	-2274.77	-8729.99	65.18	70221	67.8	2.6
6	70234	-2274.9	-8730.03	73.77	70234	76.4	2.6
7	70246	-2275.02	-8730.07	56.12	70246	59.9	3.8
5	70248	-2275.04	-8730.06	54.05	70248	59.7	5.7
5	70249	-2275.05	-8730.06	55.54	70249	59.4	3.9
5	70257	-2275.13	-8730.07	69.85	70257	72.3	2.5
5	70304	-2275.2	-8730.08	60.37	70304	68.3	7.9
6	70305	-2275.21	-8730.08	72.54	70305	68.5	-4.0
8	70423	-2275.7	-8729.54	25.93	70423	28.4	2.5
5	70438	-2275.61	-8729.51	58.81	70438	55.7	-3.1
7	70443	-2275.59	-8729.46	59.26	70443	61.4	2.1
7	70541	-2275.48	-8728.99	50.82	70541	55.3	4.5
3	70627	-2275.48	-8728.58	51.55	70627	57.3	5.8
3	70637	-2275.51	-8728.47	60.25	70637	56.4	-3.9

Figure 7-5: Selected outliers generated by VBox for the kinematic test No5

Some outliers generated during the kinematic test No5 can be filtered based on high values of HDOP or number of satellites. This is visible, for example, in Figure 7-3 for the outliers shown in light red. However, other measurements show no signs of problems based on either number of satellites in view or HDOP. The same result was observed for the remaining receivers tested during the kinematic test No5 and in fact any other test conducted during this research.

Graphs of Appendix I also demonstrate no linear dependency of a speed error on HDOP for selected test drives and GNSS receivers.

Considering the results from the above test drives and consistency across all the receivers under test, it is possible to conclude that HDOP is not a reliable measure to filter individual speed outliers. The above tables and figures prove that it is not possible to solely rely on HDOP values when analysing each individual speed record for its integrity. HDOP values calculated by the receivers in the areas where multipath is present and specifically around overpasses might be misleading. Possibly, this is because the reflected GNSS signal from one or two specific satellites makes HDOP value looking good, whereas the real value of HDOP simply cannot be calculated by the receiver correctly. As a result, reliance on individual GPS/GNSS speed records based on the number of satellites and HDOP reported in such records might be unrealistic. This conclusion agrees with Zabrieszach (2013) where a statement is made that reliance on a single GPS speed observation is not appropriate. This is because the localised interferences may not necessarily be identified and corrected by the GPS receiver. As a result, the approach which analyses an array of speed observations for integrity is most optimal.

7.2 Signal to noise ratio as a measure to filter potentially unreliable speed records

The goal of this investigation was to investigate if it is possible to filter speed outliers based on changes in SNR between the neighbouring speed records.

SNR might change when a signal is reflected from structures like buildings or overpasses (Comp & Axelrad 1998; John A Dutton e-Education Institute 2015). In such instances, post-processing analysis might be conducted and outliers determined based on changes in SNR value for problematic speed readings compared to the neighbouring speed readings.

For this investigation, several speed outliers from kinematic tests No3 to No5 were taken for further analysis.

In Table 7-11 two selected outliers are presented for the kinematic test No3.

Table 7-11*:* Examples of GPS parameters for two selected outliers for the test route on Monash Fwy

	Speed error, km/h	Horizontal Dilution of Precision (HDOP)	Number of satellites used for navigation
Outlier No1 (time 01:37:46 UTC)	2.2	1.2	9
Outlier No2 (time 01:50:32 UTC)	5.5	1.3	9

Both outliers in Table 7-11 show very good GPS visibility. The environments where such outliers were generated (see Figure 7-6) represented typical freeway situations with speed differences 2.2 km/h (left) and 5.5 km/h (right).

Figure 7-6: Examples of the environments where selected speed outliers were generated by Novatel GPS receiver with a 5° mask angle on Monash Fwy

To further determine if it is possible to use SNR for filtering potentially unreliable speed records, NMEA data for such outliers should be assessed, including NMEA sentences for neighbouring records. Below is an example of NMEA data records generated by the GPS receiver Novatel ProPak-V3-L1 with 5° mask angle when the first outlier was generated as indicated in Table 7-11.

It should be noted that NMEA data format is stipulated in NMEA 0183 Standard (2013) and the relevant $GPGSV and $GPRMC messages generated by the receivers according to this Standard have the following structure:

$GPGSV,2,1,08,01,40,083,46,02,17,308,41,12,07,344,39,14,22,228,45*75

where:

GSV = Satellites in view;
2 = Number of sentences for full data;
1 = Sentence 1 of 2;
08 = Number of satellites in view;
01 = Satellite Pseudo Range Noise (PRN) number;
40 = Elevation, degrees;
083 = Azimuth, degrees;
46 = SNR - higher is better for up to 4 satellites per sentence; and

*75 = the checksum data, always begins with *.

$GPRMC,123519,A,4807.038,N,01131.000,E,022.4,084.4,230394,003.1,W*6A

where:

RMC = Recommended Minimum sentence C;
123519 = Fix taken at 12:35:19 UTC;
A = Status A=active or V=Void;
4807.038,N = Latitude 48 deg 07.038' N;
01131.000,E = Longitude 11 deg 31.000' E;
022.4 = Speed over the ground in knots;

084.4 = Track angle in degrees True;

230394 = Date - 23rd of March 1994;

003.1,W = Magnetic Variation; and

*6A = The checksum data, always begins with *.

In Figure 7-7 NMEA sentences are shown for the Outlier No1 (see Table 7-11) and the surrounding records.

Figure 7-7: NMEA data for the outlier generated at 01:37:46 UTC and the surrounding records

Considering the structure of the GSV and RMC messages, from the NMEA data shown in Figure 7-7 it is possible to see the following. The outlier with the magnitude of 2.2 km/h was generated in the environment where the speed record generated 1 sec before (at 01:37:45 UTC) is valid. However, the record after the outlier is determined by the receiver as invalid (at 01:37:47 UTC), i.e. excluded by the receiver from the assessment. Validity of records is based on the relevant field in $GPRMC message where V or A symbol is represented. There is no difference in SNR for all satellites used by the receiver for the outlier itself compared to neighbouring records. As a result, the user is totally unaware of the outlier looking at NMEA data. Further analysis demonstrated that similar situations are present for the outlier No2 (see Table 7-11) and in fact for almost any other outliers generated by GPS/GNSS receivers during this test.

The above example highlights that in environment where overpasses cause speed outliers, it is not always possible to rely on SNR for filtering potentially unreliable speed records. To further validate this conclusion for situations when outliers are generated in tree foliage environment, specific outliers were selected for kinematic tests No4 and No5.

In Table 7-12, two speed outliers are shown as examples for the kinematic test No4. These two records belong to the GPS receiver Novatel ProPak-V3-L1 with 10° mask angle. GPS parameters for these specific outliers and times of their generation in UTC are as follows:

Table 7-12: Examples of GPS parameters for outliers generated during the kinematic test No4

	Speed error, km/h	Horizontal Dilution of Precision (HDOP)	Number of satellites used for navigation
Outlier No1 (time 23:25:42 UTC)	3.1	2.4	4
Outlier No2 (time 23:36:43 UTC)	-4.8	7.6	4

Table 7-12 represents mixed examples of GPS parameters. While for outlier No2 an indication of the problem might be obtained from the high value of HDOP, this is not the case for the outlier No1. This is because for outlier No1 both the number of satellites and HDOP parameters are within reasonable limits. Also, the environments where such outliers were generated (see Figure 7-8) do not represent a significant challenge in the form of a grove of trees. This emphasises the fact that even individual trees may represent a challenge for GPS/GNSS receivers when precise speed measurements are required.

Figure 7-8: Examples of the environments where the Novatel ProPak-V3-L1 with 10° mask angle generated the outliers during the kinematic Test No4

For this test route, it also appears that the outliers are caused by a combination of multiple scattering of GPS signal from tree canopies and signal absorption. It is known that attenuation from a single tree at GPS frequencies takes place with different values depending on tree types as shown in Table 7-13 (Cavdar, Dincer & Erdoglu 1994):

Table 7-13: Examples of GPS signal attenuation at GPS frequency L1

Tree type	Coefficient of attenuation, dB/m	Average attenuation, dB
Pine	1.8	18.0
Maple	1.2	16.2
Poplar	0.7	3.5

It is possible that such signal attenuation as 18.0 dB or 16.2 dB, if it happens fast and randomly because of scattering and absorption from both foliage and tree branches, might not be handled by the receivers effectively. Figure 7-9 and Figure 7-10 show the NMEA data records generated by the relevant receiver at times of generation of the above outliers No1 and No2 (see Table 7-12) with the surrounding records.

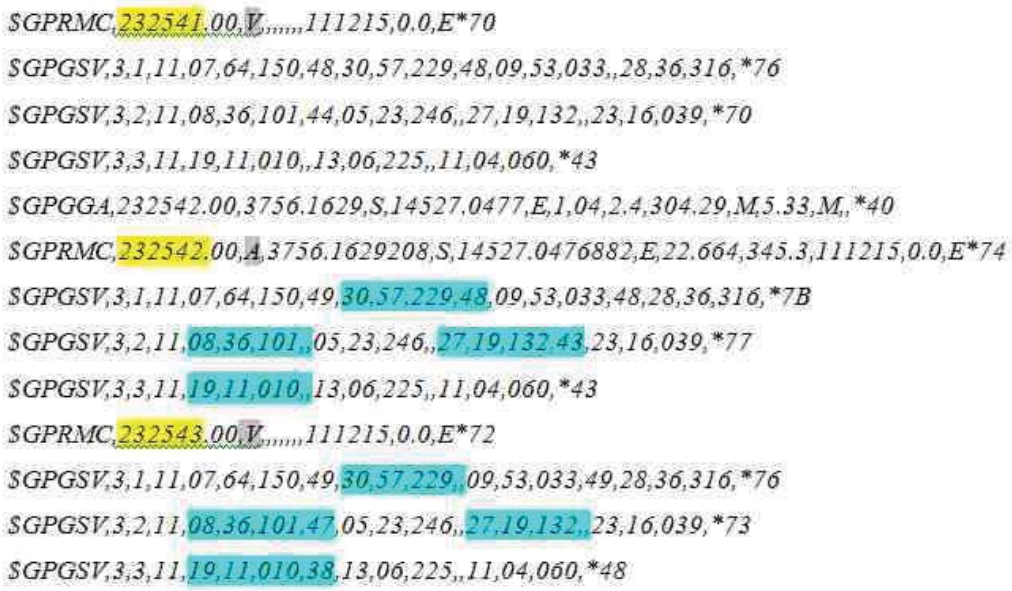

Figure 7-9: NMEA data for the outlier generated at 23:25:42 UTC and the surrounding records

From the above NMEA dataset it is noted that the outlier with the magnitude of speed error equal to 3.1 km/h (23:25:42 UTC, see Figure 7-9) was generated in environment where the immediately preceding and succeeding speed records were invalid, i.e. excluded by the receiver from the assessment. It is also noted that there is a significant difference in SNR for the satellites with PRN numbers 30, 8, 27 and 19 at the time when the outlier was generated compared to the immediately succeeding speed record generated at 23:25:43 UTC (see data in aqua colour in Figure 7-9). It is

very likely that shadowing from the tree canopies changed the SNR values for several satellites or completely prevented some satellite availability within a particular second and the receiver could not handle this situation. A similar occurrence could be seen for the outlier No2 (see Figure 7-10) where satellites PRN 8 and PRN 19 also have completely different SNR values during a 1 sec timing interval (data in aqua colour), although at a lesser scale compared to the outlier No1.

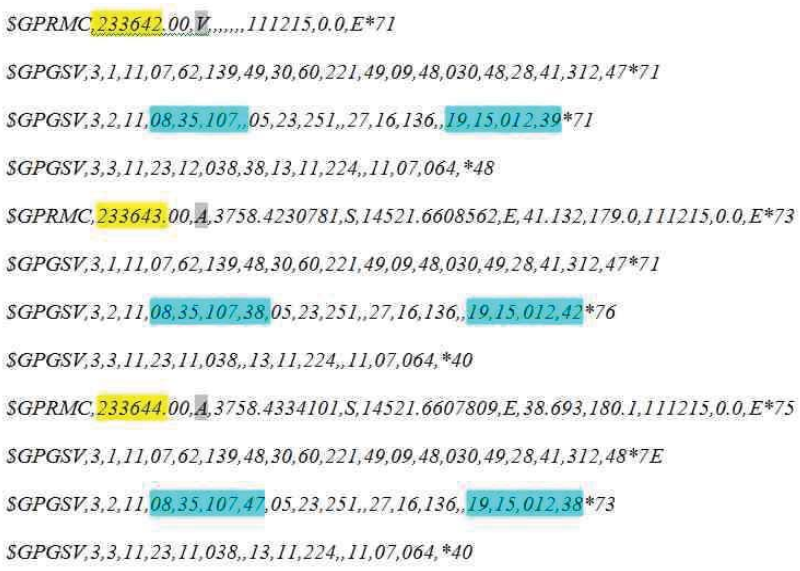

Figure 7-10: NMEA data for the outlier generated at 23:36:43 UTC and the surrounding records

One more example is selected from the kinematic test No5 in tree foliage environment for Novatel ProPak-V3-L1 GPS receiver with 5° mask angle. The selected outlier has the parameters shown in Table 7-14:

Table 7-14: GPS parameters for the outlier generated during the kinematic test No5

	Speed error, km/h	Horizontal Dilution of Precision (HDOP)	Number of satellites used for navigation
Outlier (time 07:04:23 UTC)	2.3	1.3	6

Figure 7-11 shows NMEA data records observed for the time when the outlier was generated and around this time:

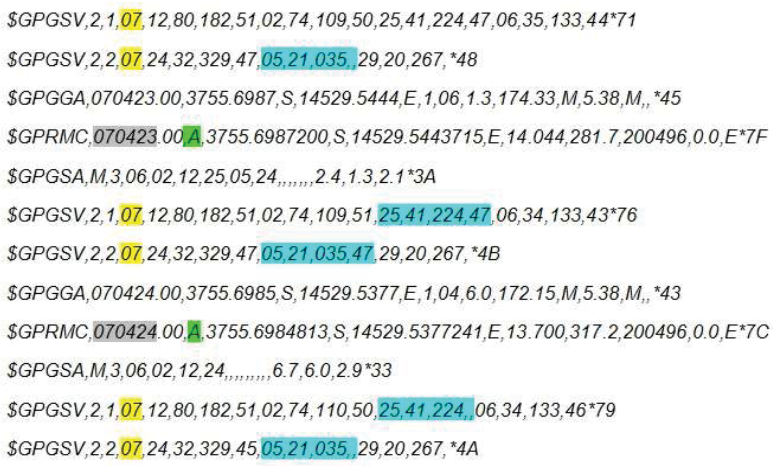

Figure 7-11: NMEA data for the outlier generated at 07:04:23 UTC and the surrounding records

NMEA data in Figure 7-11 (see data in aqua colour) demonstrates that for the satellites 5 and 25 the SNR value sharply changed in the problematic record compared to surrounding records. It is likely that this change caused the outlier to occur.

The above examples highlight that while sometimes it is possible to use changes in SNR as a good indication of an outlier (tree foliage environment), in other instances the use of SNR to filter the outliers might be problematic (freeway with overpasses environment). Therefore, changes in SNR might be considered as a good indication of a problem for selective GPS environments.

7.3 Higher mask angles for filtering of speed outliers

The goal of this assessment was to estimate an option of using high mask angle to filter potential speed outliers. As shown in Zhang (2007), theoretically this option is a possibility. However, as previously discussed in chapter 6, this may not be the case in practice.

Tables 7-15 to 7-17 represent the results from kinematic tests No3 to No5 in a summarised manner for receivers with mask angles of 5°, 10° and 15°.

Table 7-15: Number of speed outliers for the kinematic test No3 on Monash Fwy

GPS/GNSS Receiver	Number of GPS/GNSS speed records with the speed error greater than ± 2 km/h	Number of GPS/GNSS speed records with the speed error greater than ± 3 km/h
GPS receiver with 5^{o} mask angle	3	1
GPS receiver with 10^{o} mask angle	9	5
GPS receiver with 15^{o} mask angle	1	1
GPS + GLONASS receiver with 15^{o} mask angle	2	2

Table 7-16: Number of speed outliers for the kinematic test No4

GPS/GNSS Receiver	Number of GPS/GNSS speed records with the speed error greater than ± 2 km/h	Number of GPS/GNSS speed records with the speed error greater than ± 3 km/h
GPS receiver with 5^{o} mask angle	3	0
GPS receiver with 10^{o} mask angle	14	4
GPS receiver with 15^{o} mask angle	9	2
GPS + GLONASS receiver with 15^{o} mask angle	10	6

Table 7-17: Number of speed outliers for the kinematic test No5

GPS/GNSS Receiver	Number of GPS/GNSS speed records with the speed error greater than ± 2 km/h	Number of GPS/GNSS speed records with the speed error greater than ± 3 km/h
GPS receiver with 5^{o} mask angle	13	4
GPS receiver with 10^{o} mask angle	7	1
GPS receiver with 15^{o} mask angle	6	0
GPS + GLONASS receiver with 15^{o} mask angle	29	8

Tables 7-15 to 7-17 demonstrate that the higher mask angle does not necessarily improve the performance in the generation of outliers. Considering that the types of GPS receivers were the same ProPak-V3-L1 and all of them had identical GPS settings except the mask angle, there is no clear dependency between the mask angle and the number of speed outliers generated.

The second conclusion is that additional constellation, e.g. GLONASS, does not improve the performance of the GNSS receiver for speed determination. This is demonstrated by results between GPS only and GPS + GLONASS receivers in chapter 6.

8 CONCLUSION

8.1 Summary

Modern sophisticated navigation and control applications require speed measurement of vehicles. In many instances, speed measurements are derived from GPS/GNSS receivers. These receivers will operate in real-world environment with obstructions. As a result, GPS/GNSS receivers might produce speed records with higher errors compared to open sky environments. Therefore, it is required to evaluate the accuracy of GPS / GNSS speed measurements in challenging environments. This research specifically focused on two challenging GNSS environments: overpasses / road gantries and areas of tree foliage. To address the research objectives, a solution to test geodetic quality, medium range and consumer grade GPS/GNSS receivers for speed accuracy has been developed and implemented. The materials presented focused largely on methods of testing for speed accuracy in real-world environments and improving the robustness of the test through proper calibration of the test asset. Subsequently, the research focused on practical speed testing of several GPS / GNSS receivers of different complexities. Finally, the research included processing of GNSS speed records to understand more about GNSS speed measurements and errors associated with them. The main outcomes of this research are as follows:

8.1.1 Outcomes related to the designed speed measurement system

- The non-GPS based speed measurement system has been designed, assembled, tested and implemented. The system performed favourably during all experiments in terms of robustness and its ability to test GNSS receivers in real-world environments.
- Calibration methods and electronic diagrams supporting calibration methods were developed for the speed measurement system to maintain its accuracy.
- The uncertainty of measurement budgets were developed to determine the actual speed accuracy parameters for the speed measurement system.

8.1.2 Outcomes related to testing of GPS/GNSS receivers for speed accuracy

- The outcomes from the speed tests show that that the surrounding environment may have substantial influence on GPS/GNSS speed accuracy. This influence has been proven from both the trial test and the subsequent kinematic tests when the environmental factors got worse with each subsequent test. It has been validated that the speed error of GNSS receivers might be relatively high around overpasses where multipath may affect the accuracy of speed measurements. It has been further demonstrated that speed errors of GNSS receivers might be worse in areas where tree foliage is present compared to overpasses. The research proved that speed measurements conducted by consumer grade and medium range GPS receivers cannot be relied upon in tree foliage environment. The

number of outliers generated by these medium range and consumer grade receivers in tree foliage environment was excessively high. Tree foliage provides both scattering and attenuation of the GNSS signal causing difficulties to accurately measure speed. It was validated that even a single tree can significantly influence the speed accuracy parameter even when the receiver did not report any deterioration in the number of satellites in view and HDOP. It should be highlighted that in both challenging environments, e.g. overpasses and tree canopy, the majority of speed outliers had good GPS visibility parameters. Users are often not aware of these issues experienced by GNSS receivers in such environments.

- In this research, while high end geodetic GPS and GNSS receivers performed better compared to medium range and consumer grade receivers, they still experienced speed spikes of up to several km/h. Such spikes include instances when the receivers were configured with relatively high elevation mask filtering. Medium range and consumer grade GPS receivers may generate a substantial number of measurement outliers around overpasses with up to 10 km/h reported errors in speed measurements. The number of outliers for all GPS/GNSS receivers increases in tree canopy environment. This conclusion, however, should not be generalised. Independent testing of each receiver is encouraged to reveal its true performance in real-world environments. At the same time, it is possible to conclude that more sophisticated GPS/GNSS receivers are likely to achieve better speed accuracy in challenging environments. For applications where the GPS/GNSS speed accuracy is very important, the user should select the appropriate receivers to achieve desired outcome.
- It was determined that the benefit of having additional GNSS constellations to complement GPS speed measurements in terms of improving speed accuracy is marginal. Multiple examples were seen when GPS + GLONASS receiver had similar performance as GPS only receiver. This relates to both challenging environments tested in this research.
- The research demonstrated that the number of speed outliers generated by GPS/GNSS receivers has no direct correlation with mask angle values between 5° and 15°. This result was observed for both overpasses and tree foliage environments.
- It has also been demonstrated that the specific GPS receivers may perform well in relation to the others around overpasses; however, their relative performance may change in tree foliage environment, and vice versa. This highlighted the necessity of individual testing of GPS/GNSS receivers in each type of environment.
- The research topic of filtering potential GPS speed outliers is very broad and there are many possible methods that can be used. Since the receivers could only output HDOP, number of satellites and SNR (SNR for NovAtel only receivers), the use of these parameters to filter out unreliable GNSS speed records was investigated in this research. Such methods have been chosen because they can be used in practice for the majority of GPS receivers,

including medium range and consumer grade types. It has been demonstrated that it is not always possible to rely on SNR values to filter potentially unreliable speed records. While reliance on SNR changes might be used for GPS speed records generated in tree foliage environments, this is not always the case for records generated around overpasses or road gantries. It has been demonstrated that HDOP and number of satellites are also not suitable parameters to filter speed outliers. Therefore, reliance on individual GPS based speed measurements in challenging environments, even if such measurements demonstrate good GPS parameters, may not be justified.

The above conclusions cannot be generalised for all receivers. However, they highlight the importance of testing individual receivers to derive their true behaviour in different environments.

8.2 Future research

This research has investigated the accuracy of GNSS speed measurements in two challenging environments. It is evident that environmental conditions significantly affect the quality of GNSS speed measurements. Considering the results of this research and outliers generated by the receivers in various challenging environments, the next step of research is to develop theoretical algorithms to be embedded into GNSS receivers to improve their speed accuracy measurements in challenging environments. Also, it would be interesting to investigate the use of dual frequency GNSS receivers to understand if speed accuracy of measurements can be improved. In addition, the lack of GNSS measurement accuracy in challenging environments can be compensated with the use of accelerometers in conjunction with GNSS. This area of research is worth exploring. On top of that, the quality of GNSS antennas is worth exploring and its linkage with the speed outliers generated by identical GNSS receivers. Finally, future research should focus on developing filtering methods to eliminate GNSS speed outliers and understanding the correlation between a speed error and the direction of the Doppler measurement from the satellite versus the direction of travel of the vehicle. It is possible that the number of satellites contributing to the speed measurement solution is less important than this satellite-vehicle alignment for Doppler speed measurements.

As a final commentary, this research focused on several GNSS receivers made available in the research. There is no doubt that future development of GNSS technology will improve the accuracy of speed measurement in the real-world environments.

REFERENCES

Abd-Elazeem, M, Farah, A & Farrag, F 2010, 'Cut-off Elevation Angle Effect on GPS Positioning Accuracy', *Al-Azhar University Engineering Journal*, JAUES, Vol.5, No.1, pp.565-570.

Advantage Enterprises, Inc 2012, *PressurePro Product Catalog*, Advantage Enterprises, Inc, viewed 9 August 2014, <http://advantagepressurepro.com/images/upload/FullCatalogJune12.pdf>.

Advantage PressurePro LLC 2014, *PressurePro 10 Wheel TPMS Monitor 2014, PressurePro, Realiable Under Pressure Tire Pressure Monitoring Systems*, viewed 13 November 2013, <http://advantagepressurepro.com>.

Agilent 2009, *Agilent 81110 Family of Pulse Pattern Generators Datasheet*, Ver.1.3.

Al-Gaadi, K 2005, 'Testing the Accuracy of Autonomous GPS in Ground Speed Measurements', *Journal of Applied Sciences*, Vol. 5, pp. 1518-1522.

Applied Concepts 2016, *Stalker Scoreboard PC Application & Stalker Pro II Speed Sensor, User Manual 011-0116-00 Rev J*, Applied Concepts, viewed 15 August 2016, <https://www.stalkerradar.com/oem/downloads/011-0116-00_Pro_II_Speed-Sensor-Scoreboard_manual.pdf>.

Asia Pacific Legal Metrology Forum 2004, *Handbook on Traceability in Legal Metrology*, Asia-Pacific Economic Cooperation, Committee on Trade and Investment, Subcommittee on Standards and Conformance, viewed 27 July 2017, <http://publications.apec.org>.

ASTM International Standards Worldwide 2010, *Standard Test Method for Speed and Distance Calibration of Firth Wheel Equipped with Either Analog or Digital Instrumentation,* ASTM F457-04, viewed 11 May 2016, Retrieved from ASTM International Database.

Austroads 2012, *Commentary to AG:PT/T535 – Road Speed Calibration*, viewed 15 March 2015, < https://www.onlinepublications.austroads.com.au/items/AGPT-T535-12>.

Bahrami, M 2008, 'GNSS Doppler Positioning (An Overview)', University College London, Geomatics Lab, *A Paper Prepared for the GNSS SIG Technical Reading Group*.

Bai, Y, Sun, Q, Du, L. & Bai J 2015, 'Two Laboratory Methods for the Calibration of GPS Speed Meters', *Measurement Science and Technology*, Vol 26, viewed 1 September 2015, <http://iopscience.iop.org>.

Ballinger Technology 2015, *SDS Detector*, viewed 13 January 2014, <http://www.ballingertech.com.au/speedometer-sds-detector.html>.

Bell, S 2013, *A Beginner's Guide to Uncertainty of Measurements*, National Physical Laboratory, Issue 2, viewed on 01 March 2013, <https://www.wmo.int/pages/prog/gcos/documents/gruanmanuals/UK_NPL/mgpg11.pdf>.

Bies, L 2016, *Time Synchronisation with a Garmin GPS*, viewed 15 April 2014, <http://www.lammertbies.nl/comm/info/GPS-time.html>.

Borio, D, Sokolova, N & Lachapelle, G. 2009, 'Doppler Measurements and Velocity Estimation: A Theoretical Framework with Software Receiver Implementation', PLAN Group, Department of Geomatics Engineering, University of Calgary, ION GNSS, Savannah, Georgia.

Brzostowski, K, Darakchiev, R, Foks-Ryznar, A & Sitek, P 2012, 'The Location GNSS Modules for the Components of Proteus System', Space Research Center of the Polish Academy of Sciences, *Artificial Satellites*, Vol.47, No3, pp.91-109, viewed 2 May 2017, <https://www.degruyter.com/downloadpdf/j/arsa.2012.47.issue-3/v10018-012-0016-8/v10018-012-0016-8.pdf>.

CanMore Electronics Co Ltd 2013, *GP-101 Sport Tracker / Guide Mate,* CanMore Electronics Co Ltd, viewed 13 April 2013, <http://www.canmore.com.tw>.

Cavdar, IH, Dincer, H & Erdoglu, K 1994, 'Propagation Measurements at L-Band for Land Mobile Satellite Link Design', *Proceedings of the 7th Mediterranean Electrotechnical Conferenc*e, Antalya, Turkey, 12-14 April, pp.1162-1165, viewed 3 June 2015, <http://ieeexplore.ieee.org/document/380862/?reload=true>.

Chalko, T 2009, *Estimating Accuracy of GPS Doppler Speed Measurement using Speed Dilution of Precision (SDOP) Parameter*, viewed 1 May 2015, <http://nujournal.net/SDOP.pdf>.

Chowdhury, A, Chakravarty, T & Balamuralidhar, P 2014, 'Estimating True Speed of Moving Vehicle using Smartphone based GPS Measurement', *Conference Proceedings - IEEE International Conference on Systems, Man and Cybernetics* , article. No 6974444 , pp. 3348 – 3353, viewed 12 April 2915, <http://ieeexplore.ieee.org/document/6974444/>.

Christophersen, HB, Pickell, RW, Neidhoefer, JC, Koller, AA, Kannan, SK, & Johnson, EN 2006, 'A compact guidance, navigation, and control system for unmanned aerial vehicles', *Journal of Aerospace Computing, Information, and Communication*, Vol.3(5), pp.187–213.

Clark, T 2015, *GPS Determination of Course and Speed*, viewed 13 December 2015, <http://www.aprs.net/vm/gps_cs.htm>.

Comp, CJ & Axelrad, P 1998, 'Adaptive snr-based carrier phase multipath mitigation technique', *IEEE Transactions on Aerospace and Electronic Systems*, Vol.34, No.1, pp.264-276.

Cook, R 2002, *Assessment of Uncertainties of Measurement for Calibration and Testing Laboratories*, 2nd edn, viewed 15 March 2013, retrieved from NATA database.

Corrys Datron Sensorsystems GmbH 2008, Correvit SFII Sensors - Correvit S-350 Non-contact 2-axis Optical Sensor, User Manual, Vol.1, pp.29.

Dickey John Corporation 2013, Radar II Top-off-the-line Speed, Sensor, Dickey John Corporation, viewed 13 March 2014, < http://www.dickey-john.com/product/radar-ii/>.

Ding, W & Wang, J 2011, 'Precise Velocity Estimation with a Standalone GPS Receiver', Journal of Navigation, Vol. 64, pp.311-325.

Dobbert, M & Stern, R 2009, 'A Pragmatic Method for Pass/Fail Conformance Reporting that Complies with ANSI Z540.3 ISO17025, and ILAC G8', Agilent Technologies, NCSL International Workshop and Symposium, San Antonio, Texas, USA.

Durrant, A. & Hill, M 2005, *Technical Assessment of the DL2S GPS Data Quality including comparative data from the VBOX 3 (with optional DGPS) and an optical speed sensor*, Race Technology Ltd, May 2005.

Dybedal, J 2013, Doppler Radar Speed Measurement Based on a 24 GHz Radar Sensor, Masters of Science in Electronics, Norwegian University of Science and Technology, Department of Electronics and Telecommunications, Trondheim.

Dyukov, A 1988, *A Device to Control the Necessary Diameter of a Reel*, Patent (Author Certificate) of the USSR No 1388374.

Dyukov, A 1990, *A Device to Control the Cartridge Glue Machine Tool*. Patent (Author Certificate) of the USSR No1535812.

Dyukov, A 2016a, 'Development of an Electronic Speed Measurement System for Evaluating the Accuracy of GNSS Receivers and Statistical Analysis of Their Performance in Speed Measurements', *Universal Journal of Electrical and Electronic Engineering*, Vol.4(2), pp.33-50.

Dyukov, A 2016b, 'Mask Angle Effects on GNSS Speed Validity in Multipath and Tree Foliage Environments', *Asian Journal of Applied Sciences*, Vol.04, Issue 02, pp.309-321.

Dyukov, A 2016c, 'Test Vehicle Speed Error as a Function of Tire Pressure', *Journal of Traffic and Transportation Engineering*, Vol.4, No2, pp.102-107.

Dyukov, A, Choy, S & Silcock, D 2015, 'Accuracy of Speed Measurements using GNSS in Challenging Environments', *Asian Journal of Applied Sciences*, Vol.03, Issue 06, pp.794-811.

Eitel, E 2014, *Basics of Rotary Encoders: Overview and New Technologies*, viewed 7 May 2014, < http://www.machinedesign.com/sensors/basics-rotary-encoders-overview-and-new-technologies-0>.

Eurachem 2007, *Use of Uncertainty Information in Compliance Assessment*, Eurachem / Citac Guide, 1st edn, 15 pp.

Eurachem/Citac Guide 2011, *Quantifying Uncertainty in Analytical Measurement*, Third Edition, Eurachem, Olomouc, Czech Republic, May 2011.

Evans, J 1996, *Straightforward Statistics for the Behavioral Sciences*, Pacific Grove, CA: Brooks/Cole Publishing.

Expert Law 2012, GPS as Speed Data in Court, viewed 4 August 2012, <http://www.expertlaw.com/forums/showthread.php?t=139313>.

Fleetmatics 2015, *What is telematics*, Fleetmatics, viewed 27 January 2015, <http://www.fleetmatics.com.au/what-is-telematics>.

Garmin Corporation 2009, *Garmin GPS 72H Owner's Manual*, Rev.B, Garmin Corporation, Shijr, Taipei County, Taiwan.

Goldhirsh, J & Vogel, W 1998, *Handbook of Propagation Effects for Vehicular and Personal Mobile Satellite Systems, Overview of Experimental and Modeling Results*, The Johns Hopkins University and The University of Texas, Austin, TX.

Hannah, BM 2001, 'Modeling and Simulation of GPS Multipath Propagation', PhD Thesis, Queensland University of Technology, Brisbane.

Heng, L, Walter, T, Enge, P & Gao, G 2015, 'GNSS Multipath and Jamming Mitigation Using High Mask Angle Antennas and Multiple Constellations', *IEEE Transactions on Intelligent Transportation Systems*, Vol.16, Issue 2, pp.741-750.

How, J, Pohlman, N & Park, C 2002, *'GPS Estimation Algorithms for Precise Velocity, Slip and Race Track Position Measurements'*, Society of Automotive Engineers Inc, Cambridge.

Huang, D 2013, ‘Evidential Problems with GPS Accuracy: Device Testing’, A Thesis submitted to the Graduate Faculty of Design and Creative Technologies in partial fulfilment of the requirements for the degree of Master of Forensic Information Technology, School of Computer and Mathematical Sciences, Auckland, New Zealand.

Inside GNSS 2016, *Multipath vs. NLOS Signals*, viewed 8 February 2016, <http://www.insidegnss.com/node/3789>.

International Frequency Sensor Association 2004, *Universal Frequency to Digital Converter (UFDC-1) 2004, Specification and Application Note*, International Frequency Sensor Association, Barcelona, Spain.

Jankovic, J, Topic, Z, Cvetkovic, J & Marendic-Miljkovic, J 2012, ‘The New Method for Testing of Speed Measuring Devices in Road Traffic’, 5th International Scientific Conference on Defensive Technologies, Belgrade, Serbia, 18-19 September 2012.

John A Dutton e-Education Institute 2015, *GPS and GNSS for Geospatial Professionals, Multipath*, Department of Geography, College of Earth and Mineral Sciences, viewed 15 December 2015, <http://www.e-education.psu.edu/geog862/node/1721>.

John A Dutton e-Education Institute 2017, *Lesson 4: Receivers and Methods*, Department of Geography, College of Earth and Mineral Sciences, viewed 27 July 2017, <https://www.e-education.psu.edu/geog862/book/export/html/1659>.

Keskin, M, Sekerli, Y & Kahraman, S 2014, ‘Performance of Two Low Cost GNSS Receivers for Ground Speed Measurements Under Varying Speed Conditions’, 5th International Scientific Symposium for PhD Students and Students of Agricultural Colleges, Poland, 18-20 September 2014.

Kistler 2014, *Correvit SFII Sensors*, Kistler Group, viewed 12 February 2014, <https://www.kistler.com/?type=669&fid=60353>.

Klimanek, M 2010, ‘Analysis of the Accuracy of GPS Trimble JUNO ST Measurement in the conditions of Forest Canopy’, Journal of Forest Science, Czech Republic, 56, 2010 (2), pp.84-91.

Lachapelle, G, Henriksen, J & Melgard, T 1994, ‘Seasonal Effect of Tree Foliage Signal Availability and Accuracy for Vehicular Navigation’, *Department of Geomatics Engineering, The University of Calgary,* Salt Lake City, 21-23 September 1994.

Leica Geosystems AG 2013, *Leica FlexLine TS02/TS06/TS09 User Manual*, Leica Geosystems, Ver.1.0, Heerbrugg, Switzerland.

Leica Geosystems AG 2004, *Leica GS20 Professional Data Mapper 2004, Configuration Setting Manual, Device Management,* Survey & Engineering Division, Leica Geosystems, Heerbrugg, Switzerland.

Libelium Comunicaciones Distribuidas S.L. 2014, *Wasprome GPS Programming Guide*, Ver.4.6, Libelium Comunicaciones Distribuidas S.L., Zaragosa, Spain.

Longacre Racing Products 2016, *Longacre 2" Digital Tire Pressure Gauge*, Longacre Part # 53036, viewed 6 April 2016, <http://www.longacreracing.com/products.aspx?itemid=1715&prodid=7305>.

Lopez, I, Silva, G & Ruiz, A 2014, 'Calibration of Non-contact Velocity Sensor used in Automotive Industry', IMECO International Conferences, Cape Town, South Africa, 3-5 February 2014.

Mainline Automotive Equipment Pty Ltd 2014, Mainline DynoLog Dynamometers, viewed 3 June 2016, <http://mainlinedyno.com.au/index.php/products/dynamometers/premium-range/2wd/standard-modes-of-operation>.

McLarson, B 1997, 'VHF/UHF/Microwave Radio Propagation: A Primer for Digital Experiments', A Workshop given at the 1997 TAPR/ARRL Digital Communications Conference, Baltimore, United States, 10-12 October 1997.

Mediatek Inc 2010, *Mediatek – 3329 Datasheet 2010*, Rev.A03, Mediatek Inc, Hsinchu, Taiwan.

Mekik, C & Can, O 2010, 'Multipath Effects in RTK GPS and A Case Study', International Symposium on GPS/GNSS, Taipei, Taiwan, 26-28 October 2010.

Metrology Training International Pty Ltd 2005, *Measurement Uncertainty Estimation*, A Three Day Short Course for Laboratory and Testing Staff based on ISO Guide to the Expression of Uncertainty of Measurements, Course No008.

Metrology Training International 2006, *The Drongo's Guide to Determining Measurement Uncertainty*, Metrology Training International, Melbourne, Australia.

Microchip Technology Inc 2006a, *HPC Explorer Board FAQs and Troubleshooting Guide*, Microchip Technology Inc, Chandler, Arizona, United States.

Microchip Technology Inc 2006b, *MPLAB IDE Quick Start Guide*, Microchip Technology Inc, Chandler, Arizona, United States.

MicroEngineering Labs Inc 2005, PICBASIC PRO™ Compiler, CD Recording, MicroEngineering Laboratories, Colorado Springs, United States.

Moscitta, A, Pianegiani, F & Petri, D 2004, 'Measurement Uncertainty in Decision Assessment for Telecommunication Systems', Technical Report #DIT-04-050, University of Trento, Trento, Italy, April 2004.

National Aeronautics and Space Administration 2010, *Estimation and Evaluation of Measurement Decision Risk*, NASA Handbook NASA-HDBK-8739.19-4, pp.207, NASA, Washington, D.C., United States.

National Coordination Office for Space-Based Positioning, Navigation and Timing 2014, Official U.S. Government information about the Global Positioning System (GPS) and related topics, Applications, Timing, viewed 2 April 2016, <http://www.gps.gov/applications/timing/>.

National Marine Electronics Association 2002, *NMEA 0183 Standard*, Ver.3.01, viewed 12 December 2013, <http://www.nmea.org/content/nmea_standards/nmea_0183_v_410.asp>.

National Measurement Institute 2015, Length and Related Quantities Capabilities, viewed 17 October 2015, <http://www.measurement.gov.au/Services/calibrationtesting/Pages/LengthandRelatedQuantities.aspx>.

NovAtel Inc 2007, *OEMV Family Installation and Operation User Manual*, Rev.13, NovAtel Inc, Calgary, Alberta, Canada.

NovAtel Inc 2013, *ProPak-V3TM Product Sheet*, Rev.5, NovAtel Inc, Calgary, Alberta, Canada.

NovAtel Inc 2014a, *OEMV Family Firmware Reference Manua*l, Rev.8, NovAtel Inc, Calgary, Alberta, Canada.

NovAtel Inc 2014b, *OEM6 Family Firmware Reference Manual*, Rev.7, Novatel Inc, Calgary, Alberta, Canada.

NovAtel Inc 2014c, *OEM6 Family Installation and Operation User Manual*, Rev.8, Novatel Inc, Calgary, Alberta, Canada.

NovAtel Inc 2015, *Model List for NovAtel, D11873*, Revision 40, Novatel Inc, Calgary, Alberta, Canada.

NVS Technologies AG 2012, *Protocol Specification, GPS / GLONASS / GALILEO / COMPASS Receivers*, Ver.1.3, Oberriet, Switzerland.

Ogle, J, Guensler, R, Bachman, W, Koutsak, M & Wolf, J 2002, 'Accuracy of Global Positioning System for Determining Driver Performance Parameters', Transportation Research Record 1818, Paper No 02-1063, pp.12-24.

Ono Sokki Co, Ltd 2017, ‘GPS Speedometer LC-8100A/8200A’, viewed 1 December 2017, <https://www.onosokki.co.jp/English/hp_e/products/keisoku/automotive/lc8100_8200.html>.

Perez-Ruiz, M & Upadhyaya, S 2012, ‘GNSS in Precision Agricultural Operations’, viewed 14 January 2017, < https://cdn.intechopen.com/pdfs-wm/39780.pdf>.

Pinana-Diaz, C, Toledo-Moreo, R, Betaille, D & Gomez-Scarmeta, A 2011, ‘GPS multipath detection and exclusion with elevation-enhanced maps’, 14th International IEEE Conference on Intelligent Transportation Systems (ITSC), Washington, D.C., United States, 5-7 October 2011.

Polar Australia 2016, *Polar RCX3 User Manual*, viewed 17 February 2016, <http://www.polar.com/e_manuals/RCX3/Polar_RCX3_user_manual_English/ch04.html>.

Queensland Police Service 2016, *Chapter 6 Traffic Manual Speed Detection*, Queensland Police Service, viewed 3 March 2016, <https://www.police.qld.gov.au/corporatedocs/OperationalPolicies/Documents/TrafficManual/Chapter6.pdf>.

Racelogic 2013, *VBox Sport Guide*, Racelogic, Issue 10, Buckingham, United Kingdom.

Roberts, C 2015, ‘Factors Affecting GNSS Heighting’, Institution of Surveyors NSW, June conference, Bowral, Australia, 19 June 2015.

Sathyamorthy, D, Shafii, S, Amin, ZM, Jusoh, A & Ali SZ 2015, ‘Evaluation of the Accuracy of Global Positioning System (GPS) Speed Measurement via GPS Simulation’, Defense S and T Technical Bulletin, Ministry of Defence, Malaysia, 8 (2), pp.121-128.

Sbisa, P 2013, personal communication with U-blox, 2 July 2013.

SeaStar Solutions 2015*, GPS Speedometers*, SeaStar Solutions, viewed 14 January 2016, <http://www.seastarsolutions.com/products/instrumentation/instruments-2/gps-speedometres/>.

Serrano, L, Kim, D, Langley, RB, Itani, K & Ueno, M 2004, ‘A GPS Velocity Sensor: How Accurate Can It Be? — A First Look’, Proceedings of the ION National Technical Meeting 2004, Institute of Navigation, San Diego, California, United States, 26-28 January 2014**.**

Shier, R 2004, *Statistics: 1.1 Paired T-tests*, Mathematics Learning Support Centre, viewed 10 May 2014, <http://www.statstutor.ac.uk/resources/uploaded/paired-t-test.pdf>.

SiRF Technology, Inc 2007, *Sirfstar III Product Overview*, Rev.1.2, San Jose, California, United States.

SIRF Technology, Inc 2010, *SIRFStarIV GSD4E, High-sensitivity GPS Location Processor with Built-in CPU and SiRFaware Technology, Product Overview*, San Jose, California, United States.

Supej, M & Cuk, I 2014, ‘Comparison of Global Navigation Satellite System Devices on Speed Tracking in Road (Tran)SPORT Applications’, *Sensors*, Vol.14, pp.23490-23508.

Szarmes, M, Ryan, S, Lachapelle, G. & Fenton, P 1997, ‘DGPS High Accuracy Aircraft Velocity Determination Using Doppler Measurements’, Proceedings of International Symposium on Kinematic Systems in Geodesy, Geomatics and Navigation - KIS97, Department of Geomatics Engineering, The University of Calgary, Banff, Canada, 3-6 June 1997.

Terminal software 2013, Freeware downloadable from <https://sites.google.com/site/terminalbpp>, downloaded 3 December 2013.

Texas Tech University 2015, Principles of GPS Operation, viewed 15 February 2014, <http://gis.ttu.edu/gist4310/documents/lectures/>.

Tranquilla, JM, Carr, JP & Al-Rizzo, HM 1994, ‘Analysis of a choke ring ground plane for multipath control in Global Positioning System (GPS) applications’, *IEEE Transactions on Antennas and Propagation*, Vol.42, No7, July 1994, pp.905-911.

Transystems Inc 2011, G-Log 760 GPS Recorder User’s Manual, Ver.1.1 pp.28.

Truebridge, N 2014 'GPS speeds „accurate"', viewed 12 December 2014, <http://www.stuff.co.nz>.

Tyre Size Calculator 2014, viewed 8 December 2014, < http://www.inawise.com/tyre-calculator/tyre-size-calculator.html>.

U-blox 2011, *MAX-6 U-blox 6 GPS Modules*, Data Sheet, U-blox, Thalwil, Switzerland.

U-blox 2013a, *3GPP Test Report U-blox M8 FW2.01 with 4dB margin*, U-blox, Thalwil, Switzerland.

U-blox 2013b, *U-blox 6, Receiver Description Including Protocol Specification 2013, Document Number GPS.G6-SW-10018-F, Revision 7.03 (Public Release)*, U-blox, Thalwil, Switzerland.

U-blox 2013c, *U-blox 7, Receiver Description Including Protocol Specification V14, Document Number GPS.G7-SW-12001-B, Protocol Version 14.00 (Public Release)*, U-blox, Thalwil, Switzerland.

U-blox 2014, *MAX-7 U-blox 7 GPS Modules*, Data Sheet UBX13004068-R05, U-blox, Thalwil, Switzerland

United States of America Department of Defence 1996, NAVSTAR GPS User Equipment Introduction, Public Release Version, September 1996.

United States of America Department of Defence 2008, Global Positioning System Standard Positioning Service Performance Standard, 4th edn.

United States Department of Transportation 2014, *Study of the Impact of a Telematics System on Safe and Fuel-efficient Driving in Trucks*, Federal Motor Carrier Safety Administration, viewed 4 April 2015, <https://ntl.bts.gov/lib/51000/51800/51836/13-020-Study_of_the_Impact_of-a_Telematics_System_Full_Report.pdf>.

Van Dierendonck, AJ, Fenton, P & Ford, T 1992, 'Theory and performance of narrow correlator spacing in a GPS receiver', *NAVIGATION*, Vol.39, No3.

VicRoads 2016, *Intelligent Speed Assist*, VicRoads, viewed 1 August 2016, Available at: <https://www.vicroads.vic.gov.au/safety-and-road-rules/driver-safety/speeding/intelligent-speed-assist>.

Victory Co Ltd 2011, Columbus V-990 Multifunction GPS Data Logger User Manual 2011, Ver.1.0.

Vishay Semiconductors 2010, *4N25 Optocoupler Phototransistor Output with Base Connection Datasheet*, Rev.1.8, Malvern, Pennsylvania, United States.

Viswanathan, R 2005, 'Evaluation of Ground Speed Sensing Devices Under Varying Ground Surface Conditions', A Thesis Submitted to the Faculty of the Graduate College of the Oklahoma State University in the partial fulfilment of the requirements for the degree of Master of Science, Stillwater, OH, United States.

Wachendorff Automation GmbH & Co 2013, Encoder WGD 58H 2013, Online Data Sheet, pp.14.

Wainwright, R 2007 'Father and son stick to guns to prove radar wrong', *The Sydney Morning Herald,* 12 March, viewed 25 November 2014, <http://www.smh.com.au/news/national/father-and-son-stick-to-guns-to-prove-radar-wrong/2007/03/11/1173548023012.html>.

Witte, TH & Wilson AM 2004, 'Accuracy of non-differential GPS for the determination of speed over ground', Journal of Biomechanics, Vol. 37, pp. 1891-1898.

Zabrieszach, D 2013, 'ITS Activity in Australia, Australian Report 204WG9N0177, ISO TC 204', *WG9 Meeting*, Seattle, Washington, USA, 15-16 April 2013.

Zhang, J 2007, 'Precise Velocity and Acceleration Determination Using a Standalone GPS Receiver in Real Time', PhD Thesis, RMIT University, School of Mathematical and Geospatial Sciences, Melbourne, Australia.

Zhang, J, Zhang, K, Grenfell, R & Deakin R 2006, 'On the relativistic Doppler effect for precise velocity determination using GPS', Journal of Geodesy, Vol.80, pp.104-110.

Zhao, C 2015, *GPS Timing*, ASIGA Research Presentation, Edith Cowan University, viewed on December 15, 2015, <http://www.gravity.uwa.edu.au/docs/ANZAC/GPS_Timing.pdf>.

Zhao, W, Goodchild, A & McKormack E 2011, 'Evaluating the Accuracy of Spot Speed Data from Global Positioning Systems for Estimating Track Level Speed', *Transportation Research Record: Journal of the Transportation Research Board*, Vol.2246, pp.101-110.

Zhuang, W 1994, 'Performance Analysis of GPS Carrier Phase Observable', IEEE Transactions on Aerospace and Electronic Systems, Vol.32, No2, pp.754-767.

Appendix A: UFDC-1 CONNECTION DIAGRAM

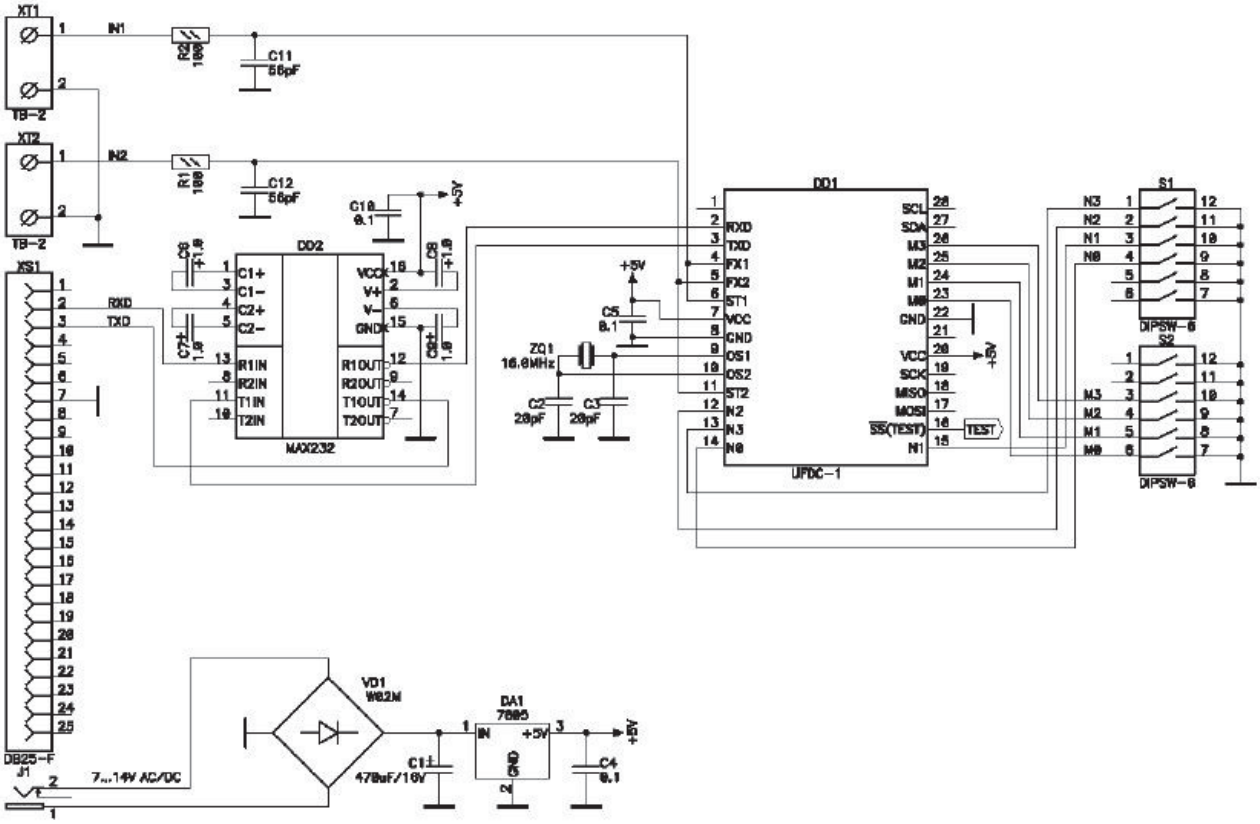

Figure A.1: Full UFDC-1 connection diagram

Appendix B: TRIAL TEST ROUTE

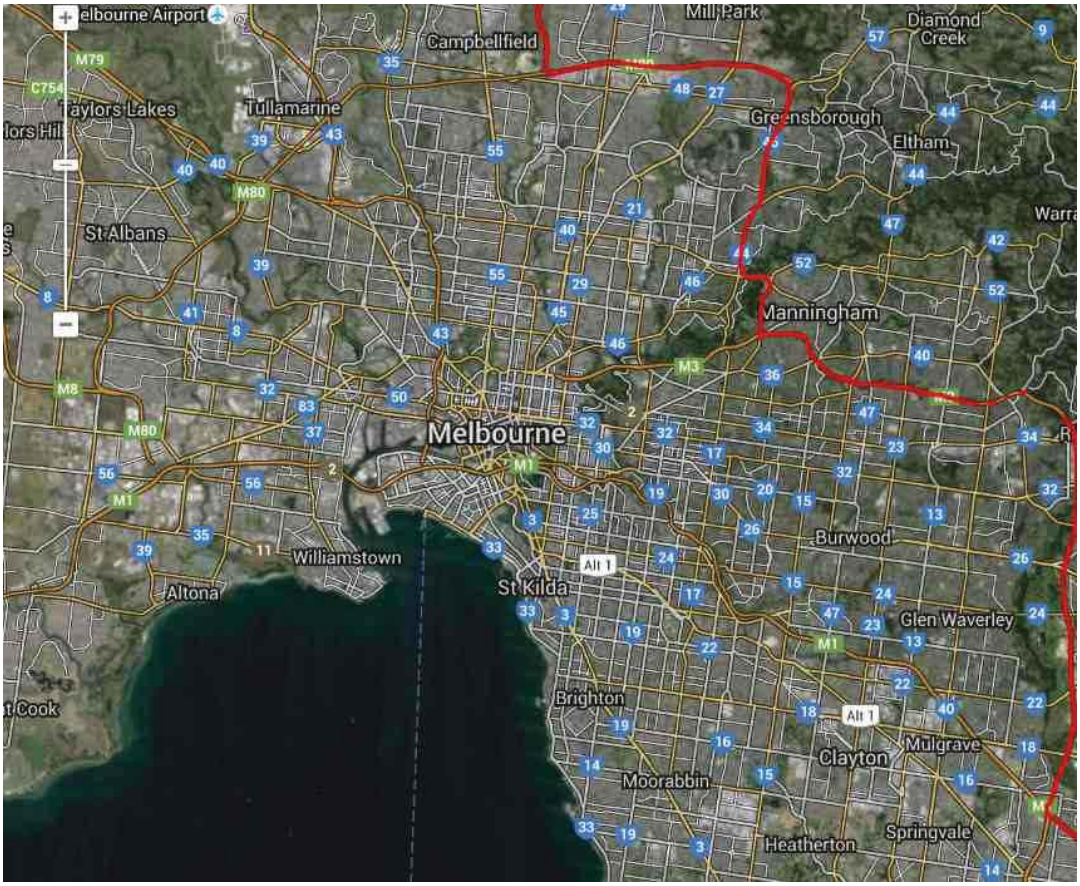

Figure B.1: Trial test route in Melbourne area

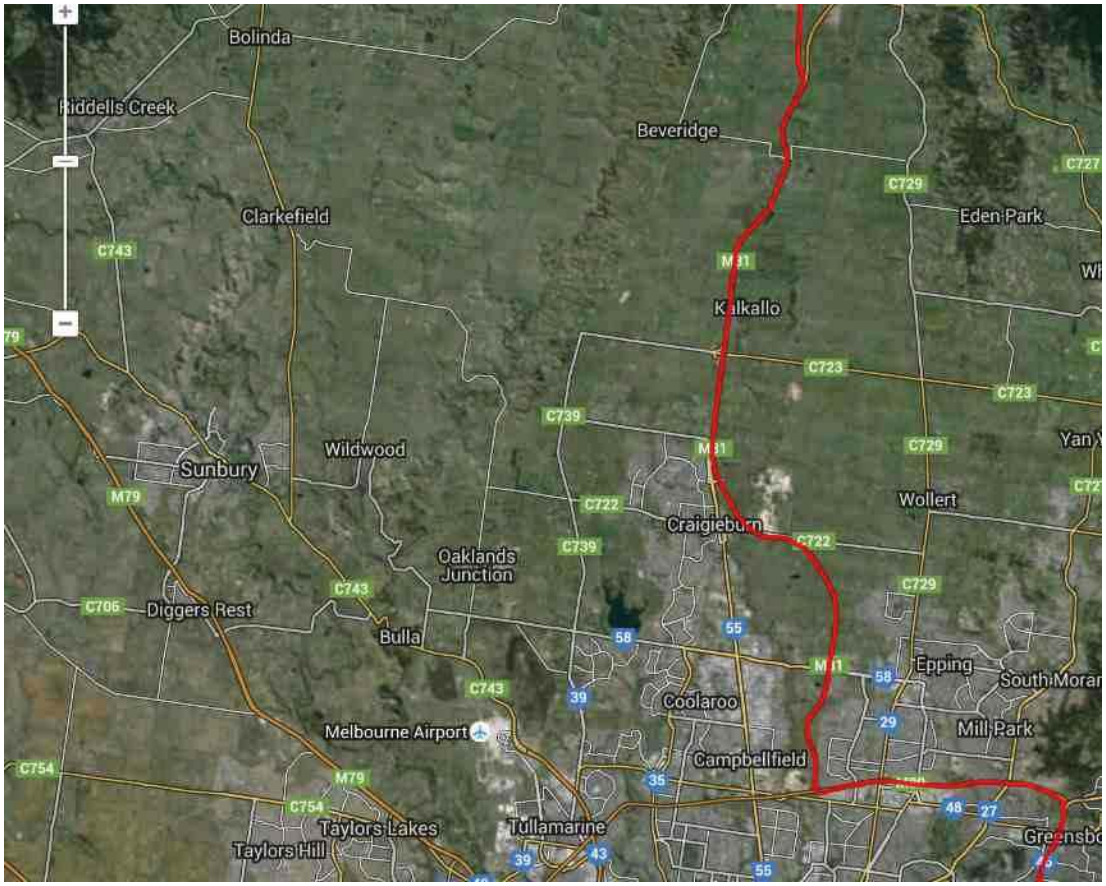

Figure B.2: Trial test route in the countryside

Appendix C: SPEED DIFFERENCE DISTRIBUTIONS AFTER PROCESSING OF THE TRIAL TEST DATA

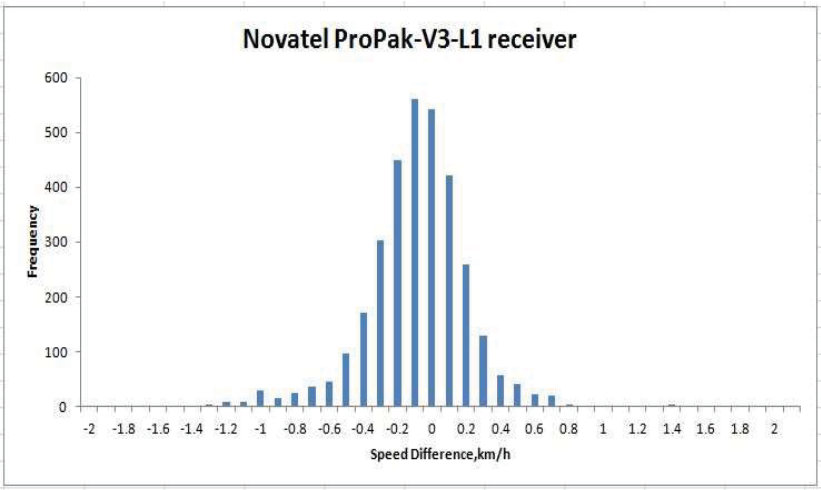

Figure C.1: Speed difference distribution for Novatel ProPak-V3-L1 GPS receiver

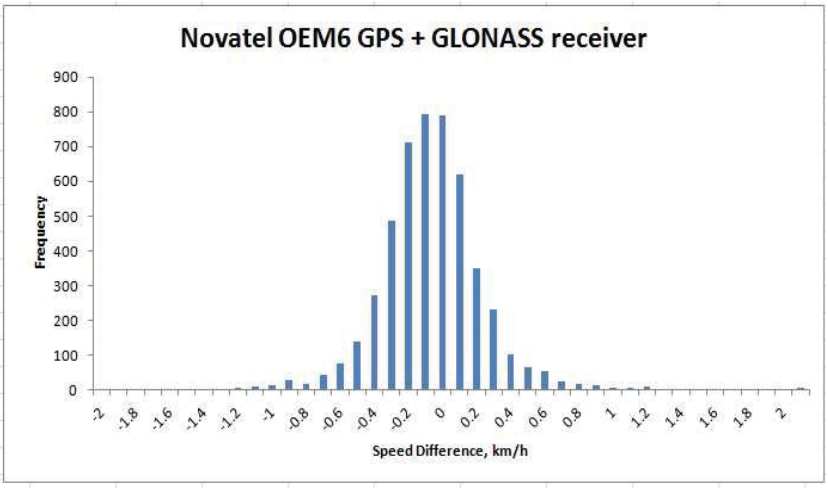

Figure C.2: Speed difference distribution for Novatel OEM6 GPS + GLONASS receiver

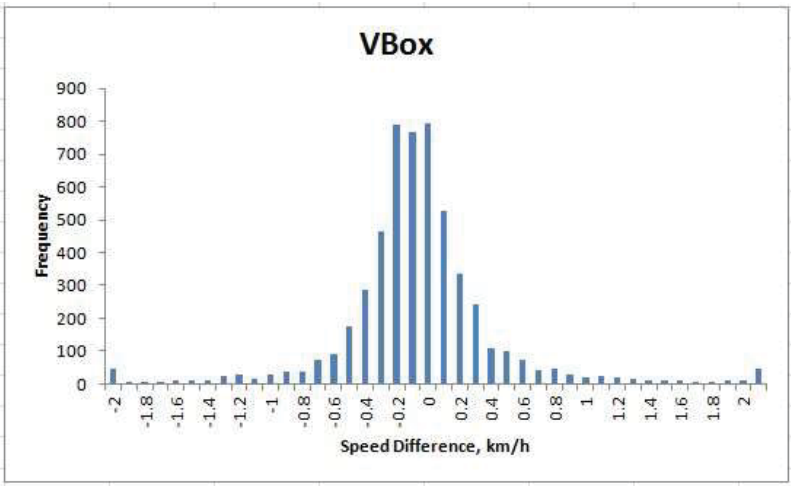

Figure C.3: Speed difference distribution for VBox GPS receiver

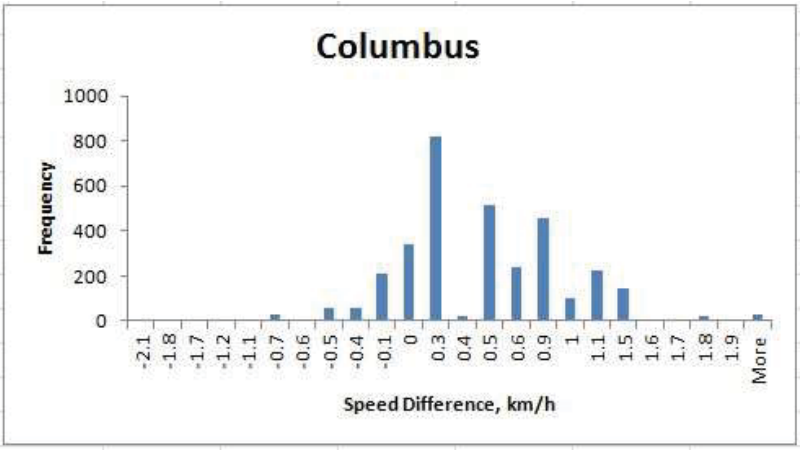

Figure C.4: Speed difference distribution for Columbus GPS receiver

Appendix D: EXAMPLES OF THE ENVIRONMENTS WHERE GPS SPEED OUTLIERS WERE GENERATED DURING A TRIAL TEST

Figure D.1: Example of the environment where an outlier was generated by Novatel OEM6

Figure D.2: Example of the environment where an outlier was generated by VBox

Figure D.3: Example of the environment where an outlier was generated by Columbus

Appendix E: SPEED DIFFERENCE DISTRIBUTIONS FOR A TEST CONDUCTED AT MONASH FWY WITH OVERPASSES

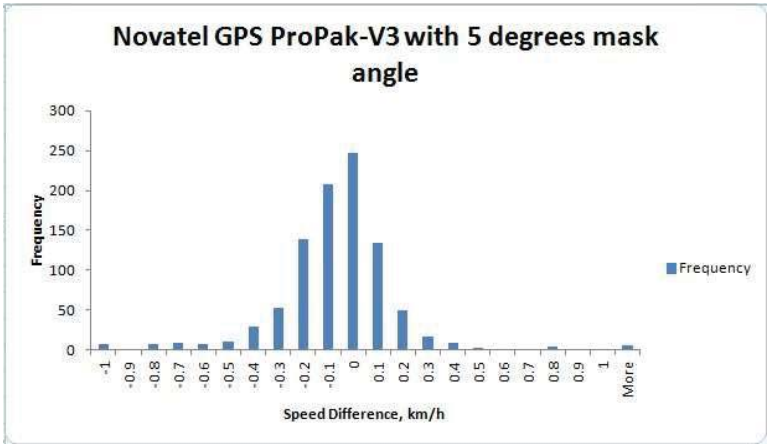

Figure E.1: Speed difference distribution for the Novatel GPS ProPak-V3-L1 with 5° mask angle

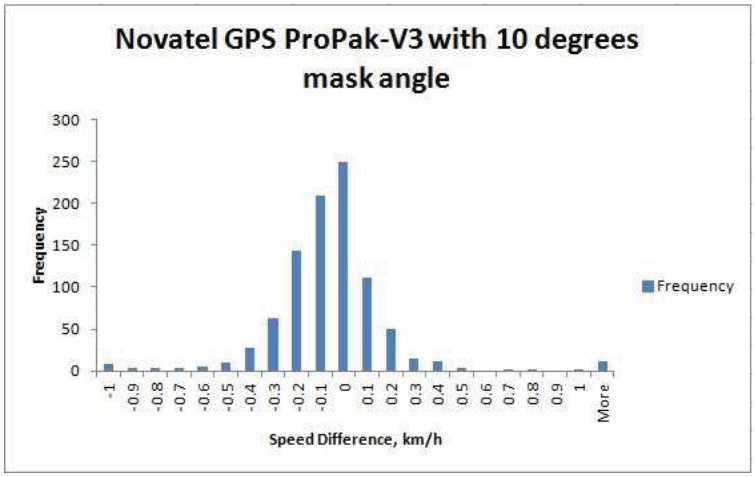

Figure E.2: Speed difference distribution for the GPS Novatel GPS ProPak-V3-L1 with 10° mask angle

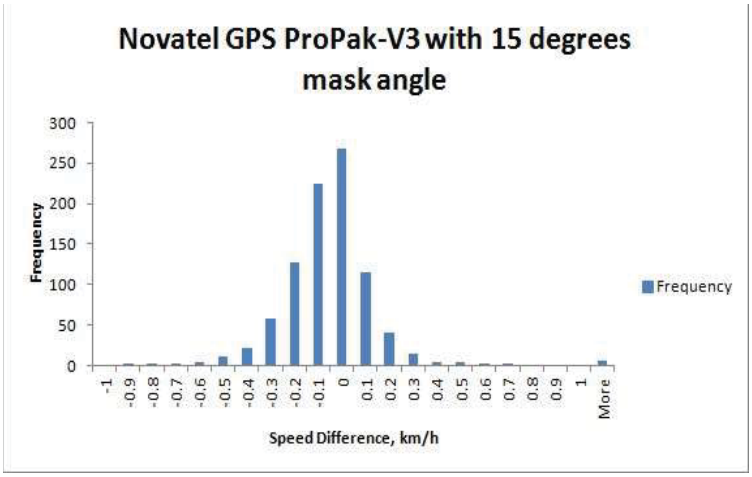

Figure E.3: Speed difference distribution for the Novatel GPS ProPak-V3-L1 with 15° mask angle

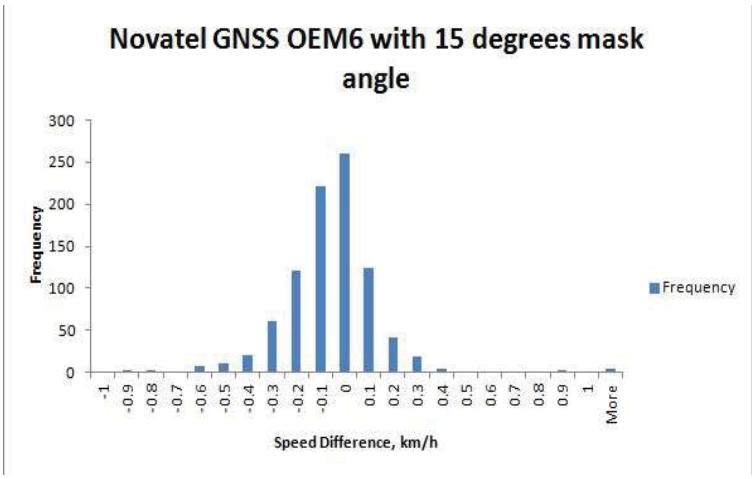

Figure E.4: Speed difference distribution for the Novatel OEM6 GPS + GLONASS receiver with 15° mask angle

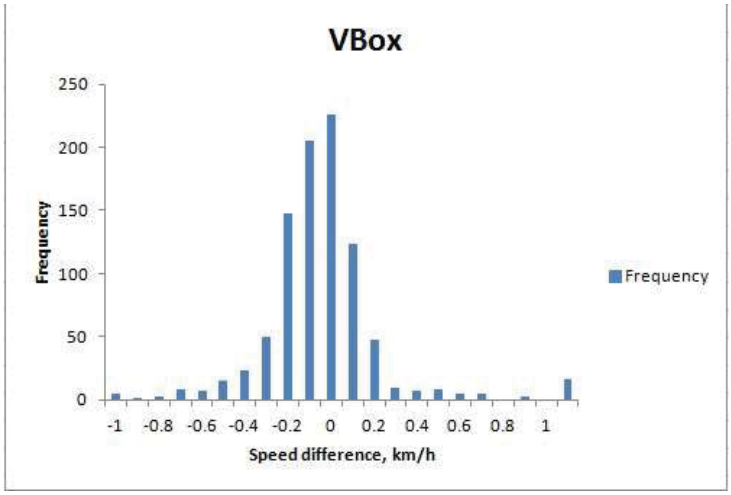

Figure E.5: Speed difference distribution for VBox

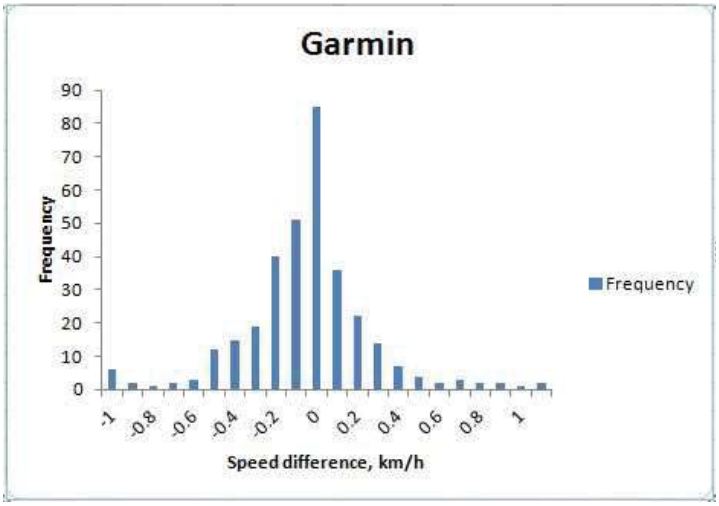

Figure E.6: Speed difference distribution for Garmin

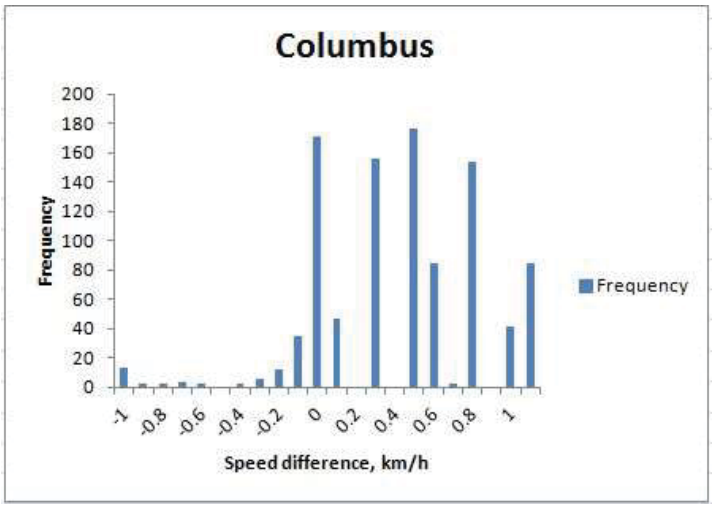

Figure E.7: Speed difference distribution for Columbus

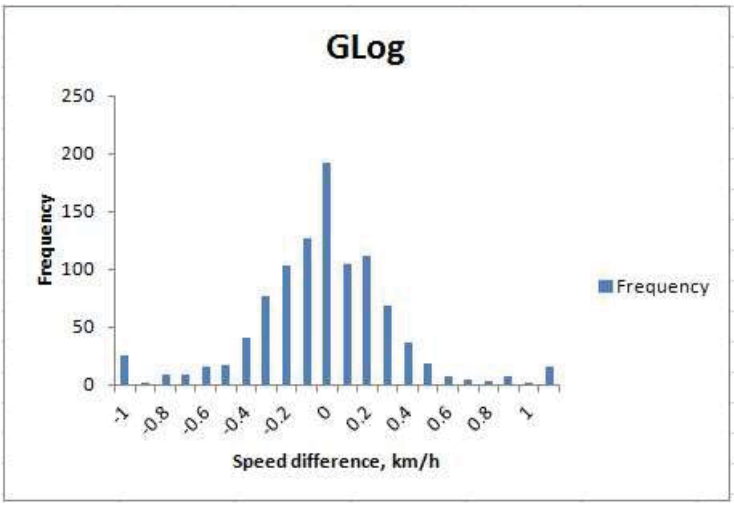

Figure E.8: Speed difference distribution for G-Log

Appendix F: EXAMPLES OF THE ENVIRONMENTS WHERE GPS SPEED OUTLIERS WERE GENERATED DURING A TEST DRIVE AT MONASH FWY

Figure F.1: An outlier of Novatel with a 10° elevation mask around a road gantry (Speed error = 12.6 km/h, Number of satellites in view = 5, HDOP = 3.5)

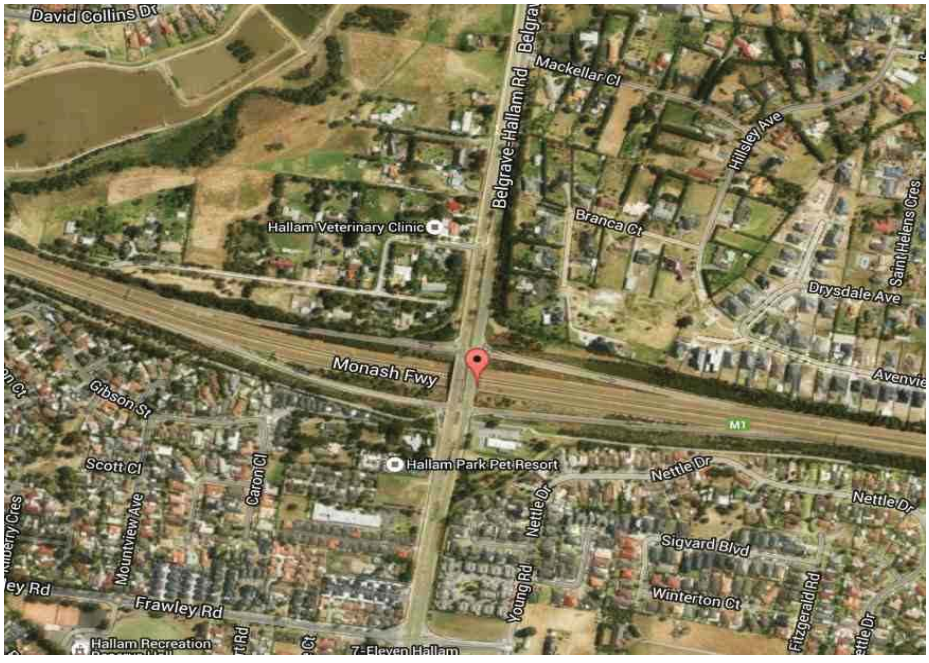

Figure F.2: An outlier of Novatel with 15° elevation mask (Speed error = 4.6 km/h, Number of satellites in view = 7, HDOP = 1.4)

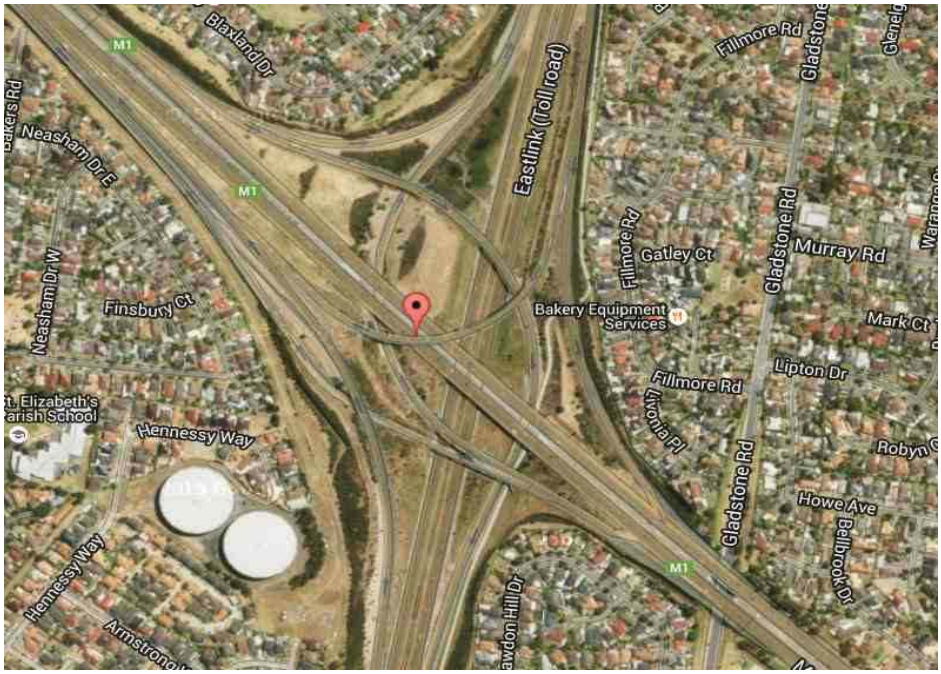

Figure F.3: An outlier of Novatel OEM6 GPS + GLONASS with a 15° elevation mask (Speed error = 9.8 km/h, Number of satellites in view = 7, HDOP = 9.9)

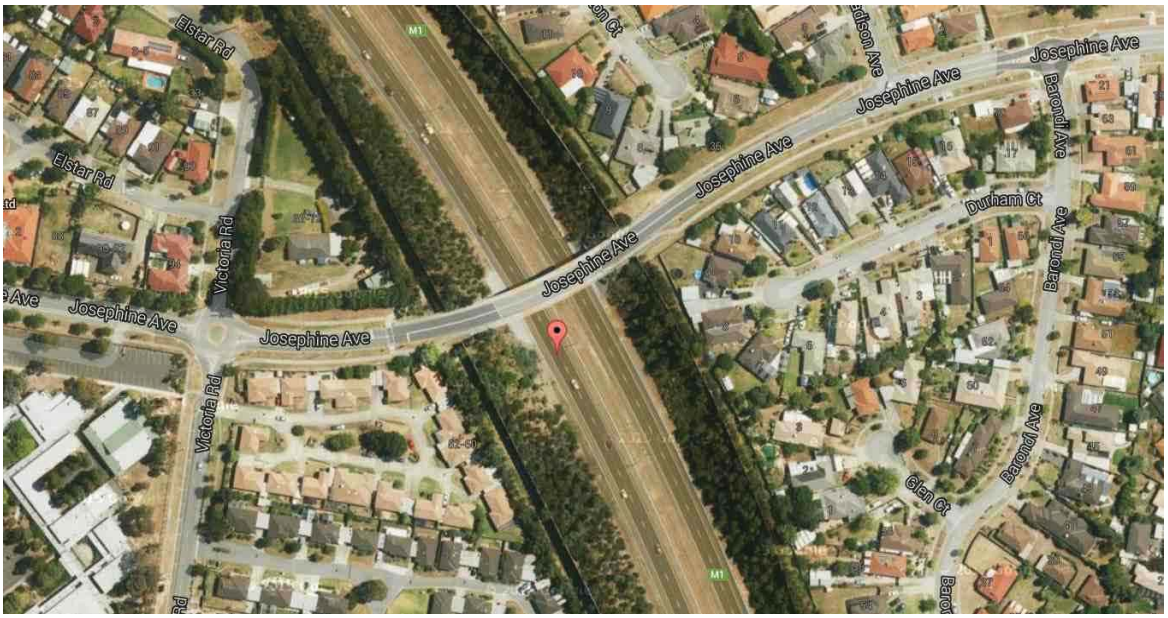

Figure F.4: An outlier of VBox with a 7º mask angle (Speed error = 11.5 km/h, Number of satellites in view = 10)

Figure F.5: An outlier of Garmin (Speed error = -9.1 km/h, Number of satellites in view = 11, HDOP = 0.8)

Figure F.6: An outlier of Columbus (Speed error = 13.4 km/h, HDOP = 1.1)

Appendix G: EXAMPLES OF THE ENVIRONMENTS WHERE GPS SPEED OUTLIERS WERE GENERATED ON ROADS WITH TREE FOLIAGE

Figure G.1: An aerial view for an outlier of Novatel OEM6 with 15° mask angle (Speed error = 12.74 km/h, Number of satellites in view = 7, HDOP = 3.9)

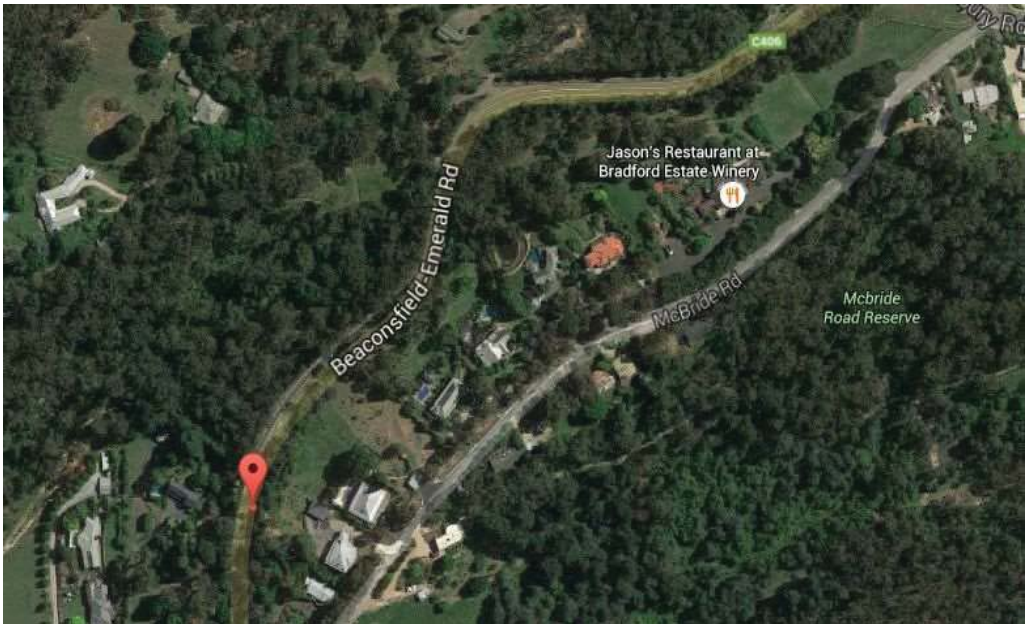

Figure G.2: An aerial view for an outlier of VBox (Speed error = 15.1 km/h, Number of satellites in view = 9)

Figure G.3: Street view for an outlier of Garmin GPS (Speed error = 2.3 km/h, Number of satellites in view = 8. HDOP = 0.8)

Figure G.4: An aerial view for an outlier of G-Log (Speed error = 4.11 km/h, Number of satellites in view = 8, HDOP = 0.95)

Figure G.5: An aerial view for an outlier of Columbus (Speed error = 5.9 km/h, HDOP = 0.9)

Two selected examples where VBox GPS receiver generated enormous speed outliers are shown in Figure G.6 and Figure G.7.

Figure G.6: Street view for an enormous outlier of VBox (Speed error = -176.9 km/h, Number of Satellites = 4)

Figure G.7: Street view for an enormous outlier of VBox (Speed error = -21.8 km/h, Number of Satellites = 6)

Appendix H: SPEED DIFFERENCE DISTRIBUTIONS FOR TESTS CONDUCTED IN TREE FOLIAGE ENVIRONMENTS

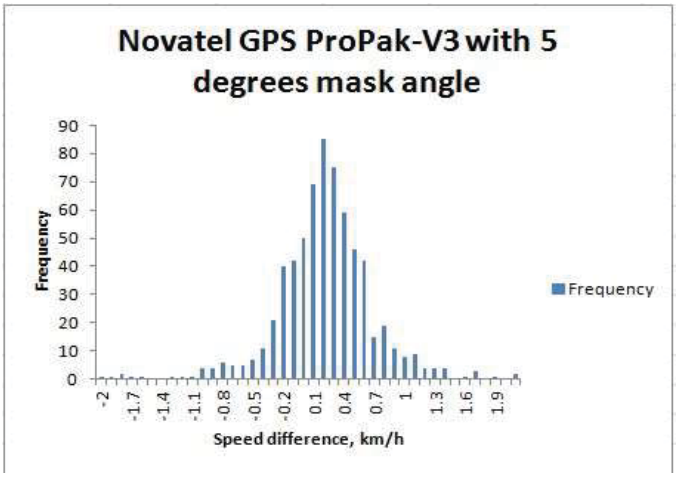

Figure H.1: Speed difference distribution for Novatel ProPak-V3-L1 GPS receiver with 5° mask angle

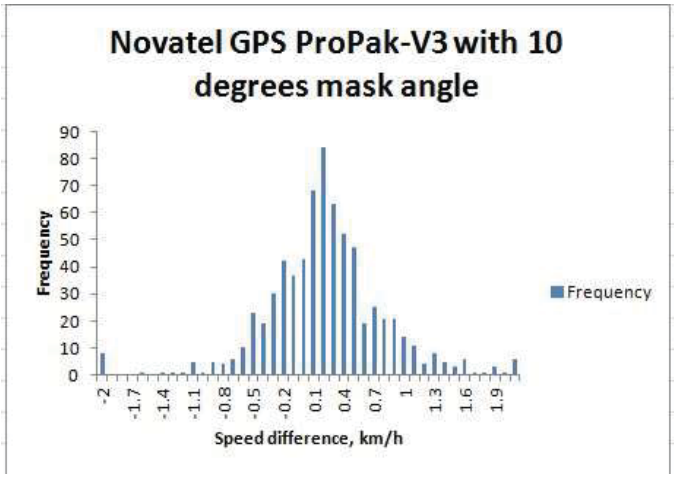

Figure H.2: Speed difference distribution for Novatel ProPak-V3-L1 GPS receiver with 10° mask angle

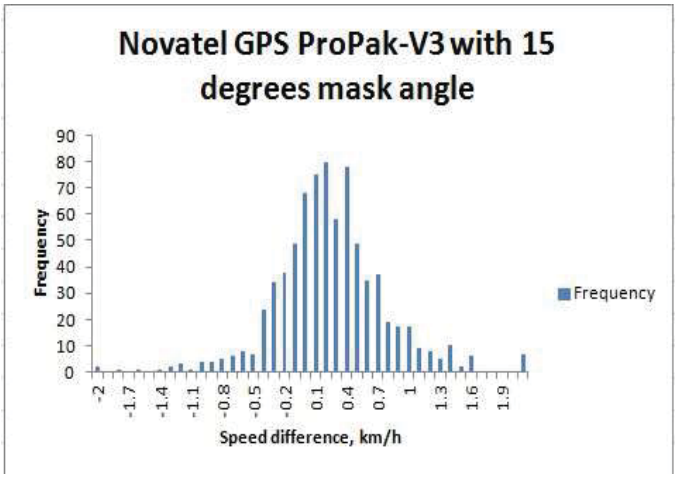

Figure H.3: Speed difference distribution for Novatel ProPak-V3-L1 GPS receiver with 15° mask angle

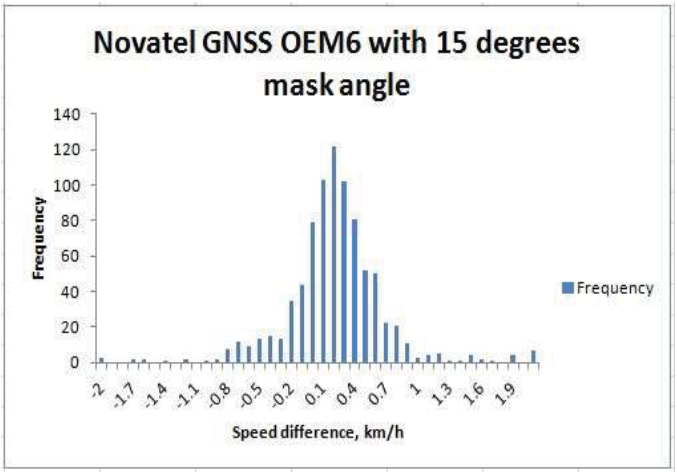

Figure H.4: Speed difference distributions for Novatel OEM6 GPS + GLONASS receiver with 15° mask angle

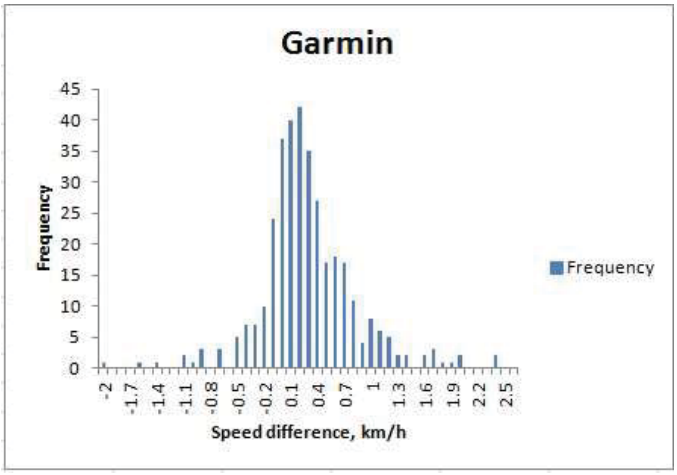

Figure H.5: Speed difference distribution for Garmin

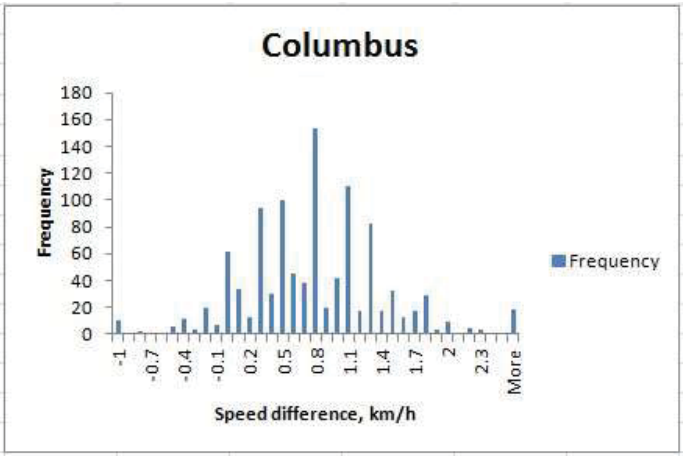

Figure H.6: Speed difference distribution for Columbus

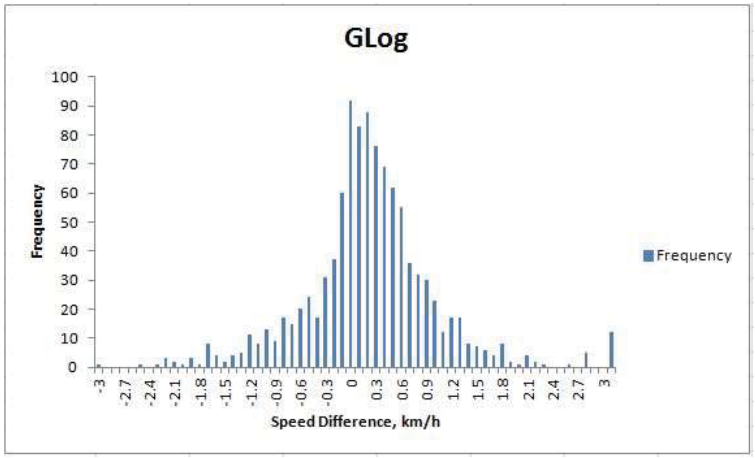

Figure H.7: Speed difference distribution for G-Log

Appendix I: SPEED ERROR AS A FUNCTION OF HDOP FOR KINEMATIC TESTS AND SELECTED GNSS RECEIVERS

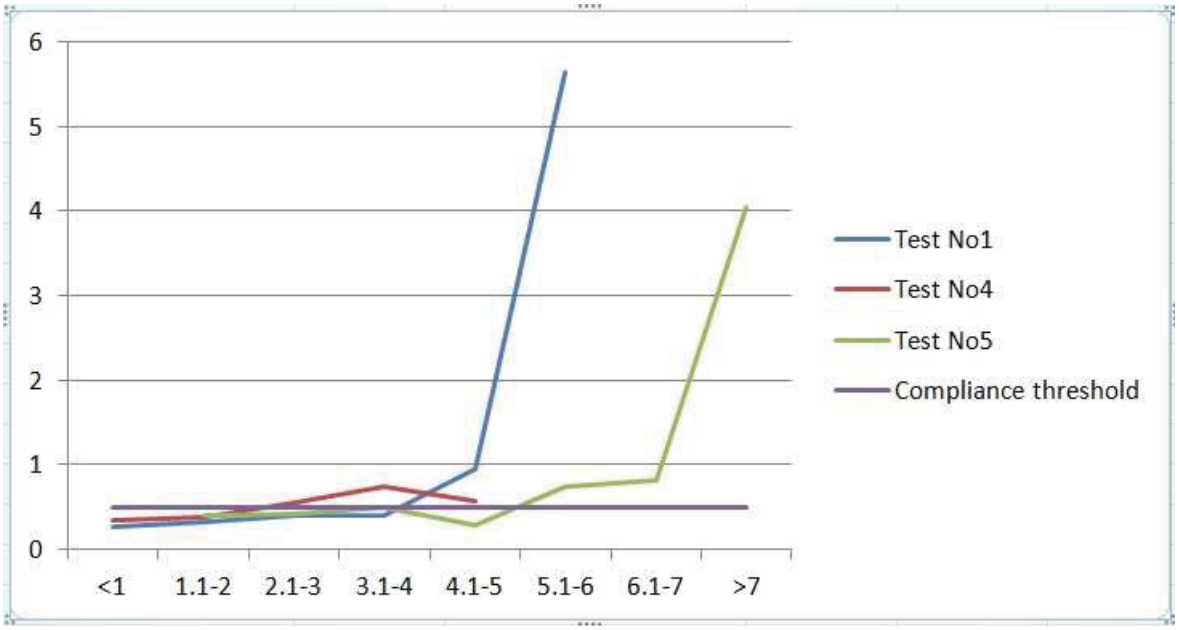

Figure I.1: Speed error as a function of HDOP for Novatel ProPak-V3-L1 GPS receiver with 5° mask angle

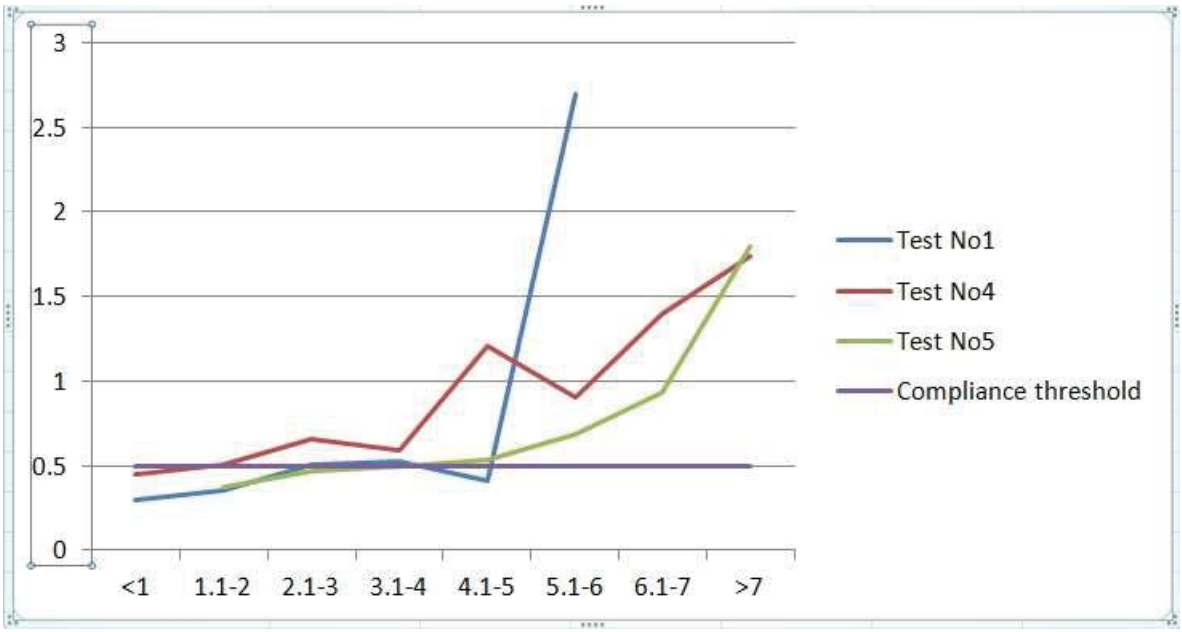

Figure I.2: Speed error as a function of HDOP for Novatel ProPak-V3-L1 GPS receiver with 10° mask angle

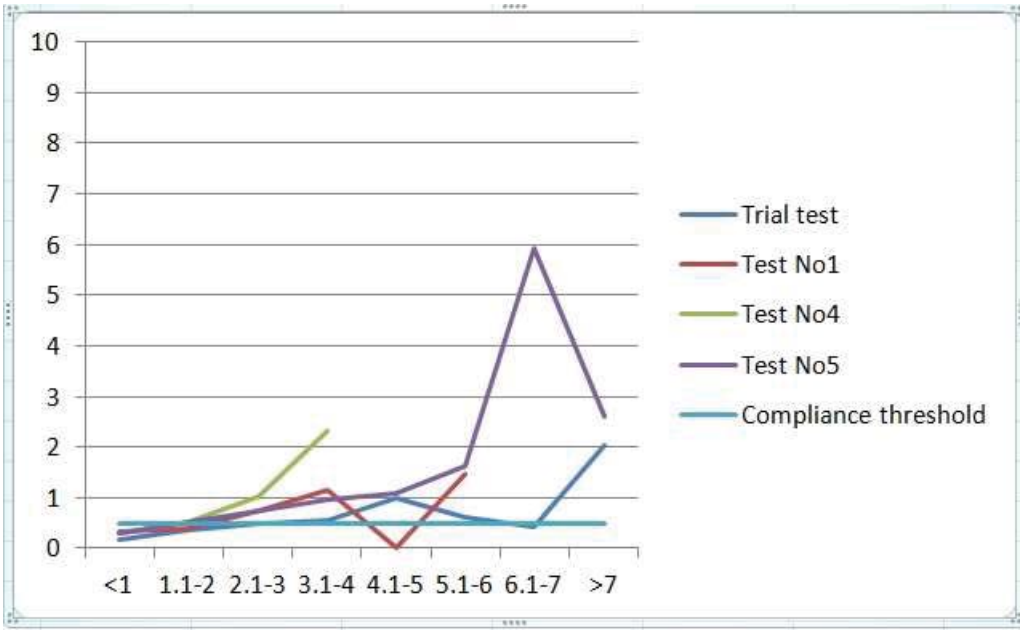

Figure I.3: Speed error as a function of HDOP for Novatel OEM6 GPS + GLONASS receiver with 15° mask angle